Roles of HR23B, HDAC6 and Myd88 and their interplay in response to HDAC inhibitor treatment

Thesis submitted for D.Phil in Oncology

University of Oxford

By

Maria New

Linacre College

September 2014

Declaration

All of the work in this thesis has been carried out entirely by myself and no part of my thesis has been accepted or is currently being submitted for any other degree or diploma in this university or elsewhere. My research was carried out under the supervision of Professor Nicholas La Thangue, Laboratory of Cancer Biology, Department of Oncology, University of Oxford.

Maria New

August 2014

Publications during D. Phil

New, M., et al., Myd88 mediated cytokine signalling regulates cell sensitivity to HDAC inhibitors. In preparation, 2014.

New, M., et al., A regulatory circuit that involves HR23B and HDAC6 governs the biological response to HDAC inhibitors. Cell Death Differ, 2013.

New, M., H. Olzscha, and N.B. La Thangue, HDAC inhibitor-based therapies: can we interpret the code? Mol Oncol, 2012.

Olzscha H., **New M**.,and N.B. La Thangue, Clinical Exemplification of HDAC Inhibitors: From Bench to Clinic, and Back Again. J of Oncopath 2013

Olzscha H., **New M.**,and N.B. La Thangue, Personalised Cancer Medicine: Fulfilling the Promise. eLS, 2013

Acknowledgements

I would like to thank all members of the Laboratory of Cancer Biology for their support and advice during the Dphil. In particular, the group leader, Professor Nicholas La Thangue for his supervision, encouragement and scientific insight, Dr Heid Olzscha for being a great collaborator on our joint publications, and for the thorough and patient reading and helpful comments and corrections on this thesis.

I would also like to thank Dr Amanda Coutts, Dr Shonagh Munro and Dr Geng Liu for their continued support, and advice both on project direction and experimental optimisation, as well as Dr Sandra Maniam, Dr Semira Sheikh and Dr Simon Carr for providing much great company and conversation during my four years in the lab, as well as all other members of the Laboratory of Cancer Biology, past and present.

I would also like to thank Dr Benedikt Kessler and his group, particularly Marie-Laetitia Thesenas and Rebecca Kozietny, for advice with sample preparation for mass spectrometry, and performing mass spectrometry on the submitted samples, with yielded a novel post-translational modification site for my protein of interest.

I must also thank clinical collaborators Dr Semira Sheikh, Dr Avinash Gupta, Dr Graham Collins and Dr Francesco Pezella for assistance with provision of clinical samples, their staining, and analysis; as well as ensuring the translational focus of our research.

This study would not have been possible without funding from Leukaemia and Lymphoma Research, and I would like to thank this organisation for its financial help and support.

I would like to thank members and staff of Linacre College, Oxford for providing a wonderfully friendly community for me to be a part of and the Department of Oncology, University of Oxford for administrative support.

Finally, and most importantly of all I would like to express sincere gratitude to my family, especially my Grandmother Liya, Parents Inna and Peter, and sister Katherine for their love and support throughout my studies.

Interplay of HR23B, Myd88 and HDAC6 in response to HDAC inhibitor treatment

Maria New, Linacre College

Submitted for degree of D. Phil

Michaelmas term, 2014

Abstract

Abnormal epigenetic control is a common early event in tumour progression, and aberrant acetylation in particular has been implicated in tumourigenesis. Histone deacetylases (HDACs) are enzymes that regulate acetylation of chromatin and a variety of other non-histone substrates. Significantly, HDAC inhibitors are potent anti-proliferative agents and exhibit clinical activity in lymphoproliferative and haematological maligancy. However, the mechanistic details by which HDAC inhibitors affect proliferation remain to be elucidated. I have explored the cellular processes affected by HDAC inhibitors, and begun to illuminate a new pathway, regulated by HDAC, which impinges on the cellular effect of HDAC inhibitors. My results suggest that the proteins HR23B and Myd88 are important sensitivity determinants for HDAC inhibitor treatment, and that their interplay with HDAC6 dictates cell fate choice between survival by autophagy or apoptosis.

TABLE OF ABBREVIATIONS

HDAC	histone deacetylase
HAT	histone acetyl transferase
HSP90	heat-shock protein 90
CTCL	cutaneous T-cell lymphoma
NER	nucleotide excision repair
3-MA	3-methyladenine
GFP	green fluorescent protein
UPS	Ubiquitin proteasome system
KD	knockdown
WT	wild-type
NT	non-targeting
GRP78	glucose-regulated protein 78
LC3	light chain 3
CFA	colony formation assay
HDI	histone deacetylase inhibitor
IHC	immunohistochemistry
IL	interleukin
SAHA	Suberoylanilide hydroxamic acid

TABLE OF CONTENTS

CHAPTER 1. INTRODUCTION

1.1 Epigenetic control of gene expression

The vast amount of genomic DNA in eukaryotic cells is assembled onto histone proteins to allow it to be accommodated within the nucleus. An octamer of histones, consisting of an H3-H4 tetramer and two H2A-H2B dimers makes up a nucleosome, around which 146 bp of DNA is wrapped [8, 11-15]. Nucleosomes interact with the linker histone H1 and other chromatin-associated proteins to achieve further compaction of DNA to form chromatin [16].

These histones, in particular their N-terminal amino-acid tail regions undergo a wide variety of enzyme modifications, including acetylation, methylation, phosphorylation and ubiquitination, which have significant effects on gene expression, and are referred to as the "histone code" [17]**.** The "histone code" is important for regulation of transcription, which is regulated not only through the binding of specific DNA sequences by transcription factors, but also via epigenetics. Epigenetics is gene expression regulation without alteration in DNA sequence, but rather through post-translational modifications of DNA-binding proteins (such as histones), and post-translational modifications of the DNA itself (such as DNA methylation and CpG islands). Binding of regulatory factors to specific DNA sequences or to particular chromatin structures (such as combinations of acetylated histone tails) leads to changes in chromatin structure which affects DNA accessibility.

Multiple lysine residues in the N-terminal tails of core histone proteins are reversibly and dynamically acetylated at multiple lysine residues, which plays a key role in modifying chromatin structure and regulating gene expression in

eukaryotes. This takes place both by affecting the intrinsic properties of histones and their interactions with other proteins and DNA [18]. The balance of histone acetylation is controlled by the activities of two enzyme groups: histone acetyl transferases (HATs) which add acetyl groups to the side chain of lysine residues, and histone deacetylases (HDACs), which deacetylate lysine residues and counterbalance activity of HATs [18].

Histone acetylation and deacetylation must be balanced as a result of correct HAT and HDAC activity, and any disruption of this balance can lead to aberrant gene expression which is associated with carcinogenesis. For example, recruitment of HDACs alongside SMRT (silencing mediator for retinoid and thyroid hormone receptors) to retinoic acid responsive target genes results in repression of transcription of genes associated with myeloid differentiation, which then leads to acute promyelocytic leukaemia [19]. The reason for this is a translocation between chromosomes 15 and 17 that causes formation of a PML-RARα fusion protein that binds to retinoic acid response elements in promoter and recruits other corepressors which include HDACs – all resulting in aberrant gene expression.

1.2 Histone deacetylase classes.

The HDAC family of enzymes regulates not only the acetylation level of histones in chromatin, but also a variety of non-histone substrates, which include many proteins that are involved with tumour progression, cell cycle control, apoptosis, angiogenesis and cell invasion [20]. The HDAC family is comprised of 18 genes which are subdivided into classes I, II, III and IV (Figure 1, adapted from [21]) based on their homology to yeast orthologues Rpd3, HdaI and Sir2 [22]. HDAC inhibitors typically target the "classical" class I, II and IV HDACs, which comprise 11 family members in humans [20]. For these HDACs, the catalytic centre contains a zinc ion chelated by aspartate and histidine residues [21] which is within a catalytic domain comprising of an eight-stranded β –sheet located over twelve α-helices.

Class III HDACs are named sirtuins (SIRT1-7) and differ from classical HDACs in that they use NAD^+ as the essential cofactor, whereas classical HDACs contain a Zn^{2+} catalytic ion in their active site [23]. There is increasing evidence for class III HDACs being important in transcriptional regulation, for example SIRT1 upregulation in cancer cells induces CpG island methylation and aberrant silencing of tumour suppressor genes such as E-cadherin [23]. This class of HDACs will not be covered in detail (reviewed in [24]).

Figure 1.1

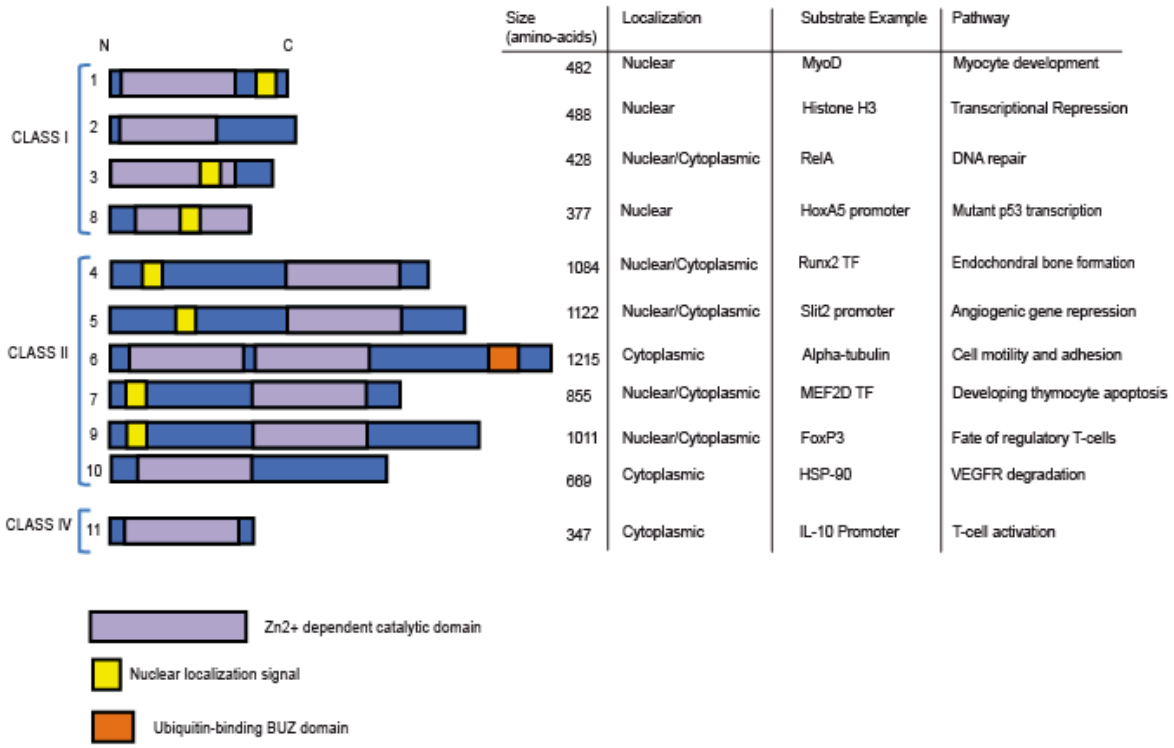

Size (amino-acids)	Localization	Substrate Example	Pathway
482	Nuclear	MyoD	Myocyte development
488	Nuclear	Histone H3	Transcriptional Repression
428	Nuclear/Cytoplasmic	RelA	DNA repair
377	Nuclear	HoxA5 promoter	Mutant p53 transcription
1084	Nuclear/Cytoplasmic	Runx2 TF	Endochondral bone formation
1122	Nuclear/Cytoplasmic	Slit2 promoter	Angiogenic gene repression
1215	Cytoplasmic	Alpha-tubulin	Cell motility and adhesion
855	Nuclear/Cytoplasmic	MEF2D TF	Developing thymocyte apoptosis
1011	Nuclear/Cytoplasmic	FoxP3	Fate of regulatory T-cells
669	Cytoplasmic	HSP-90	VEGFR degradation
347	Cytoplasmic	IL-10 Promoter	T-cell activation

Schematic organisation of Class I, II and IV HDACs showing their domain composition, size, cellular localization, target proteins and the cellular processes which are consequently regulated. The HDAC deacetylase catalytic domains are shown in purple, nuclear localization targeting sequences in yellow, and the ubiquitin-binding BUZ domain of HDAC6 is in orange. A single substrate example is given alongside each enzyme, as well as the process in which this substrate participates. Figure adapted from New et al, 2012

1.3. HDACs and cancer

There are two ways in which mutations, altered expression and deregulation of HDAC genes are linked to tumour development: through modification of gene transcription and via the non-histone HDAC substrates. Although somatic mutations of HDAC genes are rare, HDAC4 mutations have been identified in breast cancer samples during a large scale sequencing study [25]. Additionally, mutations which result in HDAC2 protein truncation have been described in human epithelial cancer cell lines [26]. The altered expression profiles of various HDACs in different cancer types observed in studies so far and their potential prognostic relevance is summarised in Table 1.

Deregulation of HDAC expression and activity frequently induces aberrant transcription of key genes regulating cell proliferation, cell-cycle and apoptosis. This takes place by HDACs acting as components of multi-protein complexes containing corepressor DNA-binding proteins such as NcoR, SMRT and Sin3A [18, 27]. The consequent transcriptional repression of tumour suppressor genes then promotes carcinogenesis. However, microarray analysis has indicated that only 2-5% of genes are influenced by HDAC inhibition [28] and approximately equal numbers of genes are induced and repressed [29]. This suggests that mechanisms other than regulation of transcription are important in HDAC effects on cellular processes. For example, regulation of the acetylation status of the diverse range of non-histone HDAC substrate proteins is likely to be important.

Table 1.HDAC expression in various cancer types and possible prognostic relevance (adapted from [21])

	Levels in cancer types	**Prognostic relevance**
Class I HDACs		
1	Upregulated in gastric, colorectal, oesophageal and pancreatic cancer	High expression in pancreatic cancer associated with poor prognosis In hepatocellular carcinoma, high HDAC1 associated with invasion into the portal vein In lung cancer, high HDAC1 associated with later stages of disease Better disease-free survival in breast cancer
2	Upregulated during early colorectal cancer at the polyp stage Upregulated in cervical dysplasia and invasive carcinoma	High levels in colorectal cancer associated with poor patient survival Associated with advanced stage disease in gastric, colorectal and prostate cancer Associated with aggressive CTCL
3	Upregulated in lung cancer, prostate and colon cancer	High levels in colorectal cancer associated with poor patient survival Associated with advanced stage disease in gastric, colorectal and prostate cancer Poor prognostic indicator for post-liver transplantation HCC
8	Upregulated in neuroblastoma	Higher expression associated with poorer outcome and advanced stage disease in paediatric neuroblastoma
Class IIA		

HDACs		
4	Upregulated in breast cancer samples compared with renal, bladder and colorectal cancer	No data available
5	Upregulated in colorectal cancer in contrast to renal, bladder and breast cancer Downregulated in cancer and acute myeloid leukemia	Low expression associated with poor prognosis in lung cancer
7	Upregulated in colorectal cancer in contrast to bladder, renal and breast cancer	May present an anti-angiogenesis target
9	Overexpressed in medulloblastoma/astrocytoma	High levels associated with poor prognosis and survival in childhood acute lymphoblastic leukaemia
Class IIB HDACs		
6	High in oral squamous cell carcinoma	Associated with favourable outcome in CTCL in higher survival in breast cancer
10	Overexpressed in hepatocellular carcinoma	Poor prognostic indicator in lung cancer
Class IV		
11	Overexpressed in breast cancer	No data available

The function of many transcription factors, chaperones and structural proteins depends on their acetylation state, which in turn impacts on a multitude of physiological pathways. For example, HDAC6 deacetylates HSP-90 which enhances ATP binding and thus promotes assembly of functional HSP-90 chaperone complexes [30]. β-catenin is another HDAC6 substrate which is frequently mutated in anaplastic thyroid cancer. Epidermal growth factor (EGF) induces HDAC6 translocation, after which HDAC6 associates with β-catenin and deacetylates it, causing nuclear localisation of β-catenin which promotes Wnt signalling and c-myc activation [31]. This implicates HDAC6 as a link between EGF and Wnt signalling during tumour progression, and suggests that inactivation of HDAC6 could be beneficial in tumours where such signalling is deregulated [31]. HDACs 1 and 2 are also implicated in Wnt signalling via disruption of the β-catenin-TCF interaction [32]. Also, Wnt-dependent increased HDAC2 expression as a consequence of the loss of the adenomatosis polyposis coli tumour suppressor gene is found in the majority of human colon cancers, where increased levels of HDAC2 are thought to prevent apoptosis [33].

Acetylation also influences function of key oncoproteins, including c-Myc and E2F1 and tumour supressors, such retinoblastoma (pRb) and p53. Increased histone deacetylase activity has been shown to be a cause of repression of transcription by the E2F-Rb complex during the G1 phase of the cell cycle. Acetylation of highly conserved lysine residues near the DNA-binding domain of E2F1 increases E2F1 DNA-binding activity trans-activation potential and half-life [34].

1.4 HDAC6 structure and function

HDAC6 is a unique HDAC in a number of ways, and affects a variety of cellular processes. As Figure 1.1 indicates, HDAC6 is the only HDAC without a nuclear localization sequence, which means it is the only cytoplasmic HDAC. It is also the only HDAC with a ubiquitin binding BUZ domain – a C-terminal zinc finger domain which binds free ubiquitin, as well as ubiquitinated proteins with high affinity [35]. In addition HDAC6 contains two catalytic domains, and its substrates include tubulin. HDAC6 is found partially associated with the microtubule network [35].

HDAC6 also associates with the AAA-ATPase p97/VCP, which is important for proteasomal degradation of misfolded proteins, which subsequently form polyubiquitinated aggregates [36]. HDAC6 promotes aggregation of such misfolded polyubiquitinated proteins into aggresomes, thus protecting cells from apoptosis as a result of misfolded protein stress [37]. In addition, HDAC6 regulates the activity of its substrate HSP90, and controls induction of this heat-shock protein on accumulation of ubiquitinated protein aggregates [30]. Mice in which HDAC6 is absent have elevated tubulin acetylation, and exhibit an impaired immune response, but they are viable and undergo normal development [38].

Interestingly, HDAC6 is directly involved in autophagy by recruiting actin-remodelling machinery, causing autophagosome-lysosome fusion [14], which suggests that HDIs which target HDAC6 could also inhibit autophagy.

1.5. HDAC inhibitors

Historically, interest in HDAC inhibitors (HDIs) was due to their ability to promote neurogenesis in the treatment of bipolar disorder [39] and to increase gene expression, for example the HDI phenylbutyrate was used in anaemic patients to increase haemoglobin expression [40]. The development of these compounds for cancer treatment was also based on their ability to enhance expression of genes involved in apoptotic pathways [40]. HDIs have been observed to cause apoptosis in cell-based studies, hence there has been great interest to develop these drugs as potential anti-cancer agents, as well as agents to dissect HDAC roles [41]. A simple explanation for the tumour inhibiting activity of HDI treatment is that such treatment causes chromatin to be in a more open structure due to increase in lysine acetylation, which means some charge of the positively charged lysines in histones is neutralised and they are thus bound less tightly to negatively charged DNA. This leads to activation of gene expression to cause tumour growth inhibition, through reactivation of protective genes which were silenced by mutations or aberrant epigenetic modifications within a tumour. Ideally, if the tumour type is correct and the required genes are reactivated, this would lead to an arrest in tumour cell proliferation to cause apoptosis, cell cycle arrest or differentiation. However, due to the range of HDAC functions, the ways in which HDIs exert their effects are often more complex and cannot be explained through gene expression changes alone.

HDAC inhibitors which are being used and developed as anticancer therapies primarily target HDACs in classes I, II and IV, although there is increasing interest in the class III sirtuin family [42]. Many HDAC inhibitor compounds are

in clinical trials or other stages of preclinical development. HDIs can be classified according to their chemical structure into hydroxamates, cyclic peptides, benzamides and fatty acids [43], or according to their specificity for various HDAC classes (summarised in Table 2). Chemoproteomic approaches which combine quantitative mass spectrometry with affinity capture have been useful in identifying which HDAC complexes (rather than isolated HDACs) are targeted by HDIs. For example, valproate affects the Sin3 complex to a lesser degree compared to other class I complexes with the same catalytic subunit [44]

The inhibitory effect of a large number of HDAC inhibitors depends on the Zn^{2+} dependency of HDAC enzymes [42]. A classic example of this is trichostatin A (TSA), which was one of the first HDIs to be identified. As shown by the crystal structure of TSA bound to HDPL, an HDAC analogue isolated from Aquifex aeolicus, the conserved deacetylase active site contains two Asp-His charge relay systems necessary for the enzymatic activity, as well as a tubular pocket and a zinc-binding site. The tubular pocket in the HDAC accommodates the aliphatic long chain of TSA, and the zinc is coordinated by the carboxyl and hydroxyl groups of the hydroxamic group at the end of this chain [45]. The hydroxamic group of SAHA chelates the zinc ion in the same way, but SAHA's aliphatic chain makes fewer van-der-Waals contacts with the HDAC tubular pocket compared to TSA, explaining the weaker inhibitory activity of SAHA relative to TSA [45]. A number of other HDIs have a similar mechanism of action including belinostat, givinostat, panobinostat and dacinostat [46].

Table 2. HDI Classification by Chemical structure and Clinical Trial Use (adapted from [21])

Classification by chemical structure	Named Examples (INN)	HDAC specificity	Clinical trial Stage
Hydroxamates	SAHA (vorinostat)	Pan-inhibitor	Approved for CTCL, phase III alone or in combination
	PXD101 (belinostat)	Pan-inhibitor	Phase II alone or in combination
	LBH589 (panobinostat)	Pan-inhibitor	Phase III alone or in combination
	ITF2357 (givinostat)	Class I and II	Phase II alone or in combination
	4SC-201 (resminostat)	Pan-inhibitor	Phase II alone or in combination
	PCI 24781 (abexinostat)	Class I and II	Phase II alone or in combination
Cyclic Peptides	Depsipeptide/FK228 (romidepsin)	Class I	Approved for CTCL and PCTL , phase III alone or in combination
Benzamides	MS-275 (entinostat)	Class I	Phase II alone or in combination
	MGCD0103 (mocetinostat)	Class I	Phase II alone or in combination
Aliphatic Fatty acids	Valproic acid	Class I and IIa	Phase II alone or in combination
	Butyrate	Class I and IIa	Phase II alone or in combination

1.6. HDI specificity

As discussed above, some HDIs such as TSA and SAHA act as pan-inhibitors against multiple HDACs by interfering with the zinc ion in their active site. Others such as romidepsin and CXD101 are only active against Class I HDACs, whereas some are only specific against one or two enzymes. Entinostat, for example has no activity against HDACs 4, 6, 7 or 8 but inhibits HDAC1 and has some activity against HDACs 2, 3 and 9 [47], whereas Tubastatin A only inhibits HDAC6 [48]. More recently, compounds in development which are not just specific against just one HDAC, but inhibit only one of several catalytic activities of an enzyme. An example of this is Tubacin, which binds to only one catalytic domain of HDAC6 and inhibits only α-tubulin deacetylation by HDAC6 [13]. Tubacin treatment does not affect microtubule stability but it did cause a decrease in cell motility, and as such may have therapeutic applications as an antimetastatic agent [13]. Development of HDAC6 inhibitors is of clinical relevance and there are some reports of clinical efficacy of compounds such as tubacin and tubastatin [49].

1.7 Various cellular outcomes of HDI treatment

HDI treatment leads to a variety of cellular responses, including apoptosis, autophagy, cell cycle arrest, cell differentiation, and anti-angiogenesis, as summarised in figure 1.2. It also impacts on cellular DNA repair and protein quality control. The various effects of HDI treatment are discussed in the sub-sections below. Autophagy as a cellular outcome of HDI treatment is described separately in section 1.8 as it has particular importance for this project as it can be seen as an alternative cell fate to apoptosis.

Figure 1.2

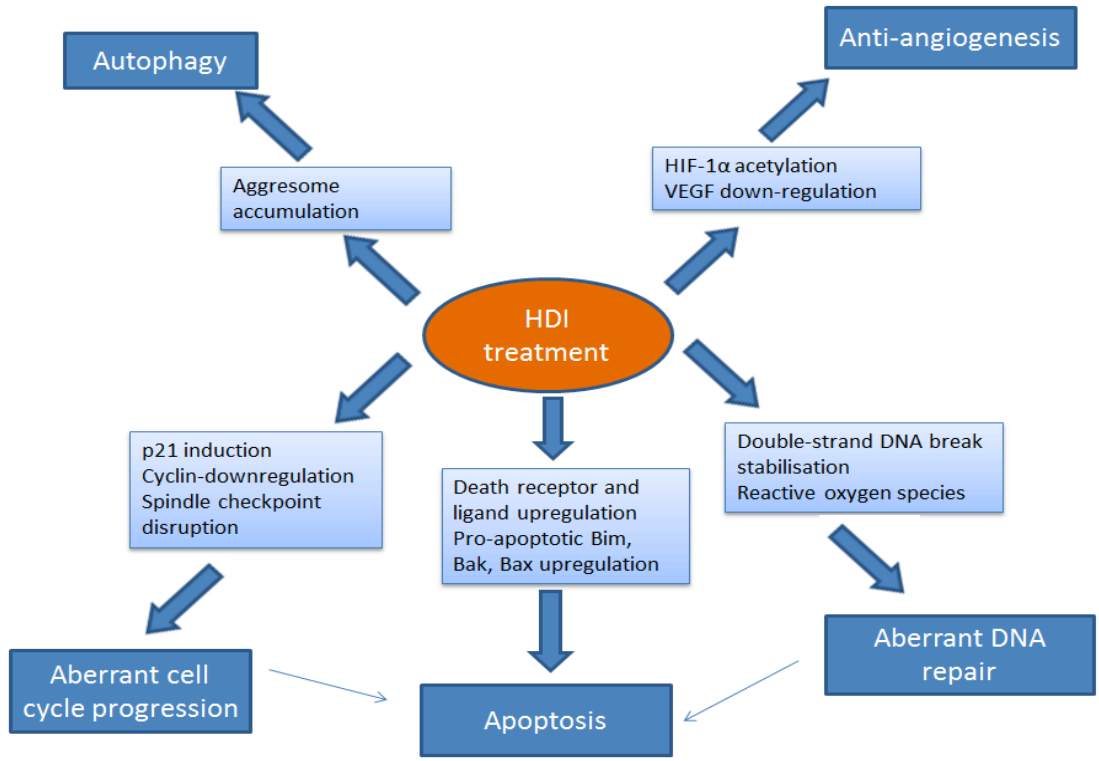

Summary of cellular outcomes and processes that take place upon treatment with HDAC inhibitors (adapted from Olzscha et al, 2013)

1.7 A. Apoptosis

Cancer cell death can be considered the especially desired outcome of HDI treatment, and HDI treatment induces apoptosis by activating both the extrinsic route via death receptor activation by ligands such as TRAIL and the intrinsic route via mitochondrial membrane disruption, which causes pro-apoptotic protein release [50]. Studies in cancer cell lines, mouse models and patient samples have shown many HDIs to cause selective up-regulation of pro-apoptotic proteins, such as death receptors and ligands [46]. For example, TRAIL expression in breast cancer has been shown to increase on treatment with both SAHA and entinostat, an effect mediated by the SP1 transcription factor and enhanced by adriamycin [51]. This caused adapter protein recruitment and caspase-8 activation, which then cleaves executioner caspases 6 and 7, resulting in apoptosis [50]. Caspase-independent serine protease-dependent apoptosis can also be activated by HDI treatment, via increasing Bax tumour suppressor protein levels causing apoptosis activating factor (AIF) to be released from the mitochondria [52]. Furthermore, cells which are resistant to TRAIL can be sensitised by HDI treatment through induction of pro-apoptotic Bax and Bak and inhibition of anti-apoptotic Bcl-2 and Bcl-xl [53]. HDAC inhibition may also directly affect acetylation patterns of proteins which determine whether apoptosis takes place, such as p53 acetylation at certain lysines (K382 and K381) as a result of HDI treatment leads to induction of PUMA (p53 upregulated modulator of apoptosis) expression and cell death [54]. HDAC1 is able to deacetylate p53, thus destabilising it, so HDI treatment may contribute to p53 stabilisation via HDAC1 inhibition thus enhancing its activity as a tumour suppressor [55].

1.7 B Anti-angiogenesis

New blood vessel formation from existing blood vessels, or angiogenesis, is an important process during tumourigenesis and metastasis to provide the tumour with nutrients and oxygen, while removing waste products. Hypoxia-inducible factor 1α (HIF-1α) is stabilised under hypoxic conditions, and acts as a transcription factor to increase expression of proteins involved in angiogenesis including vascular endothelial growth factor (VEGF). Under conditions of normal oxygen levels (normoxic conditions) HIF-1α is acetylated and hydroxylated, which leads to rapid degradation through interaction with the von-Hippel-Lindau (pVHL) ubiquitin E3 ligase complex. Levels of HDACs 1, 2 and 3 increase under conditions of oxygen deprivation, which leads to decreased pVHL, and consequent increases in HIF-1α, VEGF and angiogenesis, which is prevented by HDI treatment [56]. To the contrary, reduction in expression of HDACs 3 and 1 can cause HIF-1α degradation, and these HDACs bind directly to HIF-1α [57]. HDACs 4 and 6 can also bind HIF-1α, but regulate it via the proteasome independent of pVHL [58]. HDI treatment also results in negative regulation of some matrix metalloproteinases MMPs via gene expression regulation [59] thus suppressing tumour invasion and angiogenesis.

1.7 C Cell cycle effects

Cell cycle progression and proliferation involve a number of HDACs and are often targeted during cancer therapy. HDAC1 has been shown to be a transcriptional proliferation activator through a number of mechanisms including negative regulation of Prss11, a tumour suppressor protein which is a member of an oxidative stress-response family of proteases [60]. HDAC2 is thought to act together with HDAC1 to promote G1-S phase progression, through repression of

p21 and p57 expression [61]. HDAC4 has also been seen to down-regulate p21 transcription in cell lines and appears to be expressed primarily in the proliferative zone of the small intestine, and to be silenced during differentiation [62]. Similarly, silencing HDAC3 stimulates p21 promoter activity and HDAC3 is deregulated in colon cancer [63]. It makes sense therefore that HDI treatment leads to cell cycle arrest, as HDACs repress various mediators of cell growth arrest, such as p21. There has also been evidence that HDI treatment affects cell cycle progression by cyclin down-regulation, such as the down-regulation of cyclin D1 via causing enhanced acetylation of the NF- κB subunit p52 which then interacts with the NF- κB subnit p65 and prevents it binding to the cyclin D1 promoter [64].

Mitotic progression is another target for cancer drugs such as taxanes which target microtubules. HDIs can also have this effect by causing delayed and aberrant mitosis though disruption of the spindle assembly checkpoint and chromosomal passenger proteins such as BubR1, CENP-F and CENP-E [65].

1.7 D DNA repair

HDI treatment affects disrupts DNA repair in a number of ways including DNA double-strand break stabilisation, down-regulation of expression of DNA repair factors and ROS accumulation [46], as explained further in Table 2. These effects on DNA repair explain the synergistic activity of DNA-damaging agents and HDIs, which has led to clinical trials involving combined use of the two compounds.

Table 3. The effects of HDI treatment on DNA repair processes

HDI effect on cancer cell DNA	**Evidence**	**Mechanism**	**Consequence**
Stabilisation of DNA double strand breaks (DSBs)	Accumulation of phosphorylated H2AX nuclear foci [66]	Increased histone acetylation causes chromatin structure to become more open	DNA becomes exposed to further damage from cytotoxic drugs, radiation etc
Down-regulation of homologous DSB repair	Immunofluorescence showed inhibition of subnuclear repair foci on HDI treatment Reduction in transcription of genes associated repair, such as RAD51 [67]	HDACs regulate gene transcription, including genes coding for DNA repair proteins HDACs may assist assembly of repair protein complexes [67]	Lack of DNA repair leads to cell death and inability to replicate
Reactive oxygen species (ROS) accumulation[68]	Pre-exposure of leukaemia cells to HDI induces ROS increases that lead to sustained	Mechanism not fully understood	DNA damage, oxidative stress, and eventually

	DNA damage [68] Co-treatment with ROS scavengers decreases HDI-caused cell death		apoptosis
Inactivation of DNA repair machinery components by acetylation	HDAC1/2 are recruited to DNA damage sites and affect ability of NHEJ factors to bind to DSB sites [69]	HDACs1 and 2 deacetylate proteins involved in DNA repair, which is required for their normal function	Inability of cells to repair DNA

1.7 E Protein quality control

Various interconnected protein control mechanisms exist to maintain the balance of the proteome in cells in order to react to endogenous and environmental changes [70]. The adjustment of protein folding and conformation, concentration, localisation and interaction is controlled by the processes of protein synthesis, the molecular chaperones, the ubiquitin proteasome system (UPS) and autophagy as well as post-translational modifications.

HDIs impact on these pathways in several ways, for example, through inhibition of HDAC6, which binds polyubiquitinated misfolded proteins and recruits them to dynein motors for transport to aggresomes [14, 37].

HDAC6 interacts with and deacetylates Hsp90 chaperones. Consequently, HDI treatment leads to reversible Hsp90 hyperacetylation, impairing its function and releasing HSP90 client proteins such as Akt, Bcr-Abl, c-Raf and ErbB2. These client proteins could then undergo poly-ubiquitination with subsequent proteasomal degradation [71, 72].

1.7 F Cytokine production and immunity

Cytokine signalling is frequently aberrant in haematological malignancies, such as persistently activated STAT3 (signal transducer and activator of transcription), which promotes pro-oncogenic inflammatory pathways by interacting with the NF-κB family member RelA, causing it to remain in the nucleus and constitutively activate the NF-κB signalling pathway which leads to production of inflammatory mediators such as interleukin-6 [73]. HDACs dynamically regulate STAT acetylation [74], and HDI treatment causes hyperacetylation, which impacts on tumour cell survival, suggesting that cytokine-producing pathways are important targets of HDI treatment. Protein acetylation plays a key part in the functioning of the immune system and HDACs regulate immunity in a number of ways, such as myeloid cell development, toll-like receptor signalling regulation and negative regulation of inflammatory cytokine production [75]. These pleiotropic roles in immune cell development and function mean that broad-spectrum HDIs often have negative immune-related effects in patients such as down-regulation of genes involved in host defence, including pattern recognition receptors and cytokines [75]. However, there is therapeutic potential in developing specific HDIs to target tumour-linked inflammation or increase tumour immunogenicity. For example, treatment with tubastatin A, a specific HDAC6 inhibitor resulted in significant inhibition of the cytokines IL-6 and TNF in human macrophages and paw tissue of arthritic mice [76].

1.8. Autophagy

The word autophagy comes for the Greek “auto” meaning self and “phagy” meaning to eat, which means it is a process of self-digestion. Autophagy takes place in a wide range of eukaryotic organisms and has a number of functions during starvation, tissue remodelling and cell death [77]. There are three types of autophagy: microautophagy, macroautophagy and chaperone-mediated autophagy [8]. Microautophagy is the formation of vesicles at the lysosomal surface by invagination, protrusion and membrane separation, whereas macroautophagy (hereafter referred to as autophagy) is the formation of a double-membrane vesicle in the cytosol which sequesters part of the cytoplasm, which subsequently fuses with the lysosome to create an acidic degradative compartment [77]. Macroautophagy can be further classified into “induced autophagy”, which occurs during starvation to produce amino acids and “basal autophagy” during which cytosolic components are constitutively recycled [8]. Autophagy is a process separate from degradation of extracellular and membrane proteins by lysosomes following endocytosis and also separate from the ubiquitin-proteasome system (UPS) which is selective and specific to ubiquitinated proteins, whereas autophagy is thought to be a generally non-selective degradation process, although there are exceptions, such as HDAC6 shuttling of monoubiquitinated proteins [8]. Another key function of autophagy is for elimination of intracellular microbes after Toll-like receptors have been activated [78].

Autophagy is typically triggered by nutrient starvation such as the depletion of certain amino acids and can be viewed as a process to yield resources during time of need. However, it can also be induced by other extracellular stress, including

hypoxia and oxidative stress, or intracellular stress such as accumulation of damaged organelles or protein aggregation. The fact that all these various stimuli act as autophagy triggers reflects the multiple signalling pathways involved in the process [79]. Autophagy-related genes are known as ATG and their protein products as Atg, and these are conserved amongst eukaryotic organisms [79]. For example, Beclin1, the mammalian ortholog of yeast Atg6 initiates autophagosome formation through interaction with the phosphatidylinositol (PtdIns) 3-kinase class III, which is also required for autophagy [80], as indicated in Figure 1.3. Beclin 1 is of particular interest as it is an autophagy related tumour suppressor gene, and has been shown to inhibit tumourigenesis through its autophagy-promoting activity [81]

As shown in Figure 1.3a, mTOR (mammalian target of rapamycin) is a negative regulator of autophagy at the centre of the signalling pathways culminating in autophagy, through its suppression of the Atg1 kinase complex, which is thought to be required for autophagy [6]. As shown in figure 1.3, insulin is a major down-regulator of autophagy, and IRS (insulin receptor) activation triggers a signalling cascade which leads to mTOR activation, and autophagy downregulation [6]. High levels of cellular amino-acids and ATP also suppress autophagy, as well PI3 kinase (class I), Rheb and PDK1, where as PI3 kinase (class III) is required for PAS (preautophagosomal structure) generation (Figure 1.3).

mTOR is a highly conserved protein which forms two multiprotein complexes – mTORC1 and mTORC2 and controls processes related to cell growth and metabolism such as hypoxia response and development [81]. However, there are other pathways regulating autophagy in an mTOR-independent way, such as the inositol signalling pathway, the calcium/calpain pathway, the cAMP pathway and

other mTOR-independent small molecules such as the disaccharide trehalose, which induces autophagy [82].

The various steps of autophagy are summarised in figure 1.3b. First, cytoplasmic components such as proteins or organelles are sequestered by a phagophore or isolation membrane, which then elongates and expands to form an autophagosome which can sequester materials, typically a double membrane organelle with LC3 (Atg8) localised on its inner membrane [8]. The next step is for the autophagosome to fuse with lysosomes after which the inner autophagosome membrane and cytoplasmic-derived materials are degraded by lysosomal hydrolytic enzymes. Monomeric units such as amino-acids are then exported to the cytosol so that they can be reused, for example in the glucose-alanine cycle through which glucose can be produced during starvation, or as an energy source during the TCA cycle [8].

Figure 1.3

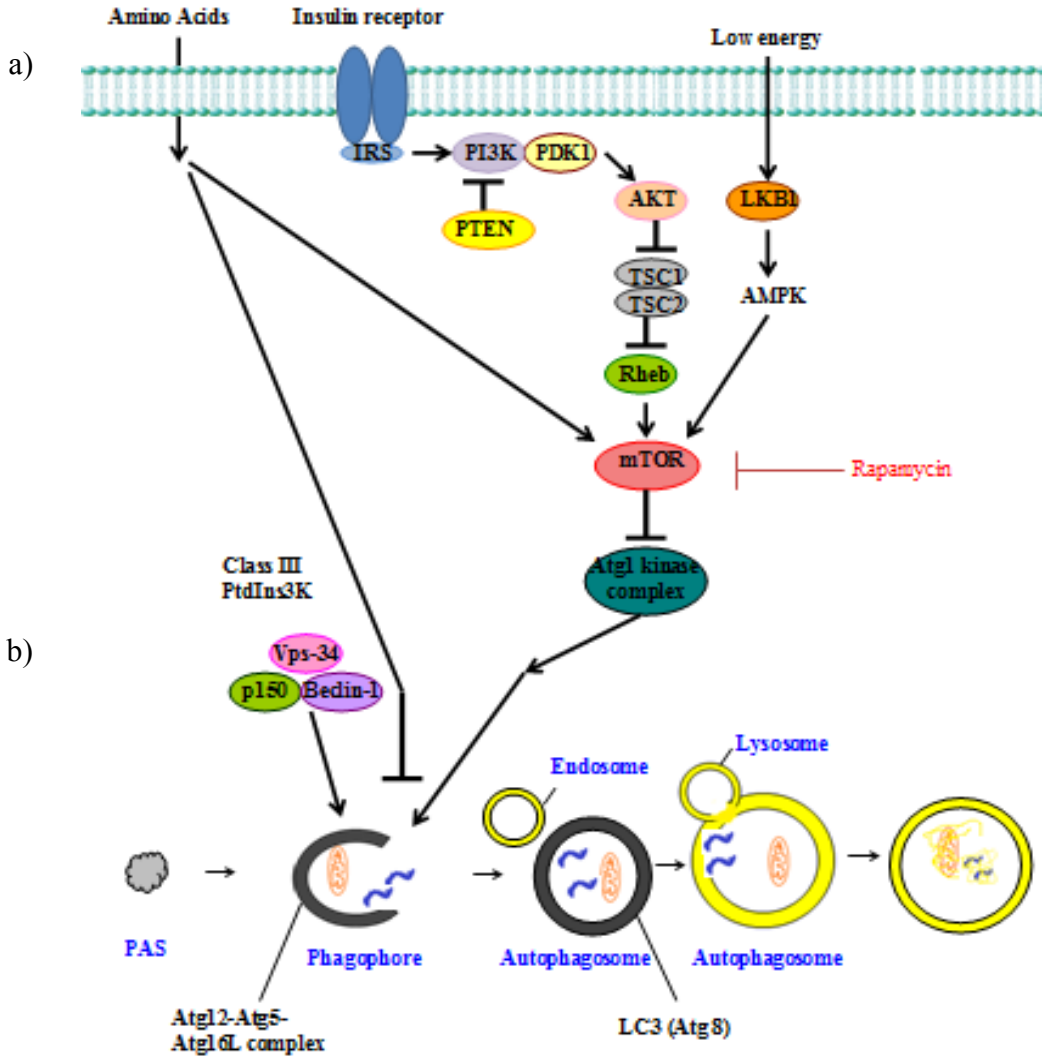

a) Schematic representation of autophagy regulation (adapted from [3] and [6]). mTOR is the major suppressor of autophagy, and is regulated by insulin (also suppressed autophagy), energy levels which activate the AMP kinase pathway, and amino-acid levels.

b) Summary of the various steps which take place during autophagosome formation, adapted from (adapted from [8] and [9]). The PAS (pre-autophagosomal structure) requires the class III PI3 kinase complex which includes Beclin-1 (Atg6). Elongation of isolation membrane (phagophore) to form and autophagosome requires the ubiquitin like modification systems Atg12 and Atg8 (LC3), the latter of which associates with the autophagosome as a conjugate with phosphatidylethanolamine [6].

1.9. Autophagy and cancer

Similarly to several other anti-cancer therapies, HDIs induce autophagy in human cancer cell lines. However these results are difficult to interpret as autophagy has been associated with contradictory roles both in cell death, tumour suppression and cell survival during cancer (see table 1) [50].

Table 1. Evidence and mechanism of controversial pro-survival and pro-death autophagy functions (adapted from Olzscha et al, 2013)

Pro-death autophagy functions	Pro-survival autophagy functions
Persistent autophagy in response to cellular stress such as chemotherapy can act as death signal [50].	Allows cells to gain ATP during hypoxia or nutrient deprivation, which are typical tumour conditions [50].
In some cells lines such as chondrosarcoma, SAHA shown to induce autophagy-associated cell death [83].	Co-administration of autophagy inhibitors such as chloroquine with HDIs enhances apoptosis in colon cancer cells [84].
Autophagic cell death mechanisms are not fully defined, but generally caspase independent [50].	siRNA depletion of the essential autophagy gene Atg7 enhances apoptosis in colon cancer cells [84].

1.10. Methods of measuring autophagy.

As autophagy has so many important biological roles, a number of methods have been established to measure this process. These methods can be divided into morphological methods, biochemical methods, and specific markers for autophagy [85].

Morphological methods are those which observe physical changes in the cells. An example of these is electron microscopy (EM) which was in fact the method used to originally discover autophagy by Ashford in 1962, where "polymorphic dense bodies" distinct from lysosomes were described in which parts of mitochondria could be visualised [86]. EM can be used to observe double-membraned autophagosomes and quantification is possible if the volume of autophagosomes is divided by the total cytoplasmic volume and expressed as a ratio, using specially developed computer software. However, electron microscopy is a skill and time-requiring technique and it is very difficult to distinguish autophagic vacuoles from other structures such as heterophagic vacuoles (with endocytosed material), swollen endoplasmic reticulum organelles in stressed cells, or even just a double-membraned structure arising from a portion of a cell protruding into the next cell and then being cut perpendicular to the axis of protrusion [85]. More recently, immunoelectron microscopy has been developed where specific antibodies against autophagosomal markers are used [87].

A biochemical method for monitoring autophagy is looking at the bulk degradation of long-lived proteins by a pulse-chase experiment where cells are labelled with valine containing heavy isotopes of carbon or hydrogen so that all

cellular proteins are labelled, after which cells are incubated with an excess of unlabelled valine for a short period of time, after which they are incubated again in unlabelled media. This results in specific labelling of long-lived proteins the degradation of which can be measured by precipitating proteins with TCA (trichloroacetic acid) and measuring radioactivity in culture supernatant. This is a useful measurement method as autophagy is a means to degrade long-lived proteins (as opposed to proteasomal degradation of short-lived proteins), but it is not specific for macroautophagy [85]. Observing specific markers for autophagy is the method used to monitor autophagy during this project. One of the most widely used such markers is microtubule-associated protein 1 light chain 3 (LC3) a homologue of yeast Apg8p. Immediately after synthesis, LC3 undergoes ubiquitin-like post-translational modifications which causes it to be targeted to the isolation membrane, after which it's C-terminal region (5 amino-acids in human cells) is cleaved by mammalian homologues of yeast Atg4 [87]. This initial processed form is called LC3-I and resides in the cytosol. Once autophagy is activated, LC3-I is transferred to a specific E2 (Atg3) and conjugated to PE. This final form of LC3 associates with the autophagosomal membrane and is called LC3-II. The localisation of LC3-II on the autophagosome membrane was shown by immunoelectron microscopy, and the amount of LC3-II correlates with autophagosome formation [58]. The two forms of LC3 migrate differently on an SDS-PAGE gel, so give two bands on an immunoblot with an α-LC3 antibody. The apparent mobility of LC3-I is 18 kDa and the apparent mobility of LC3-II is 16 kDa [87]. The number of autophagosomes correlates with either the amount of LC3-II or the LC3-II/LC3I ratio [58]. A limitation of this method is that LC3-II represents only the autophagy levels at that particular moment in time, rather than

the magnitude of flux through the autophagic pathway in general. This is because the autophagosome is a transient structure and the lifetime of LC3-II is relatively short [85]. Another potential problem is that LC3-II may be more sensitive to immunoblot analysis than LC3-I due to its conformation or hydrophobicity and its levels are therefore overrepresented. In some cases even in the absence of starvation the LC3-II band is stronger than LC3-I [87]. However, immunoblot analysis of LC3-II remains a common accepted way to measure autophagic activity of mammalian cells as it is simple and semi-quantitative. A chimeric GFP-LC3 fusion protein has been generated which makes it possible to observe autophagosomes by immunofluorescence and it has been confirmed that ectopic GFP-LC3 does not interfere with endogenous autophagy [85]. GFP-LC3 transgenic mice have also been created and used to show that autophagy takes place in most tissues as a result of starvation [88].

1.11. Autophagy inhibitors and activators

Autophagy plays a role in human disease including neurodegenerative diseases and cancer, and investigating the role of autophagy in these diseases is very important as it may be a useful therapeutic target. However, as discussed in section 1.10 methods available to monitor autophagy are limited and have drawbacks, which means it is informative to enhance or block autophagy and observe the effects on cellular processes to understand more completely the role of autophagy in disease processes.

Some inhibitors such as bafilomycin function by inhibiting vacuolar type H (+) ATPase and therefore acidification of the lysosomes and endosomes [79]. There is also some evidence that bafilomycin prevents fusion between autophagosomes and lysosomes which means that the content of the autophagosome cannot be "digested", as acidification of the luminal space of the autophagosome cannot take place [89]. This leads to autophagosome accumulation which can be observed by electron microscopy in combination with specific dyes for acidic cellular compartments [89]. Others, such as 3-methyladenine (3-MA), which was the first autophagy inhibitor to be identified and is the most widely used, functions by inhibiting class III PI 3 kinase, which has a vital role in autophagosome formation in mammalian cells [79]. Other, less frequently used autophagy inhibitors include the protein biosynthesis inhibitor cycloheximide, which also inhibits segregational steps which take place just before autolysosome formation and compounds which impair lysosome function by alkalysing lysosomes, such as chloroquine, and hydroxychloroquine [79].

There are also a number of ways in which autophagy can be activated experimentally, for example through depleting cell media of amino-acids, or through use of the mTOR inhibitor rapamycin and its derivatives, which inhibit the kinase activity of mTOR through formation of a complex with the FKBP12, which stabilises raptor-mTOR association [90]. Other autophagy activators include trehalose, an mTOR independent autophagy activator, inositol monophosphatase (IMPase) inhibitors, which cause depletion of free inositol, and class I PI3 kinase inhibitors such as such as acetyl-D-sphingosine [79].

Although chemical activators and inhibitors of autophagy are useful tools for investigation of the autophagy process and its functions, most chemical inhibitors are not entirely specific, so genetic intervention is a useful alternative [79]. The ATG genes which are essential for autophagy can be deleted, or knocked down through use of RNAi [79], and microRNAs (small RNA molecules that post-translationally modify mRNA and therefore influence gene expression) such as miR-30a have been shown to down-regulate expression of Beclin-1 and ATG-5, therefore inhibiting autophagy [91].

1.12. Recognition of protein acetylation sites by bromodomain containing proteins

The balance of lysine acetylation in cellular proteins is controlled by the action of HATs which mediate acetylation, and HDACs which carry out deacetylation, as described in sections 1.1 and 1.2. The acetylated lysines are in turn recognised and bound to by bromodomain-containing proteins, and this "reading" is key in the regulation of chromatin control. Acetylation also occurs on a variety of non-histone proteins with different biological functions, such as chaperone proteins, glycolytic enzymes and cell cycle proteins [92], and these acetylated proteins frequently function in pathways that may contribute to oncogenesis.

ε-N-lysine acetylation is specifically recognised by bromodomain protein modules. There are 46-bromodomain containing proteins in the human genome, of which 11 are cytoplasmic and the remainder are located in the nucleus, where they recognise acetylated histones, and other nuclear proteins, such as p53 [93]. A number of three-dimensional structures of bromodomain proteins from various organisms have been determined in-solution and by crystallography, and it appears that bromodomains adopt a conserved structural fold of a left-handed four-helix bundle, with a flexible loop to enable the dynamic nature of the acetyl-lysine bundle, and a conserved asparagine, which hydrogen-bonds to the acetylated lysine [94]. Sequence-specific recognition of residues surrounding the acetylated lysine is made possible by the flexible ZA and BC loops surrounding the conserved acetylated-lysine [94].

Biological functions of bromodomain-containing proteins are primarily concerned with regulation of gene expression. Examples include chromatin remodelling through nucleosome displacement, which leads to recognition of target promoters

by transcription factors [94], and coupling of histone acetylation to transcription by BRD2 and BRD3, which associate with histone H4 modifications and thus allow RNA polymerase II to transcribe through nucleosomes [95]. There are still many human bromodomain proteins which do not have well-characterized functions.

Genetic rearrangement and overexpression of bromodomain protein have been linked to tumour development, for example BRD4-NUT (nuclear protein in testis) rearrangement blocks cellular differentiation and is frequently found in aggressive poorly differentiated carcinomas of the head or neck, due to recruitment and activation of the CBP/p300 HAT by BRD4-NUT, which leads to p53 inactivation [96, 97]. Inhibition of BRD4-NUT through use of a competitive inhibitor has led to tumour shrinkage and survival in BRD4-NUT xenograft mice and RNAi depletion of BRD-NUT results in cell cycle arrest [98]. Bromodomain proteins also serve as targets for treatment of inflammation and neurological disorders, as well as cancer [99]. Bromodomains present a particularly attractive target for inhibition of protein-protein interaction due to their relatively weak interaction with their substrate, and the large number of available crystal structures which enables rational design of inhibitors [99].

1.13. Need for personalized cancer treatment

Having discussed the histone deacetylase family and the effects and cellular outcomes of treatment with inhibitors of these enzymes, the broader view of cancer treatment will now be considered, in terms of the necessity for personalized therapy development. This may be achieved through identification of biomarkers for certain drug classes, with histone deacetylase inhibitors being of particular interest for this project.

Personalised medicine is a broad concept which refers to the utilisation of unique patient characteristics such as clinical, genetic, and environmental state in order to improve and ensure the most efficient medical care for each individual both in treatment, early stage detection and disease prevention [100]. This approach is becoming possible thanks to advanced molecular understanding of disease and enables patient stratification from a diverse group into those that are likely to benefit from the treatment and those who will not (Figure 1.4). Personalised medicine in its application to cancer relates specifically to the transition from treatment with broadly acting cytotoxic drugs to the use of more specific, targeted therapies which are selected individually for each patient. An expanding group of cancer drugs have now been approved as “personalised therapies”, and are used in treatment depending on presence of a certain genetic events.

Personalized medicine is needed because of the frequent variable response to standard cancer therapy, even in cases where patients have the same diagnosis, as indicated in Figure 1.4. An example of variable response to standard cancer therapy is post primary-tumour resection, which may be sufficient to be curative, depending on how malignant the primary tumour is. In some, but not all, cases

aggressive systemic therapy such as chemotherapy is required to remove any remaining tumour cells, which is known as adjuvant therapy [101].

Figure 1.4

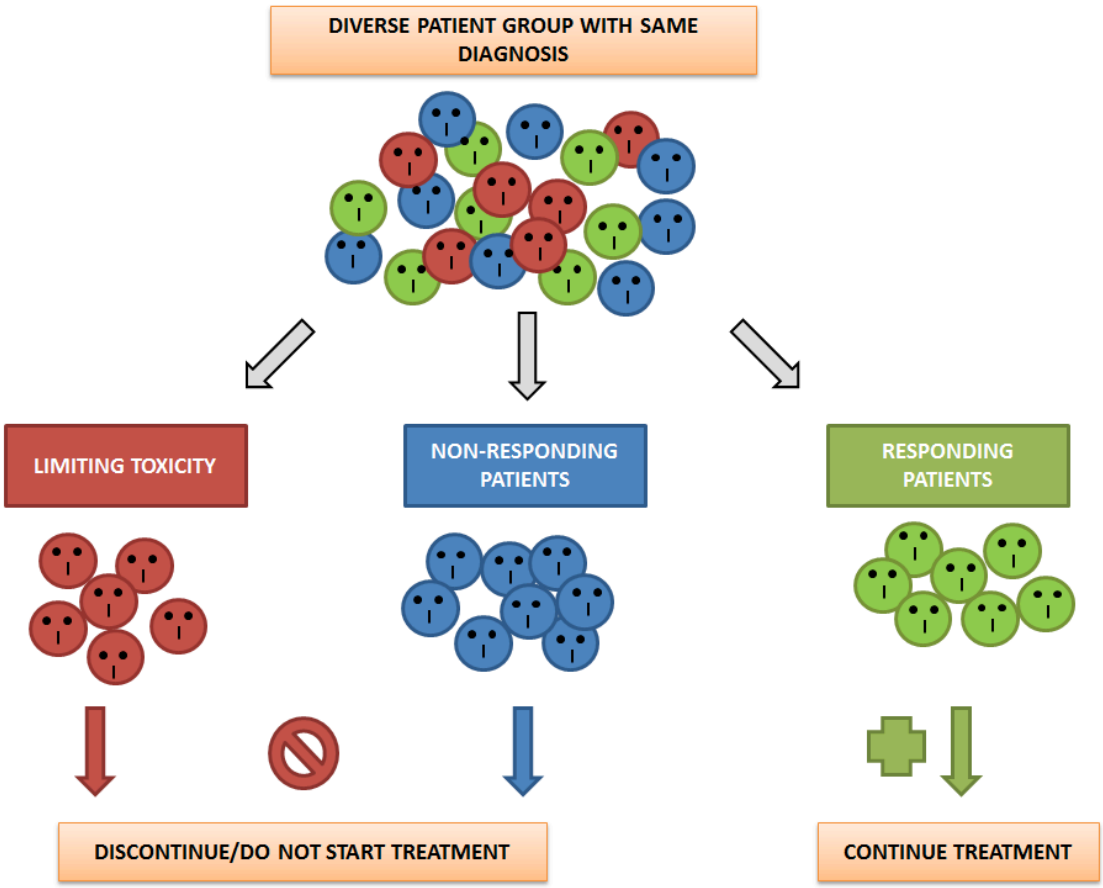

Schematic representation of a diverse patient group which have the same diagnosis, but may respond differently to treatment (adapted from Olzscha et al, 2013)

Such variable therapy response is a key issue which frequently arises during cancer treatment. For example, colorectal cancer is most commonly treated with combination therapy including 5-fluorouracil prior to surgery, however there is variability in survival rate of patients even in cases where the initial clinical stage is the same [102]. A study of 148 such patients with stage II/III colorectal cancer showed that tumours are more responsive to treatment when they express wild-type KRAS, and less responsive if they express mutant KRAS [102]. KRAS is a signalling protein necessary for growth, and its mutation leads to resistance to targeted therapies through persistent activation of the KRAS signalling pathway including focal adhesion kinase and mitogen activated kinase, which leads to faster tumour growth and metastasis formation [102].

Another example of such variability in therapy response, and its impact on patients is a result the analysis of 18000 young female patients with early stage lymph-node negative breast cancer, in which tumour removal and localised radiotherapy alone results in recurrence in 20-30% of cases, but it is not possible to predict which patients will relapse [103]. Therefore, up to 95% of such patients receive chemotherapy as additional treatment, which has many toxic side effect and causes unnecessary patient suffering in the 70-80% of women for whom tumour removal and localised radiotherapy would have been sufficient [103]. Studies such as the two presented above emphasize the need for development of personalized cancer therapy where only the subset of patients which will benefit from the treatment receive it.

An important factor which contributes to such variable response to treatment is the heterogenous nature of tumours. A crucial role in tumour development is played by constituents of the tumour microenvironment, which

include the extracellular matrix (ECM), as well as stromal endothelial cells, adipocytes and macrophages [104]. The ECM refers to all molecules immobilised outside cells, many of which influence tumour progression and treatment. Failure and resistance of tumours to cancer therapy is likely to be at least partially due to the differences between patients in components of the tumour microenvironment, such as varying secretion of hepatocyte growth factor by non-cancerous stromal cells, which leads to activation of MAPK signalling pathways in cells nearby, resulting in accelerated tumour growth and treatment resistance [105].

Patient derived tumour xenografts have been grafted into immune-deficient rodents as an model for the tumour microenvironment as part of preclinical studies, which retain histological features of the parent tumour [106]. Such studies have been used to validate KRAS mutation as a predictive biomarker which leads to cetuximab-resistance in colorectal cancer tumours [106].

The maitrix metalloproteinase (MMP) group of enzymes are upregulated in many cancer types, and this upregulation differs between tumour subtypes and patients [107]. MMPs are zinc-dependent endopeptidases which are present in the ECM, and some of these enzymes are secreted by tumour stroma cells, whereas others are produced by cancer cells [107]. MMPs are thought to contribute to cancer progression by carrying out proteolysis of growth factor precursors to result in growth factor release and degradation of structural ECM components to enable greater cancer cell migration [107]. For example, xenograft experiments have shown that when the level of the MMP stromelysin-3 is increased, tumours in nude mice are established and tumour cell apoptosis is reduced [108].

Subsequent studies showed that MMPs levels can act as cancer treatment biomarkers, such as MMP-9 levels in breast cancer tumour tissue indicate therapy

response and tumour recurrence [109], although clinical trials targeting MMPs have not been successful [107].

Interestingly, recent studies have shown MMPs to act as tumour suppressors rather than metastasis promoting enzymes [110], such as the inhibition of human melanoma progression by wild-type MMP8 [111], and the association of this enzyme with improved survival in tongue cancer [112], indicating the complex role of extracellular matrix components in cancer progression.

1.14 Biomarkers in personalized cancer treatment

Biomarker identification typically requires molecular disease diagnosis. This term refers to the measurement of gene modification and expression, rather than conventional disease diagnosis, which is based on distinguishing tumour stages through observation of microscopic cell morphology. During molecular disease diagnosis, microarrays can be used to determine messenger RNA levels to indicate gene expression levels, which can be correlated with various tumour traits [103].

The three types of biomarkers that assist development of personalized cancer treatment are: prognostic, predictive and pharmacodynamics. A prognostic biomarker anticipates the clinical outcome of an illness which helps elucidate whether further treatment will be needed, and a predictive biomarker indicates the likelihood of response to the treatment given. The effect of disease therapy can be measured by using a pharmacodynamic biomarker, and this effect can also be correlated with a clinical endpoint. In the case of histone deacetylase inhibition treatment, an example of a pharmacodynamic biomarker would be histone acetylation, whereas for kinase inhibition this would be phosphorylation level of the enzyme substrate [113].

As an example of a prognostic biomarker, a gene-expression signature of 70 genes (including genes regulating tumour invasion, metastasis, cell cycle and angiogenesis) can be used to classify primary breast adenocarcinoma into high-risk and low-risk, through correlation of the gene expression signature with the time until metastasis at distant sites from the initial tumour appear [114]. This 70 gene signature has been validated in large independent tumour sets [114] and is commercially available as MammaPrint (Agendia) (www.agendia.com).

Interestingly, another 76 gene signature as a breast cancer metastasis marker has been obtained by a similar method as the one above, but by a different research group, which had only 3 genes in common with the 70 gene signature [115]. A reason for this may be the wide range of different genes that result in expression of proteins which participate in the same biological process.

An example of a gene expression signatures acting as a predictive biomarker is transcription signature of cancer-related genes (measured in tumour tissue biopsies) Onco*type* DX® Test (www.oncotypedx.com), which predicts recurrence of stage II and III breast and colon cancer.

A key example of predictive biomarker, which relates to drug response is mutation in the catalytic domain of BCR-ABL (breakpoint cluster region - Abelson murine leukaemia viral oncogene homologue) which correlates with resistance to imatinib treatment [116]. Another example of a predictive biomarker is HER2 which correlates with poor prognosis and is over-expressed in around 25% of breast cancer patients [117, 118]. Other examples are breast cancer susceptibility genes BRCA1 and BRCA2 (breast cancer 1 and 2), which, when mutated, enhance cancer susceptibility and response to PARP inhibitors [119, 120], and code for proteins which are components of the homologous recombination (HR) DNA-repair pathway.

A large proportion of biomarkers that have proved to be useful in the clinic have been identified through retrospective analysis of clinical trial data. Recently developed molecular tools should allow identification of biomarkers through top-down prospective- driven approaches [121]. An example of a biomarker revealed by such a screen-driven approach is HR23B (human UV excision repair protein RAD23 homolog B), which is involved in DNA repair and shuttling proteins to

the proteasome [15], and acts as a sensitivity determinant to HDAC inhibitor treatment. Further investigation showed that HR23B governs the sensitivity of CTCL (cutaneous T cell lymphoma) cells to HDAC inhibitors [41]. These cell-based findings are supported by a recent clinical study using the HDAC inhibitor belinostat for patients with unresectable hepatocellular carcinoma, where a relationship between HR23B and clinical response was reported [122]. The screen used to identify HR23B and its other outcomes will be discussed in greater detail in section 1.14.

1.14 Biomarkers for HDI treatment and their identification by genome-wide shRNAscreen

Although the mechanisms and pathways through which HDI treatment inhibits tumour cell proliferation are still not fully understood (see section 1.6), it is known that certain tumour types are more responsive to HDI treatment than others. In particular haematological malignancies such as CTCL undergo a more favourable response to HDI treatment. However, as mechanisms through which HDI exert anti-proliferative effects and give rise to different biological outcomes remain to be determined, the process of potential biomarker identification to predict tumour response on HDI-based treatment has been hampered.

One of the ways in which potential sensitivity determinants and insights to the mechanism of HDI anti-tumour activity have been discovered is through a genome-wide loss-of-function screen performed in our research group with the aim of identification of genes governing sensitivity of cells to HDI treatment. An shRNA library targeting the vast number of genes involved in human cancer was used to silence these genes effectively over a prolonged period of time under conditions of SAHA treatment [15] (see figure 1.5). Silencing genes required for HDI-induced apoptosis allowed cells in which such a gene is silenced to survive and then be isolated. Cells were allowed to grow for 25 days under conditions of 2μM SAHA and transfection with the pRETRO shRNA library and surviving colonies were isolated, after which the gene silenced in each particular colony was validated [15].

Figure 1.5

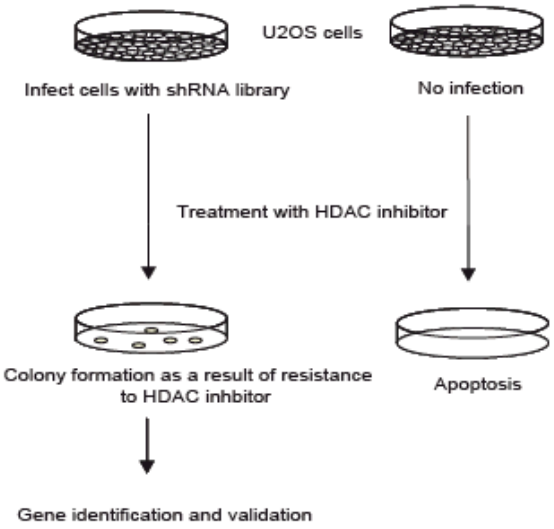

Schematic of shRNA screen (adapted from [106]). U2OS cells were transfected with a library targeting a large number of genes involved in human cancer alongside an untransfected control. The cells were then treated with the general HDAC inhibitor SAHA at 2μM and allowed to grow for 25 days. The colonies which survived where those in which a potential SAHA sensitivity determinant gene was silenced.

After the genome-wide screen was completed, the initial follow up investigation was focussed on the HR23B protein. The fact that the shRNA sequence used in the screen does reduce the level of HR23B protein was confirmed by immunoblotting [15]. The function of HR23B as a sensitivity determinant to HDAC inhibition was validated in mouse embryonic fibroblasts (MEFs), which were HR23B -/- and HR23B +/+ and the latter were more sensitive to HDI-induced apoptosis [15]. It was also shown that the HR23BA form of HR23B has no role in HDI-induced apoptosis, and that the role of HR23B in nucleotide excision repair [123] is not the HR23B-dependent mechanism through which HDAC inhibitors induce apoptosis. This was established by treatment with SAHA of XP4A cells which carry a defective XPC gene and thus exhibit low NER activity, which were as sensitive to SAHA as control U2OS and M2C5 fibroblasts in which NER activity was normal [15].

The genome-wide loss-of function screen identified a number of proteins other than HR23B which act as sensitivity determinants for HDI-based therapy [15]. One of these was Myd88 (Myeloid differentiation primary response gene 88), an adaptor molecule for Toll-like receptors (TLRs) and interleukin (IL)-1 receptor [124], as summarised in the signalling pathway in Figure 1.7) and discussed in more detail in section 1.16.

1.15. Established roles of HR23B.

HR23B has at least two cellular roles: Nucleotide excision repair (NER) [123] and the targeting of ubiquitinated proteins to the proteasome [125]. HR23B involvement in NER does not affect its function in sensitizing HDI treated cells to apoptosis [15]. However, further studies indicated that the protein shuttling activity of HR23B is partly responsible for aberrant proteasome activity displayed by HDI-treated tumour cells [15, 41], which is likely to underpin the role of HR23B as an HDI sensitivity determinant. A simplified domain structure of HR23B is shown in Figure 1.6; it is the ubiquitin-like domain (UBL) in HR23B which interacts with the proteasome, whereas two ubiquitin-associated domains (UBA) interact with the ubiquitinated substrate proteins thus allowing HR23B to shuttle proteins to the proteasome for degradation [126].

Increased HR23B association with the proteasome and aberrant proteasome activity has been shown in HDI treated cells [15], which suggests the role of HR23B in transporting proteasomal substrates is important in HR23B-mediated apoptosis. Depletion of HR23B allowed cell proteasomal activity to return to normal, confirming that HR23B has a direct influence on protein turnover mediated by the proteasome [15]. Although aberrant proteasome activity was shown to be a consequence of HR23B activity, it was not completely clear at this stage how apoptosis is mediated through HR23B as a result of HDI treatment.

The role of HR23B as a sensitivity determinant to SAHA treatment has since been evaluated not only by siRNA depletion of HR23B ([15]), but by ectopically increasing levels of HR23B in an inducible U2OS cell line [41], which correlated with an increased rate of cell death on HDI treatment, as shown both by FACS analysis and PARP cleavage. The sensitivity determinant role of HR23B was also

confirmed in CTCL cells [41], which is of more clinical relevance then previous experiments in U2OS cells, as SAHA has been approved for use in CTCL by the FDA. Proteasome activity was measured in CTCL cells using a fluorigenic substrate which was cleaved as a result of proteasome activity, in combination with HDI treatment and HR23B depletion, and it was shown that under conditions of HR23B depletion, HDI treatment no longer causes a decrease in proteasome activity, indicating that proteasome activity is influenced by HR23B during HDI treatment [41].

HR23B has been found to be a promising predictive biomarker in a study of 65 CTCL patient biopsies from a phase II clinical trial of SAHA, whereby HR23B expression was monitored and correlations with clinical response was observed [41]. Although the number of biopsies is limited, a statistically significant coincidence was seen between high HR23B levels and clinical response to HDI treatment. It was encouraging to see a positive predictive value of 71.7%, which indicates a much higher chance for a CTCL patient with high tumour HR23B levels to undergo clinical benefit on HDI treatment than the existing frequency of response in patients without biomarker utilisation [41].

To summarise, prior to the start of this project, it has been established that HR23B levels are important in determining cell fate on SAHA treatment and that the proteasome is important in HR23B-mediated cell death, but it remained to determined exactly how and why some cells undergo apoptosis on HDI treatment where as others escape this fate, and what cellular processes regulate the levels of HR23B.

Figure 1.6

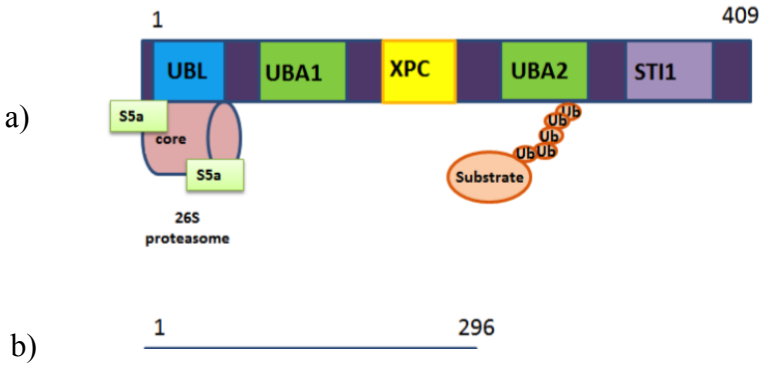

a) Domain structure of HR23B, showing the ubiquitin-like (UBL) and two ubiquitin-associated (UBA) domains. The UBL domain is shown bound to the 26S proteasome subunits, and the UbA domain is bound to a ubiqutinated substrate. The XPC domain refers to the region of HR23B which binds to its nucleotide excision repair partner, XPC [1]. STI1 is a heat shock chaperonin binding motif (www.uniprot.org).

b) Domain structure of Myd88 showing the death domain (DD), intermediate domain (ID) and Toll-like receptor interacting (TIR) domains. The death domain binds to the death domain of IRAK1 and IRAK4 to activate subsequent signalling pathways, and the TIR is shown bound to a Toll-like receptor. Myd88 dimeriation is likely to be mediated through its intermediate domain and its death domain, but not its toll-like receptor interacting domain[4].

1.16. Role of Myd88 in Toll like receptor (TLR) signalling

TLRs are found in a number of cellular compartments, and their localisation depends on their function. TLRs that recognise protein and lipid membranes of pathogens are localised on the plasma membrane (TLR1, 2,4,5,6), whereas those which recognise viral protein are located on the endolysosomal compartment (TLR 3,7,9) [127]. They function through one or more of the four adapter proteins: Myd88, TICAM1, TIRAF and TICAM2 [127]. Myd88 has been shown to be essential for all TLR family members except TLR3 to create the downstream inflammatory response [128]. Myd88 deficient mice are unable to respond to lipopolysaccharide (a ligand for TLR4) in terms of cytokine production or B cell proliferation, although the NF-κB pathway and MAP kinase activation were not affected, which means that the role of Myd88 is not simply due to lack of activation of MAP kinases or NF-κB [129]. Similarly, such mice were not able to respond to the TLR2 ligands peptidoglycan or lipoprotein, or the TLR9 ligand CpG DNA. They were also unable to produce IL-6 in response to the TLR5 ligand flagellin which indicates that Myd88 is essential for inflammatory responses mediated by all TLR family members [129].

As shown in the figure with the simplified domain structure of Myd88 (Figure 1.6), Myd88 has a toll-like receptor interacting (TIR) domain in its C-terminal region and a death domain (DD) in its N-terminal. Myd88 dimerisation is likely to be mediated through its intermediate domain and its death domain, but not its toll-like receptor interacting domain[4]. Myd88 is associated with the TLRs through its TIR domain and, during stimulation it recruits the IL-1 receptor-associated kinase (IRAK) through interaction of the death domains of both proteins. Once

IRAK is recruited to TLRs, it is phosphorylated which activates it; and associates with TRAF6. This causes activation of two distinct signalling pathways, as shown schematically in Figure 1.7.

TLR simulation leads to activation of a number of signalling pathways, including NF-κB, MAP kinases, p38, interferon regulator factor, and JUN N-terminal kinases (JNKs). These are all needed for the orchestration of the adaptive and innate immune responses [127].

In addition, TLRs have been shown to regulate cell death, both positively and negatively. TLRs can induce cell-autonomous apoptosis through TICAM1, FADD and caspase 8 during bacterial and viral infection, but they can also promote cell survival through activation of the PI3K-Akt signaling pathway [127].

Inflammation and TLR signaling in particular has been shown to have a role in tumourigenesis. TLR agonists such as lipopolysaccharide (LPS) have been shown to have anti-tumour activity [130]. This may be due to various mechanisms, including TLR activation causing apoptosis of tumour cells directly, and through stimulation of the adaptive immune system which will no longer tolerate tumour self-antigens [127]. TLRs may also reduce changes of tumourigenesis by preventing infection with pathogens that are associated with cancer development, such as the human papilloma virus and *Helicobacter pylori* [127]. On the other hand, TLR activation has also been shown to drive tumourigenesis, during studies where adoptive transfer of a tumour or a tumour cell line was followed by LPS administration, which caused increased survival and proliferation of tumour cells [127].

One of the key outcomes of TLR signalling is release of inflammatory cytokines [131]. It is important however, to keep in mind the distinction between inflammation which induces cancer, and cancer-induced inflammation [127]. Tumour promotion and progression is associated with the production of inflammatory mediators including cytokines, and recruitment of macrophages, with consequent processes such as neoangiogenesis and tissue remodelling [127]. Cytokines are proteins that regulate the growth, activation and differentiation of tumour cells, and they can be secreted or membrane-bound. Local cytokine expression is likely to change during tumourigenesis and cytokines produced in the tumour microenvironment have important roles in cancer pathogenesis [132]. A number of cytokines and growth factors are important during repair of damaged tissue and removal of apoptotic cells. Some of these such as interleukin-1β are proapoptotic where as others (e.g. transforming growth factor-β are antiapoptotic) [12].

1.17. IL-6 functions

IL-6 is one of the cytokines released as a result of NF-κB signalling, and affects a variety of biological functions related to inflammation. Its known roles are primarily prosurvival and protumourigenic. IL-6 binds to membrane bound or soluble IL-6 receptors, which in turn interact with the membrane-associated ubiquitous GP130 signal transducer unit, which leads to JAK (Janus kinase) activation through phosphorylation, leading to recruitment of adapter molecules [133]. Downstream effects of this signalling pathway include Stat3 (signal transducer and activator), Shp2-Ras, and phosphatidylinositol 3-kinase (PI3K)-Akt [133] activates the Ras-raf-Erk pathway, that leads to T cell survival, which can cause inflammation through continuous production of growth factors and cytokines. Other roles of IL-6 include tissue homeostasis and regeneration. Although IL-6 is predominantly known as a cytokine which has a role in proliferation and protection from cell death, there has also been evidence of an "inverse" role for IL-6, whereby IL-6 enhances Fas-induced apoptosis in normal lung fibroblasts [12]. This pro-apoptotic effect of IL-6 was likely to be through upregulation of the pro-apoptotic protein Bax, through a STAT-3 dependent mechanism, which causes a low Bcl-2-Bax ratio [12] The Bcl-2 family of proteins consists of members which suppress and activate apoptosis, and it is the balance of the levels of these pro- (Bax) and anti (Bcl-2) apoptotic proteins which determine if a cell undergoes apoptosis or survives. If the expression of these proteins is altered through an aberrant signaling pathway during tumourigenesis, it can cause a cell to be resistant to apoptosis.

Figure 1.7

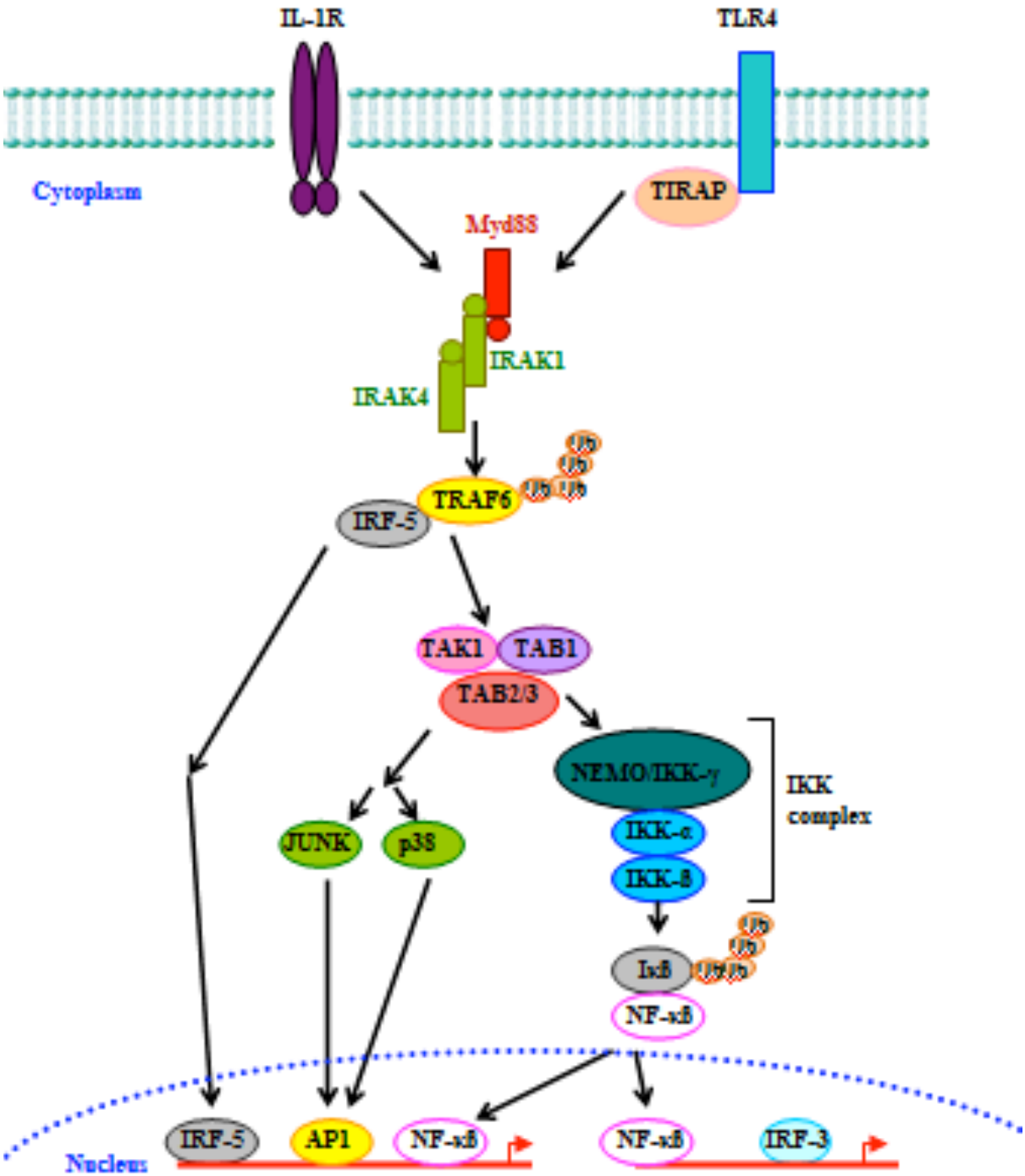

Schematic diagram indicating the role of Myd88 as an adaptor protein in Toll-like receptor (TLR) and IL-1R (interleukin 1 receptor) signalling (adapted from [2] and [5]). Stimulation with their ligands recruits adaptors such as Myd88 and TIRAP which leads to formation of a complex of IRAKs, followed by TRAF6 and IRF-5. TRAF6 is an E3 ubiquitin ligase and causes formation of polyubiquitin chains on TRAF6 itself and NEMO, which activates the TAK1 complex, which in turn carries out phosphorylation of NEMO and IKK complex activation. Phosphorylated Iκß becomes ubiquitinated and degraded, and free NF-κß enters the nucleus, where it initiates transcription of proinflammatory cytokine genes [5]. These genes are also induced through TAK1, which activates the MAP kinase cascade (involving JNK and p38).

1.18. Myd88 in Ras signalling

Myd88 appears to have other roles, which are not dependent on its role in TLR signalling which has been described above (1.16), in particular during Ras signalling. Cell growth, proliferation and differentiation is regulated by the mitogen-activated protein kinase (MAPK) pathway which is aberrantly activated in a number of cancers via mutations in proteins along the Ras-Raf-MEK-ERK pathway [7], summarised in Figure 1.7. MAPK pathways link extracellular signals to a three-tier kinase system where the first MAPK is phosphorylated and activated by a MAPKK (MAPK kinase), which is activated by phosphorylation by MAPKKK. Six groups of MAPKs have been characterized in mammals: extracellular signal-regulated kinase (ERK)1/2, ERK3/4, ERK5, ERK7/8, Jun N-terminal kinase (JNK)1/2/3 and the p38 isoforms α/β/γ (ERK6)/δ [134]. The ERK pathway is deregulated in about a third of human cancers and responds to many extracellular signals such as growth factors and mitogens, which result in activation of receptor tyrosine kinases which then trigger guanosine triphosphate (GTP) binding to the Ras GTPase which then recruits Raf kinases for activation [134], as summarised schematically in Figure 1.7. Activated Raf then phosphorylates specific serine residues in MEK1 and MEK2 (MAPKs) kinases which in turn activate ERKs that phosphorylate many cytoplasmic and nuclear proteins including transcription factors, resulting in regulation of diverse cellular processes [134].

Myd88 activates the Ras signalling pathway by preventing inactivation of the MAP kinase Erk by its phosphatase MKP3, through a mechanism where Myd88 is bound to Erk by the same motif which would usually bind to MKP3 [10]. These

finding are made particularly relevant to cancer cell transformation by the fact that Myd88 has been found overexpressed and interacting with Erk in primary human cancer tissues [10].

The role of Myd88 in Ras/Erk signalling seems essential for survival of colon cancer cells and is required for expression of DNA repair enzymes in colon cancer cells [135]. When Myd88 levels are reduced in colon cancer cell lines through RNA interference these cells are sensitised to DNA damaging agents such as cisplatin, and cell death takes place via p53 [135].

Figure 1.8

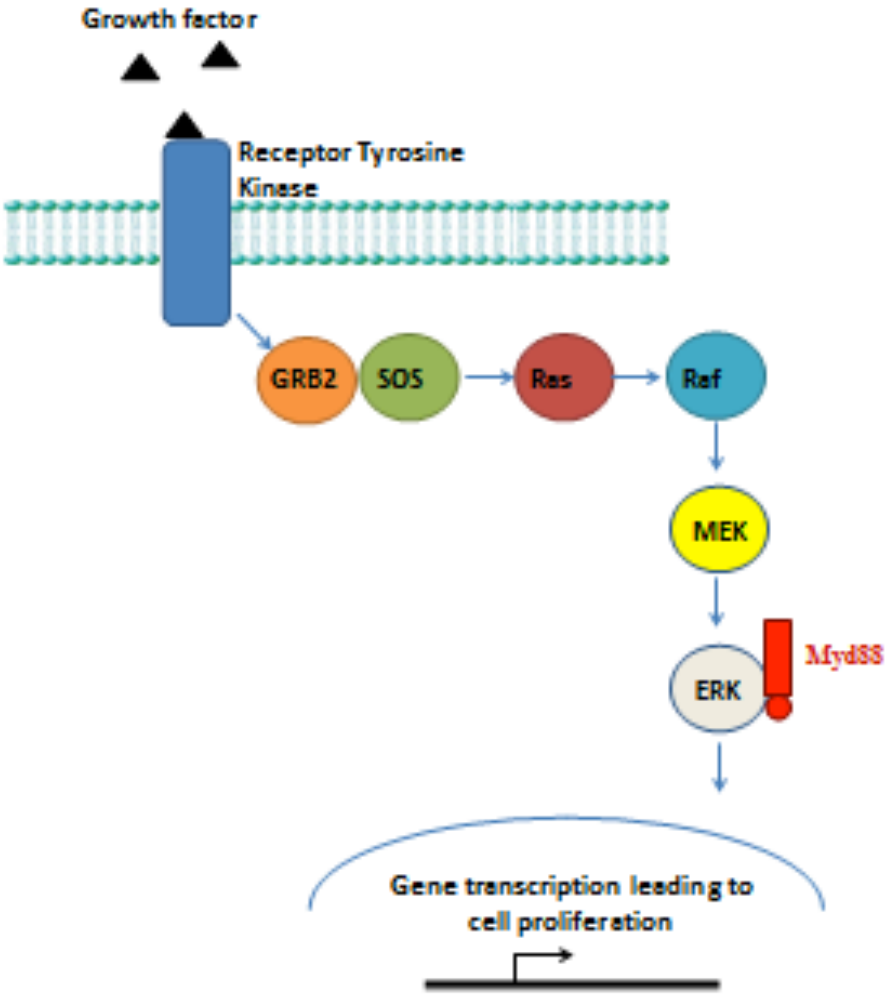

Summary of the Ras signalling, where Myd88 also plays a role, by binding to the activated form of the MAP kinase ERK and preventing its inactivation by its phosphatise MKP3 (adapted from [7] and [10]).

1.19. Myd88 and HDAC6

As Myd88 has been identified in a shRNA screen for sensitivity determinants to HDAC inhibitors, it is of interest to consider which HDAC(s) may be responsible for these effects. Myd88 is a cytoplasmic protein and the only HDAC with primarily cytoplasmic localisation is HDAC6, which has an established role in the deacetylation of cytoplasmic proteins, including alpha-tubulin [35].

Interestingly, HDAC6 has been shown to have a role in Myd88 signalling. HDAC6 is required for Myd88 aggregation together with sequestosome 1 (SQSTM1, also known as p62) [124]. Both SQSTM1 and HDAC6 have a role in the transport of Lys^{63}-linked polyubiquitinated proteins to form aggregates, which are degraded by autophagy (this is an example of the selective degradation capacity of autophagy) [136]. It has been shown that Myd88 is involved in this process, by recruiting SQSTM1 and HDAC6 as a step in aggregate formation, although the biological significance of aggresomes for cell signal transduction is not fully understood [124]. Myd88-dependent signalling has been shown to be dependent on both SQSTM1, and HDAC6, and the latter regulates the recruitment of the ubiquitin E3 ligase TRAF6 (tumor necrosis factor (TNF) receptor-associated factor 6), which then participates in a signalling cascade resulting in activation of NF-κB and transcription of genes coding for proinflammatory mediators [124].

These findings are of interest for the current study, one of the aims of which is to elucidate the role of Myd88 in response to HDI treatment, as it suggests that

HDAC6 may be the histone deacetylase which regulates Myd88 during the HDI response, which warrants further investigation.

1.20. Role of Myd88 in cancer

The genome-wide loss-of function screen [15] identified a number of proteins other than HR23B which act as sensitivity determinants for HDI-based therapy, although only HR23B was investigated in more detail during the initial follow-up investigation. One of the other identified potential biomarkers of interest that we decided could be of interest was Myd88 (Myeloid differentiation primary response gene 88), an adaptor molecule for Toll-like receptors (TLRs) and interleukin (IL)-1 receptor [124]. This initially seemed to be an interesting protein to investigate partly because of its established role in inflammation, which is shown to be of increasing importance during tumourigenesis.

The clinical relevance of Myd88 been demonstrated since the loss-of-function screen by the investigation showing that that it is frequently mutated in DLBCL [137], particularly the activated B-cell-like (ABC) subtype, which is the least curable form of this malignancy and in which 39% of cases carry the Myd88 mutation. RNA interference screening has also shown that Myd88 is essential for ABC DLBCL, and the L265P mutant particularly promotes cell survival and is a gain-of-function driver mutation. This is likely to take place via activation of the Toll-like receptor pathway which in turn causes activation of the NF-κB pathway [137], . High Myd88 levels have been shown to play a role in pro-tumourigenic transformation by interacting with the MAP kinase Erk, thus activating the RAS pathway [10]. Conversely, reducing Myd88 levels or inhibiting Myd88 function in murine mammary carcinomas slowed tumour growth rates [139]. This makes Myd88 an interesting potential biomarker to investigate.

1.21 Aims of project

The increasing interest in the use of HDI's to treat clinical malignancy and the lack of understanding of precise mechanisms by which they cause apoptosis has made it important to try to analyse what determines the cellular outcome upon HDI treatment, as well as identify sensitivity determinants for treatment with these drugs. The two potential sensitivity determinants identified by a shRNA genome-wide screen previously performed in the group were HR23B and Myd88 [15], and the initial aim of the project was to verify that pre-treatment levels of these proteins alter cell fate on HDI treatment. This was to be achieved by modifying the levels of HR23B and Myd88 through siRNA depletion, transfection and inducible cell line creation and observing the effects on cell fate after SAHA treatment. The next aim of the project was to identify mechanistically why levels of HR23B and Myd88 alter cell fate on HDI treatment, through investigation of the known roles of these proteins and determining whether these are important in cell fate outcome. In the case of HR23B, this is protein transport to the proteasome, and in the case of Myd88, this is the involvement of Myd88 in TLR signalling.

Previous studies have shown HDI (SAHA) treatment in cell culture causes both apoptosis and autophagy, and HDAC6 has been shown to have an important role in the latter. One of the directions of the project is to determine what factors are important to determine whether a cell fate on HDI treatment is autophagy or apoptosis. This is a direction which has potential for clinical relevance, as autophagy has been seen to be a means of avoidance apoptosis, and combination of autophagy inhibitors with HDIs has been shown to increase cell death levels [84].

In summary, the aim of this project is to investigate the roles of HR23B, Myd88, and HDAC6 on SAHA treatment, and how their levels and the pathways these proteins are involved in lead to various cellular outcomes on SAHA treatment, with apoptosis being of particular interest.

CHAPTER 2. MATERIALS AND METHODS

2.1 Cell lines

Cells were cultured at 37^{o}C in a humidified 5% CO_2 incubator. The cell lines U2OS, A549 WT and A549 HDAC6 KD were maintained in DMEM supplemented with 10% foetal calf serum (FCS) and 1% penicillin/streptomycin (Invitrogen). The inducible HR23B cell line was previously created by Susan Fotheringham in the La Thangue lab in U2OS cells using the Clon-tech TET-ON gene expression system, and the U2OS-TET-Flag-HDAC6, U2OS-TET-Flag-Myd88, U2OS-TET-Flag- K119R-Myd88 inducible cell lines were created by selecting cells transfected with Flag-HDAC6 or Flag-Myd88 inserted in a TET-ON gene expression system (Clontech).

The stable inducible cell lines ectopically expressing FLAG-HR23B, FLAG-Myd88, Flag-K119R-Myd88 and FLAG-HDAC6 were maintained in DMEM supplemented with 5% Tetracycline-negative FCS (PAA Laboratories), 100µg/ml G418 (Promega), 75 µg/ml hygromycin B (Invitrogen), and 1% pen/strep. Ectopic Flag-protein expression was induced by the addition of doxycycline (Dox) (Sigma-Aldrich) at 1µg/ml according to manufacturer's instructions, with subsequent addition of Dox every 24 hours.

The shRNA A549 HDAC6 WT and KD cells were a kind give from T.P. Yao (Kawaguchi et al, 2003). A retrovirus mediated pSUPER RNAi system (OligoEngine) was used to establish the A549 line expressing shRNAi for HDAC6.

2.2 Plasmids and transfections

Cells were transfected with 200ng - 5µg of plasmid using GeneJuice (Merck) according to the manufacturer's instructions. Cells were harvested 24-72 hrs after transfection.

The pcDNA-Flag-HDAC6, ΔBUZ and ΔN (439-1215) constructs were a kind gift from T.P.Yao ([37]). Ptre2-FLAG-HDAC6 was PCR-amplified from pcDNA-HDAC6 with the following primer combination: Forward (5'-GACGCGTGCTAGCATGACCTCAACCGGCCAGGATTC-3') and Reverse (5'-ACAAGCTTCATCGATTTATTTATCATCATCATCTTTATAATCC-3') and subcloned into the pTRE2 vector using Nhe1 and Cla1 restriction sites. BUZ was amplified from wild-type pcDNA-Flag-HDAC6 with the following primer combination: Forward (5'- CTACTAGCGGCCGCAATGACCTCAACACGC-3') and Reverse (5'-TAGTAGGCGGCCGCTTATTTATCATCATC-3'). The PCR products was then inserted into the pcDNA3.1 vector (invitrogen) via the restriction site Not 1 (following TSAP treatment of vector to prevent self-ligation), using the Liga Fast rapid DNA ligation system (Promega) to create a flag-tagged construct.

U2OS cells were transfected with synthetic siRNAs against HR23B; 2 (5'-UUGCAGCCCUGAGAGCCAG-3'), synthesised short hairpin siRNAs against HDAC6 (Dharmacon, M-00349900), Myd88 (Smart-pool Dharmacon) and non-targeting control N2 (Dharmacon) as indicated using oligofectamine (Invitrogen) to a final concentration of 50nM before harvesting.

2.3 Myd88 mutant derivative plasmids

The pCMV-Flag-WT Myd88 mutant derivative L265P was created using oligonucleotides designed in accordance with Stratagene's QuikChange Site-Directed Mutagenesis kit with the following primer combination: Forward (5'-CAGAAGCGACCGATCCCCAT -3') and reverse (5'-GATGGGGATCGGTCGCTTCTG-3').

The pTRE2-Flag-WT Myd88 mutant derivative K119R was created using oligonucleotides designed in accordance with Stratagene's QuikChange Site-Directed Mutagenesis kit, with the following primer combination: Forward (5'-CAAAAGTATATCTTGAGGCAGCAGCAGGAGGAG-3') and reverse (5'CTCCTCCTGCTGCTGCCTCAAGATATACTTTTG-3')

2.4 Drug Treatments

Cells were treated with compounds suberoylanilide hydroxamic acid (SAHA; Alexis Biochemicals), Tubastatin A (Chemietek), Bafilomycin (Millipore), 3-MA (Sigma-Aldrich), Puromycin (Sigma-Aldrich), bortezomib (Millenium), at the indicated concentrations and for the indicated times before harvesting. The proteasome inhibitor Z-Leu-Leu-Leu-al (MG-132) (Chemietek) was used at a concentration of 10 μM for 4 hrs unless otherwise indicated.

2.5 Antibodies

Details of primary and secondary antibodies

Antibody	Species/description	Source
FLAG-M2	Mouse monoclonal	Sigma Aldrich
cleaved PARP	Rabbit	Cell Signalling
acetylated histone H3	Rabbit	Fisher
acetylated tubulin	Mouse	Sigma Aldrich
actin	Mouse	Sigma Aldrich
HDAC6	Rabbit	Millipore
HR23B	Mouse	BD
LC3	Mouse	Nanotools
LAMP1	Mouse	Santa Cruz Biotechnology
Myd88	Rabbit	Cell Signalling
Myd88	Rabbit	Epitomics
HSP90 α/β	Mouse	Santa Cruz Biotechnology
Cleaved Caspase 3	Rabbit	Cell Signalling
His	Mouse monoclonal	Sigma Aldrich
Mono and poly	Mouse	Cell Signalling

ubiquitinated proteins		
Acetylated Lysine	Rabbit	Cell Signalling
Puromycin	Mouse	Santa-Cruz
Phospho-Chk1 (ser 317)	Rabbit	Cell Signalling
Chk1	Mouse	Santa-Cruz

2.6 Flow cytometry

Trypsin-harvested cells were fixed in 70% ethanol/PBS overnight at 4^{o}C and incubated for 30 min with 1x RNAseA and 20ng/ml propidium iodide (Sigma). Samples were run on a FACScan flow cytometer (BD Bioscience) and the analysis was carried out using CellQuestPro software and analysis was carried out using FACS Accuri C6 software. The percentage of cells in the sub-G1 phase of the cell cycle was used as an indicator of apoptosis.

2. 7 Immunoblotting and Immunoprecipitation

Cells were washed with 1 x PBS, harvested by scraping or trypsinisation and pelleted by centrifugation for 5min at 1000 *r.p.m* at 4°C, washed in PBS and lysed in 100 µl RIPA buffer (Tris 50mM, NaCl 150 mM, SDS 0.1 %, Na.Deoxycholate 0.5 %, Triton X 100, NP40 1%) for 1hr on ice. Extracts were centrifuged at 13,200 *r.p.m* for 10 mins to remove cell debri. Cell lysate was normalized (Bradford assay) and equal protein loading was confirmed with Ponceau S staining. For immunoprecipitation, cells were lysed in TNN buffer (50 mM Tris-HCl pH 7.3, 150mM NaCl, 5mM EDTA, 0.5% igepal (NP-40), 0.2mM Na_3VO_4, NaF 50mM and protease inhibitor cocktail (Roche)) for 1hr, and incubated overnight at 4^oC with the appropriate antibody, after which 30µl igG beads were added and incubated for 2h at 4^oC. The beads were washed four times with 1ml of TNN buffer, and boiled with SDS sample buffer containing 2-mercaptoethanol for 5 mins.

Protein concentration was determined using Bradford reagent (Bio-Rad), and unless otherwise indicated, equal amounts of total protein were used. Total protein was resolved by denaturing SDS–polyacrylamide gel electrophoresis before electrotransfer to polyvinylidene fluoride (PVDF) membrane and probed with antibody overnight at 4°C. Membranes were washed three times for 10 min with PBST (phosphate buffered saline/0.1% Tween 20). Membranes were incubated with corresponding secondary HRP-antibodies for 1hr30min at room temperature before washing three times with PBST as above and signal detection

using enhancen chemi-luminescence (Perbio). Representative blots from at least three experiments are shown.

2. 8. Immunofluorescence

Cells were seeded onto coverslips, which were washed in PBS and fixed in 3.7% formaldehyde for 15 minutes, then permeabilized in PBS containing 0.5% Triton X-100 for 5 minutes and then blocked in 5% FCS/PBS for 30 minutes at room temperature before incubation with primary antibody overnight at 4°C. Coverslips were then washed three times in PBS 0.05% Tween-20 and incubated with corresponding secondary antibodies for 30 min at room temperature: Alexa Fluro 488 (green fluorescence) or Alexa Fluro 594 (red fluorescence) (Molecular Probes). Finally coverslips were washed extensively in PBS 0.05% Tween-20 and mounted onto microscope slides using Vectashield containing DAPI (Vector Laboratories). Protein expression and localization was then visualized using a B202 light microscope (Olympus) and images were taken using OpenLab software (Improvision).

2. 9 Colony formation assay (CFA)

U2OS-TET-Flag-HR23B, U2OS-TET-Flag-Myd88 inducible cells or U2OS were seeded at 1000 cells/well in 6-well plates. Flag-HR23B or Flag-Myd88 were induced for 4 hours prior to 24hr of drug treatment as indicated. At 9 days post drug-treatment, cells were washed twice in PBS, fixed in methanol for 10min and stained with crystal violet solution for 30 min before extensive washing with water. The colonies were then counted.

2. 10 Immunohistochemistry pathology examination

Paraffin embedded formalin-fixed tissue slides were cleared of paraffin in histoclear (for 15 mins), and rehydrated through graded alcohol baths by incubation for 3min in 100% IMS twice followed by 70% IMS. After a rinse in water, sections were heated at 95 °C for 20 min in 1mM EDTA pH8 for antigen retrieval. Slides were incubated in 0.5% hydrogen peroxide for 15min, then washed in PBST for 5 min before being blocked in serum for 20 min. Slides were incubated in the primary antibodies overnight at 4 °C, followed by incubation with corresponding anti-HRP secondary antibodies, ABC reagent (Vector Laboratories) and then substrate (DAB; Vector Laboratories). Slides were placed in hematolysin (Sigma) for 60 seconds for nuclear counterstaining and then mounted on coverslips in AquaTex (Merck). Sections were examined under a light microscope.

2.11 Reporter assay

Cells were seeded in 60mm dishes and transfected with 200ng PCMV-β-gal and 200ng Bcl-xl reporter plasmids (the Bcl-xl reporter were a kind gift from Professor Neil Perkins, and created by Professor Ron Hay) and 1ug of relevant plasmid of interest as indicated. Cells were then treated as stated (in triplicate for each condition) and washed in PBS prior to harvesting by scraping in 300µl Reporter Lysis buffer (Promega). Eppendorfs with cell lysates were then centrifuged at 13,200 r.p.m for 2 min and 50 µl of each sample was transferred to a 96-well plate and processed with a WinGlo^{TM} 96 Microplate Luminometer (Promega) which automatically added 100 µl of Luciferase Assay Reagent (Promega) per well and recorded luciferase activity. Relative reporter gene activity was then calculated according to transfection efficiency indicated by β-galactosidase activity.

2.12. Cytokine level analysis

The levels of 6 cytokines involved in inflammation were analysed using a CBA (cytometric bead array) kit from BD biosciences. This system used antibody-coated beads with unique fluorescence intensities to capture proteins of interest (inflammatory cytokines). The unique fluorescence intensities of each of the six beads permit levels of several analytes to be simultaneously assessed and then measured using fluorescence detection by flow cytometry. Analysis was the performed with the FCAP Array v3.0 software which allows construction of a standard curve which unknown samples can be compared to giving cytokine concentrations in pg/ml.

2.13. Sample preparation for mass spectrometry analysis

Protocols adapted from Benedikt Kessler group website:

http://www.ndmrb.ox.ac.uk/protocols-and-tools

In solution digest

PCMV and Flag-Myd88 stable cell lines were seeded into P150 plates and harvested after 72 hrs at 80% cell confluence, washed in PBS and lysed in TNN (50 mM Tris-HCl pH 7.3, 150mM NaCl, 5mM EDTA, 0.5% igepal (NP-40), 0.2mM Na_3VO_4, NaF 50mM and protease inhibitor cocktail (Roche)) lysis buffer for 30mins, incubated with 60µl Flag-agarose beads (Sigma) and incubated with Flag peptide in 20mM Tris pH 7.4 at 4 C on a shaker for 1 hr for flag-tagged protein elution.

5 µl of the DTT reducing reagent (200 mM DTT in Tris buffer, pH 7.8) was added to the sample and incubated for 60 min at room temperature.

20 µl of iodoacetamide alkylating reagent (200 mM iodoacetamide in Tris buffer, pH 7.8) was added to the sample and the mixture was incubated for 60 min at room temperature. The protein sample was precipitated via Methanol / Chloroform Extraction.

During Methanol/chloroform extraction, sample was made up to 200 µl with MilliQ-H20, 600 µl methanol and 150 µl chloroform was added, sample was vortexed and 450 µl MilliQ-H20 was added. Sample was vortexed again, and centrifuged at room temperature 13,200rpm for 1min, after which upper aqueous phase was pipetted off and 450 µl methanol added to the sample containing the organic phase. Sample was vortexed and centrifuged room temperature 13,200rpm for 2 min, and supernatant removed.

Methanol/Chloroform extraction was performed twice after which 50 µl 6 M urea buffer was added and the sample was sonicated for 2 min. Urea concentration was reduced by diluting the reaction mixture with 250 µl MilliQ-H_20.
Elastase (0.2 µg/µl concentration) was added in a 1:50 ratio regarding the total protein content of sample, and digestion carried out overnight at 37 °C. Protein purification is carried out by "ZIP-TIP purification"

ZIP-TIP Purification

Sample was acidified by adding formic acid to a final concentration of 0.1%. "Ziptip" was equilibrated by aspiration of 10 µl of buffer B (65% CH3CN 35% MilliQ-H20) into the tip twice and disgarding it, after which Buffer A (98% MilliQ-H20, 2% CH3CN, 0.1% TFA or FA) was aspirated into the pip and dispensed into waste twice. 10 µl of sample was then aspirated and dispenced within the tip 10 times to bind proteins present, and dispensed. This was repeated until the entire volume of the sample had been passed through the tip 10 times. Zip tip was then washed with buffer A (10 µl) and bound proteins were eluted with 10 µl of buffer B into a new tube. Sample was then dried down in vacuum centrifuge and resuspended in 10 µl of buffer A prior to mass spectrometry analysis (Kessler Group).

2.14 Measurement of proportion of cells in S-phase by BrdU incorporation

10µM BrdU (from Becton Dickinson set, Cat. No. 550891) in PBS to the media of tissue culture dishes to be analysed 15 min before harvesting. Cells were harvested by trypsinization and fixed with 70% ethanol for 30 minutes. Cells were pelleted by spinning for 5min at 1000 rpm, and pellets were broken up and resuspended in 1ml denaturation solution **(**2N HCl, 0.5% Triton in PBS), then incubated at room temperature for 30 minutes, prior to another spin at 1000 rpm for 5 minutes. The cell pellet was then resuspended in 1ml neutralization solution **(**0.1M Na2B4O7·10H2O pH 8.5) and incubated for 30 minutes, after which the cells were pelleted again and resuspended in FITC-mouse Brd-Uantibody (from set Becton Dickinson Cat.no. 556028) solution (44µl blocking solution**(**1% BSA, 0.5% Tween 20 in PBS), 6µl AB) and left for 1 hour in the dark. 1ml PBS was added to the cells prior to a spin of 1000 rpm for 5 minutes, and resuspension in 0.5ml PBS containing 5µg/ml RnaseA and 10µg/ml PI. Cells were then left in the dark for 30 mins and analysed by FACS (cell quest Pro-software), where gating was carried out to select cells where BrdU was incorporated. A control where no BrdU was added to the cells at the start of the assay was essential to discriminate cells undergoing S-phase.

2.15 Measurement of translation levels in cells by puromycin incorporation

Cycloxehamide was added to control plates for 10min at a concentration of 100 μM to inhibit translation, and cells were placed back into incubator. All plates were then washed with PBS and media containing 1ug/ ml of puromycin was added, and cells were permitted to incorporate the puromycin during translation, prior to harvesting by trypsinization. Cells were then counted using the FACS Accuri, and immunoblotting was carried out as normal, except that each extract was loaded on the SDS-gel according to cell number in each treatment (rather than Bradford analysis) and anti-puromycin antibody was used to measure puromycin incorporation as an indicator of translation rate.

2.16 xCELLigence

5,000 cells/well were plated into E-plate 16. Experiments were carried out using the RTCA DP instrument (Roche Diagnostic GmbH, Germany) which was placed in a humidified incubator maintained at 37 °C with 5% CO_2. The electronic sensors provided a continuous and quantitative measurement of cell index in each well. Cell index is a quantitative measure of cell number present in a well e.g. lower cell index reflects fewer cells are attached to the electrodes. The E-Plate 16 was monitored over the time frame indicated.

Chapter 3. HDI TREATMENT RESPONSE AND HR23B

3.0 Introduction

Treatment of cells with pan-HDAC inhibitors such as SAHA causes a number of cellular outcomes other than apoptosis, including anti-angiogenesis, cell cycle arrest, aberrant DNA repair, protein degradation and autophagy (see Introduction section 1.5). Autophagy, or "self-digestion" in greek comes from the words "autos" – self and "phagos" – to eat. It is a process during which proteins and organelles are sequestered in intracellular membranes and delivered to the lysosome for degradation and has been associated with contradictory roles both in cell death, tumour suppression and cell survival. Under "normal" conditions, autophagy functions as a tumour suppressor pathway via degradation of damaged unnecessary cellular components. Indeed, mice that lack the essential autophagy gene, *beclin 1*, are more prone to tumour formation [140]. During starvation, autophagy functions as an important "recycling" process of cellular components such as amino-acids, although it can also act as a death signal in response to persistent stress ([141] and Introduction section 1.8).

However, once cancer has developed activation of the autophagy pathway may be utilized to generate ATP via protein recycling to overcome metabolic/hypoxic stress and maintain survival. Thus, autophagy may mediate cell death in response to cell stress such as chemotherapy in some circumstances, but it may in other cases be a mechanism of tumour cell resistance to HDAC inhibitor treatment. During cancer, the latter role of autophagy is considered more prevalent as it is generally regarded as a means of escape from apoptosis on HDI treatment, since it allows cells to gain ATP during hypoxia or nutrient deprivation, which are typical

tumour conditions [50]. In some cancer cells, autophagy-activation is a resistance-mechanism in response to apoptosis-inducing drugs, such as HDIs [142] and there is increasing evidence that tumour cells evade cell death through autophagy. This is exemplified by anti-cancer drug trials where chemotherapy drugs are combined with autophagy inhibitors such as chloroquine [143].

One of the aims of my project has been to investigate various cell fates on HDAC inhibitor treatment, and determine the reason as to what determines which cell fate a cell undergoes and why. During the initial part of my project, I focus on two cell fates: apoptosis, or cell death as a result of HDI treatment as once cell fate and autophagy as a means for tumour cells to "avoid" apoptosis. One of the ways in which the levels of apoptosis on HDI treatment can be measured is by observing Poly-ADP ribose polymerase (PARP) cleavage during immunoblotting. PARP cleavage is carried out by caspase protease into fragments of 89kDa and 24kDa during early stages of apoptosis, in particular by caspase 3[144] [145]. A useful way to measure cellular autophagy is to monitor by immunoblotting to observe conversion of microtubule-associated protein light-chain 3 (LC3) from the cytosolic form, LC3-I, to the autophagosome-associated form, LC3-II [58], as described in more detail in introduction section 1.5. LC3 is a protein which is immediately processed by mammalian Atg4s after synthesis and is present in the cytosol as LC3-I, but becomes converted into membrane bound LC3-II when autophagy is induced. LC3-II migrates faster than LC3-I on SDS gel, which makes it possible to measure LC3 conversion by immunoblotting. It is the level of the LC3-II fragment which gives an indication of the cellular level of autophagy [87].

A previous study performed in our research group identified a number of genes which are important for cell death to take place in response to HDI treatment and therefore have potential to act as predictive biomarkers for this type of treatment [15]. This genome-wide loss-of-function screen identified HR23B and Myd88 as two of the most important sensitivity determinants for HDI treatment. HR23B is a human homologue of the yeast (*S. cerevisiae)* Rad23B, which was initially identified as a component of nucleotide excision repair (NER) [146] although this role of HR23B was subsequently shown not to be important for its role as an HDI sensitivity determinant [15]. The second important role of HR23B is as a component of the ubiquitin proteasome system pathway (UPS) in shuttling ubiquitinated proteins to the proteasome for degradation [126]. The mechanism for this is through the specific recognition of polyubiquitin chains of cargo proteins by the ubiquitin associated (UBA) domain of HR23B [147] and subsequent binding of the ubiquitin-like (UBL) domain of HR23B to the 26S proteasome [148]. It was subsequently shown that proteasome activity was reduced in HDI-treated cells and HR23B is partially responsible for this reduction [41].

The aim of my initial experiments was to ascertain that two of the possible cellular outcomes: autophagy and apoptosis occur in a number of cell lines on treatment with the general HDI SAHA, after which I wanted to confirm the roles of HR23B (and eventually Myd88) as sensitivity determinants during HDI treatment, i.e that an increase in levels of HR23B corresponds to a greater level of apoptosis on HDI treatment and vice versa.

3.1 HDI treatment of U2OS cells causes apoptosis and autophagy

Cell lines treated with the broad-spectrum HDI SAHA showed an increase in both apoptosis markers (cleaved PARP) and autophagy markers (cleaved LC3) in a dose-dependent manner, as shown in Figure 3.1. Levels of acetylated Histone H3 were measured as a control to ensure SAHA exhibits activity as an HDAC inhibitor [150]. Levels of acetylated histone H3 increased on SAHA treatment as expected due to nuclear histone deacetylase inhibition of enzymes whose substrate had been histone H3.

There is variation in sensitivity of different cell lines to SAHA, for example clearly visible PARP cleavage is seen at 0.1μM SAHA in the diffuse large ß-cell lymphoma SUDHL10 cell line (Figure 3.1 c), whereas 5 μM SAHA is needed to cause such striking PARP cleavage in T-cell lymphoma MYLA cells (Figure 3.1b). Previous research shows similar variability of response to HDI treatment depending on cell line type, for example different chondrosarcoma cell lines show significant apoptosis as measured by immunoblotting for cleaved PARP at SAHA concentrations as varied as 5 and 20 μM [83]. The limitation of using immunoblotting for cleaved PARP as a measure of apoptosis and particularly for comparison between different cell lines, is that immunoblotting is not a quantative measure, and it is not possible to compare between immunoblots from different SDS-gels (as in Figure 3.1 a and b), due to the dependency of signal intensity of film exposure and on specific immunoblots conditions such as temperature variation. For more precise comparison of SAHA effects on various cell lines, MTT assays of cellular viability or FACS analysis with measurement of sub-G1 levels could be performed. However, as the aim was primarily to confirm that

both apoptosis and autophagy take place on SAHA treatment as shown in previous publications, immunoblotting for cleaved PARP was considered to be a sufficient assay.

As discussed, autophagy is another key cellular outcome of HDI treatment, and LC3 cleavage from its cytosolic form to the smaller autophagosome associated fragment can be observed in a dose-dependent manner as SAHA concentration was increased in U2OS and SUDHL10 cell lines (Figure 3.1 a and c). An alternative way to measure autophagy (rather than endogenous LC3 cleavage) is to transfect ectopically the GFP-LC3-Cherry plasmid and monitor the appearance of cleaved GFP. This fusion protein displays dual red-green fluorescence in autophagosomes but in the acidic environment of lysosomes it becomes cleaved. In this case, green fluorescence during immunofluorescence, and GFP protein in an immunoblot, can be observed (GFP-LC3-Cherry plasmid created and utilised in [151]). Although the GFP-LC3-Cherry plasmid is usually used to monitor conversion of autophagosomes to lysosomes (and thus stage of autophagy) by observing LC3-granule colour by immunofluorescence, where green fluorescence indicates later stages of autophagy, it can also be used to monitor GFP appearance in immunoblotting [151]. In U2OS cells transfected with GFP-LC3-Cherry and treated with SAHA there is cleavage of the larger GFP-LC3-Cherry protein and appearance of GFP during treatment with 5μM SAHA, and a further increase in GFP levels at 10 μM, indicating higher levels of autophagy, or perhaps simply accumulation of GFP protein (proteasome activity is compromised during HDI treatment [15]) during SAHA treatment at increased concentrations (Figure 3.1d).

Figure 3.1

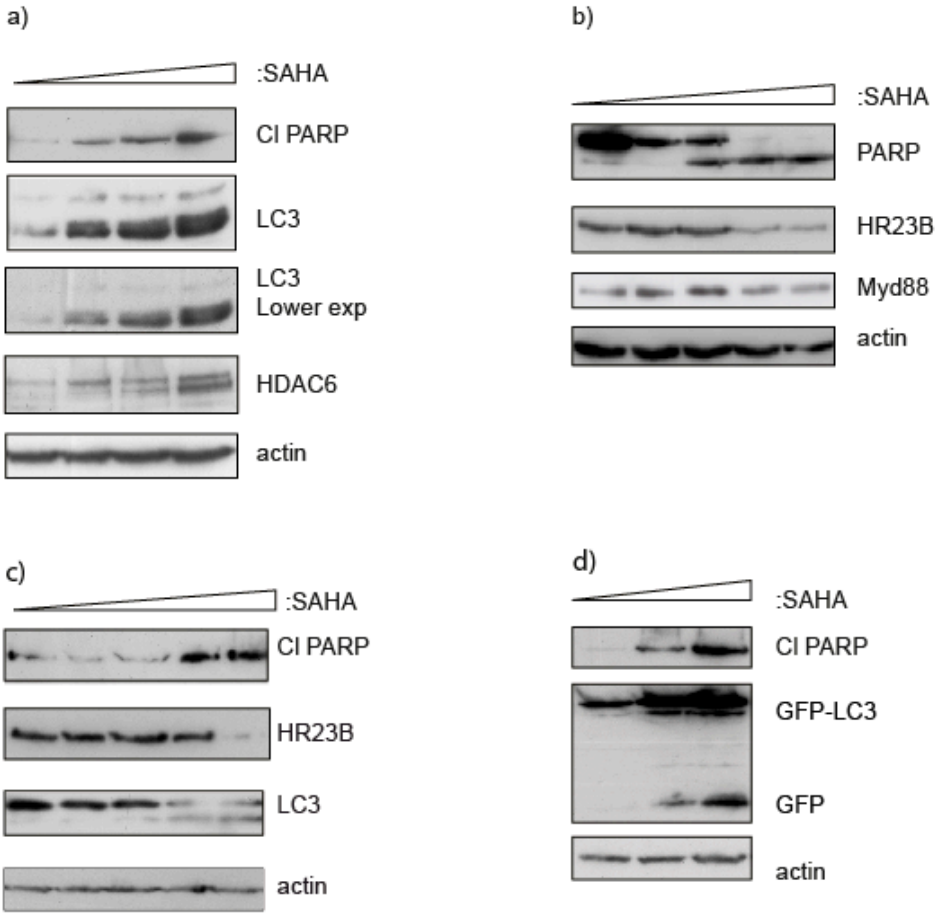

a) U2OS cells were treated with 0, 0.5, 1 and 2 μM SAHA for 24hrs prior to harvesting and immunoblotting to visualise apoptosis (cleaved PARP) and autophagy (LC3) markers. Actin serves as loading control. The example shown is representative of three independent experiments.

b) MYLA cells were treated with 0, 2.5, 5, 10,15 μM SAHA for 24hrs prior to harvesting and immunoblotting using cleaved PARP, acetylated Histone H3 (ac-H3), HR23B and Myd88 antibodies. Actin serves as loading control. The example shown is representative of three independent experiments.

c) SUDHL 10 cells were treated with 0, 0.01, 0.05 and 0.1 μM SAHA for 24hrs prior to harvesting and immunoblotting using cleaved PARP, HR23B and LC3 antibodies. Actin serves as loading control. The example shown is representative of three independent experiments.

d) U2OS cells were transfected with 1μg/P100 GFP-LC3-Cherry DNA for 24 hrs prior to 24 hrs treatment with 0, 5 and 10 μM SAHA. Immunoblotting using cleaved PARP to measure apoptosis and GFP to measure cleavage of the GFP-LC3-Cherry protein upon autophagy into GFP was subsequently carried out. The example shown is representative of three independent experiments.

In order to show that apoptosis and autophagy are separate and alternative cell fates which both arise as a result of HDI treatment, U2OS cells were treated simultaneously with a general HDI (SAHA) and the autophagy inhibitor bafilomycin. Bafilomycin treatment alone (at 100nM) did not cause any PARP cleavage (Figure 3.2a), indicating that it is not toxic at this concentration. However, autophagy inhibition in combination with SAHA treatment resulted in higher levels of apoptosis than SAHA treatment alone at the same concentration (Figure 3.2a) which suggests that these cell fates are separate outcomes of HDI treatment, and that there are cells which undergo autophagy as an alternative to apoptosis on SAHA treatment, although this conclusion cannot be drawn from the experiments above. Similar effects have been previously seen in studies where HDIs and autophagy inhibitors, such as panobinostat and chloroquine are combined during treatment of cancer cell lines to result in synergistic cell survival inhibition [152]. Figure 3.2a shows levels of the cleaved form of LC3 (which runs at a smaller size on an SDS-gel) to increase on bafilomycin treatment, which is counter-intuitive as autophagy should be inhibited under these conditions. The reason for this is likely to be that bafilomycin inhibits autophagy downstream of LC3 cleavage, which leads to autophagosome accumulation. More specifically, bafilomycin fuctions by preventing fusion of autophagosomes with lysosomes [89].

To investigate further in an alternative approach whether autophagy can indeed be seen as a pro-survival alternative fate to apoptosis on HDI treatment under the conditions used, SAHA treatment was combined with a compound that leads to autophagy induction through mTOR inhibition (see introduction figure 1.3)

labelled as AZD2014 (previously used in [153]) in figure 3.2b. Autophagy induction can be seen on SAHA treatment even without AZD, but a combination of SAHA and AZD correlates with higher levels of cleaved LC3 as shown by immunoblotting than SAHA alone (Figure 3.2 b). Autophagy induction (caused by AZD treatment) also correlates with a decrease in cleaved PARP levels, which suggested that autophagy is indeed a pro-survival mechanism under these conditions, as the cells which were previously undergoing apoptosis are now instead undergoing autophagy and surviving. This observation also indicates that SAHA induces autophagy by other means in addition to the mechanisms by which AZD induces autophagy. A factor which complicates the understanding of this experiment is the absence of cleaved LC3 even at highest AZD concentrations, unless SAHA is also present, which may imply that the compound is not working as it should in terms of inducing autophagy. A potential explanation of this is that autophagy induction through mTOR inhibition works best when there is already a high basal level of autophagy. An additional factor here is that AZD treatment causes a slight increase in uncleaved LC3 levels, which, according to previous publications can also be interpreted as an increase in autophagy levels [85].

Figure 3.2

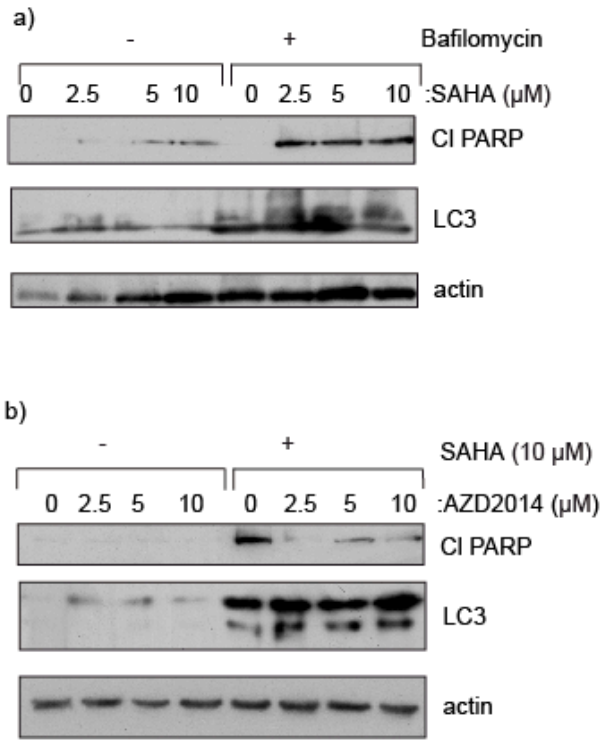

a) U2OS cells were treated with SAHA at the indicated concentrations and bafilomycin (100nM) for 24 hrs prior to immunoblotting for cleave PARP (Cl PARP), LC3 and actin. The example shown is representative of three independent experiments.

b) U2OS cells were treated with AZD2014 and SAHA at the indicated concentrations prior to immunoblotting for cleaved PARP (Cl PARP), LC3 and actin. The example shown is representative of three independent experiments.

A limitation of these experiments, in which SAHA treatment has been combined with autophagy inhibition (by bafilomycin) and induction (by AZD), is that only one compound was used to induce and inhibit autophagy. Using a range of compounds both for autophagy induction and inhibition would give more convincing evidence of the potential of cell survival through autophagy as an alternative fate to apoptosis.

It is important to note at this stage that appearance of autophagocytic markers at increasing SAHA concentrations was coincidental with decreased levels of HR23B (figures 3.1b, 3.1c), which suggests there might be a potential relationship between HR23B and autophagy which will be discussed in further detail subsequently.

3.2 HR23B overexpression increases apoptosis levels on HDI treatment

A U2OS cell line in which expression of stable ectopic Flag-tagged HR23B was under conditional control (induction upon doxycycline treatment) was used to determine the correlation between cellular HR23B levels and apoptosis on HDI treatment. The FLAG-HR23B inducible cell line (made by Dr Susan Fotheringham) was sensitive to apoptosis induced by SAHA in a dose and time-dependent manner. (Figure 3.3a) and b)). Immunoblot quantitation using ImageJ software showed a three-fold increase in cleaved PARP when FLAG-HR23B levels are induced compared to uninduced cells after 24 hours of SAHA treatment at the same concentration. This supports previous findings, which show that there is a dominant role of HR23B in regulating the cellular outcome of HDAC inhibitor treatment [41]. Although the sensitivity determinant role of HR23B has already been shown prior to the start of my project, to confirm these finding by a variety of assays and ensure that HR23B levels are indeed important in determining cell fate on HDI treatment under the conditions I am using, prior to investigation of why cells undergo a particular cell fate under high or low HR23B levels, and what factors may govern cellular HR23B levels, several methods were used to confirm the previous results.

Clonogenic or colony formation assay (CFA) is a cell survival assay measuring the ability of any single cell to grow into a colony, typically of 50 cells or more [154]. Exponentially growing cells are harvested and replated at an appropriate number of cells per well (1000 cells per well in my experiments, a number chosen after titrating several), only a fraction of which retain the capacity to produce colonies, which can then be stained with a dye and counted [154]. This assay typically tests the effectiveness of cytotoxic agents or ionizing radiation by measuring the proliferation

ability of cells and their sensitivity to treatment. An advantage of using a CFA as an additional measure of cell survival alongside markers such as cleaved PARP is that the length of the assay (9 days) means the cells have undergone at least 5 division cycles (the cell cycle length for U2OS cells is about 24 hrs) so cells in all phases of the cell cycle were present during the assay for a significant amount of time. Unsynchronised populations of cells have been used for my previous experiments with the inducible Flag-HR23B cell line so there is a possible bias due to cells being drug treated for only 24hrs during which cells in some cell phases might be represented more than others. This is particularly important for HDI treatment as histone deacetylase inhibition impacts on DNA repair, which is particularly important during S-phase (see introduction section 1.5).

The role of HR23B was further evaluated by measuring the effect of increasing its levels in CFAs, in the presence and absence of two SAHA concentrations. The expression of ectopic HR23B (+ Dox in figure 3.3cii) caused a markedly enhanced growth inhibitory effect of the drug compared to uninduced (- Dox) cells, reflected as a reduction in cell colony formation number. This reduced number of colonies is seen both at 5 μM and 10 μM SAHA treatment (for 24hrs) under conditions of HR23B overexpression, but the doxocyclin addition alone does not have an effect on colony number. It was important to consider effect of doxocyclin addition alone as a control both here and in other experiments with the HR23B-inducible cell line, as doxocyclin is an antibiotic and may cause a slower rate of proliferation, as well as changes of metabolism at high enough doses [155].

This suggests that the HR23B levels affect colony formation only during or after SAHA treatment, supporting previous findings which show HR23B to regulate cellular outcome of HDI treatment [41]. The CFA experiment was performed in

quadruplicate and statistical analysis performed on all the experiments using the student t-test, which showed that observed differences in colony number were statistically significant. It is important to note that CFA assays do not give a direct measure of cell death (as opposed to observing cleaved PARP levels in figures 3.3 a) and 3.3b), but rather give the colony formation ability of cells, which gives an indication of proliferation ability, which seems to decrease when HR23B levels are ectopically increased.

Figure 3.3

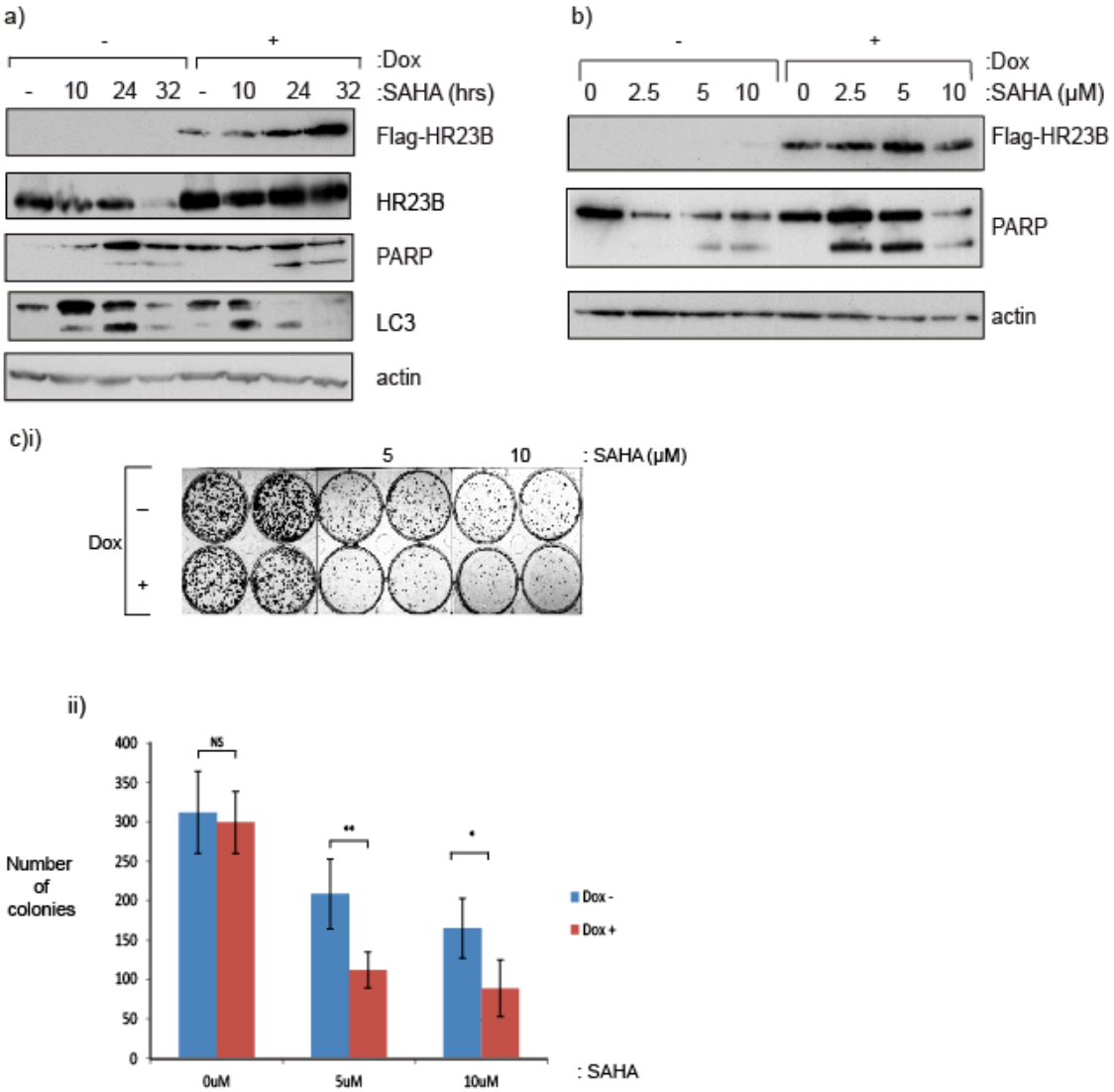

a) U2OS cells stably expressing inducible HR23B were either untreated or treated with SAHA as indicated (10μM for the indicated times) under non-induced (-) or induced (+) doxycycline treatment conditions (1μg/ml; induction for 72hr treatment). Cells were harvested and immunoblotted with anti-Flag (for ectopic HR23B), anti-LC3 or actin as indicated. cThe example shown is representative of three independent experiments.

b) U2OS stable HR23B- inducible cells were treated with SAHA at the indicated concnetrations for 24hrs and the level of apoptosis analysed by immunoblotting for PARP (cleaved and uncleaved) under non-induced (-) or induced (+) doxycycline treatment conditions as indicated. The level of ectopic HR23B and actin is shown. The example shown is representative of three independent experiments.

c) i) U2OS cells stably expressing HR23B were grown in quadruplicate in the absence (-) or presence (+) of doxycycline together with SAHA (indicated concentration in μM) and, after 9 days, the number of viable cell colonies assessed by crystal violet staining. The untreated control cells are shown for comparison. The example shown is representative of three independent experiments

ii) Graphical representation of the data in (i). Statistical analysis was performed by using the student t-test. Ns: non-significant difference P≥0.05 (P=0.7 in this case). * P≤0.05 difference is statistically significant ** P≤ 0.01difference is very statistically significant.

3.4 HR23B depletion reduced the growth inhibitor effect of SAHA.

In addition to investigating the effect of increasing HR23B levels ectopically on cell fate during HDI treatment, it was of interest to determine whether reduction of endogenous HR23B by siRNA has the converse effect, i.e. whether cells with low levels of HR23B survive SAHA treatment and have a higher colony formation ability.

CFAs were performed with U2OS cells where HR23B levels were depleted with siRNA alongside non-targeting (NT) siRNA treated controls (Figure 3.4a) and larger number of colonies were seen in plates where endogenous HR23B levels were lower, both at 5 and 10μM SAHA. This is the converse result to that of Figure 3.3 c which shows that higher HR23B levels upon overexpression of the ectopic protein correspond to lower numbers of colonies in SAHA-treated cells. The control untreated CFA is shown for comparison and the number of colonies formed is the same both for HR23B siRNA and NT treated cells ensuring that reducing HR23B levels alone does not impact on colony formation ability in the absence of drug treatment. It is important to note at this stage the reduction in HR23B levels on SAHA treatment, both in cells with NT siRNA and HR23B siRNA. This has been observed in previous figures (Figure 3.3 a), and typically reduction in HR23B levels on SAHA treatment correlates with appearance of autophagocytic markers (LC3 cleavage), which will be discussed in more detail in subsequent sections (section 3.6). In order to confirm HR23B level depletion, immunoblots were performed both at set-up of CFA, labelled “0 days” in figure 3.6b) and after 9 days at the same time as CFA cells were crystal violet stained, labelled “9 days” in figure 3.4 c). These show that endogenous HR23B was

depleted successfully in the cells used for the CFA and the level of HR23B was still lowered in HR23B siRNA at the end of the assay, compared to NT siRNA treated cells. Immunofluorescence was also performed after 9 days treatment to look at cellular HR23B localisation and levels and confirmed that HR23B levels were still reduced at the end of the CFA in both untreated and SAHA-treated cells (Figure 3.4c).

The two CFA experiments where HR23B levels are both increased through ectopic overexpression in the inducible cell line and depleted using siRNA when taken together give convincing evidence of HR23B levels having an impact on colony-forming ability. It is important to note, however, that clonogenic assays do not necessarily reflect cell apoptotic rate (better measured by PARP cleavage such as in figure 3.4b), but rather indicate the growth inhibitory effect of SAHA is impacted by HR23B levels.

Figure 3.4

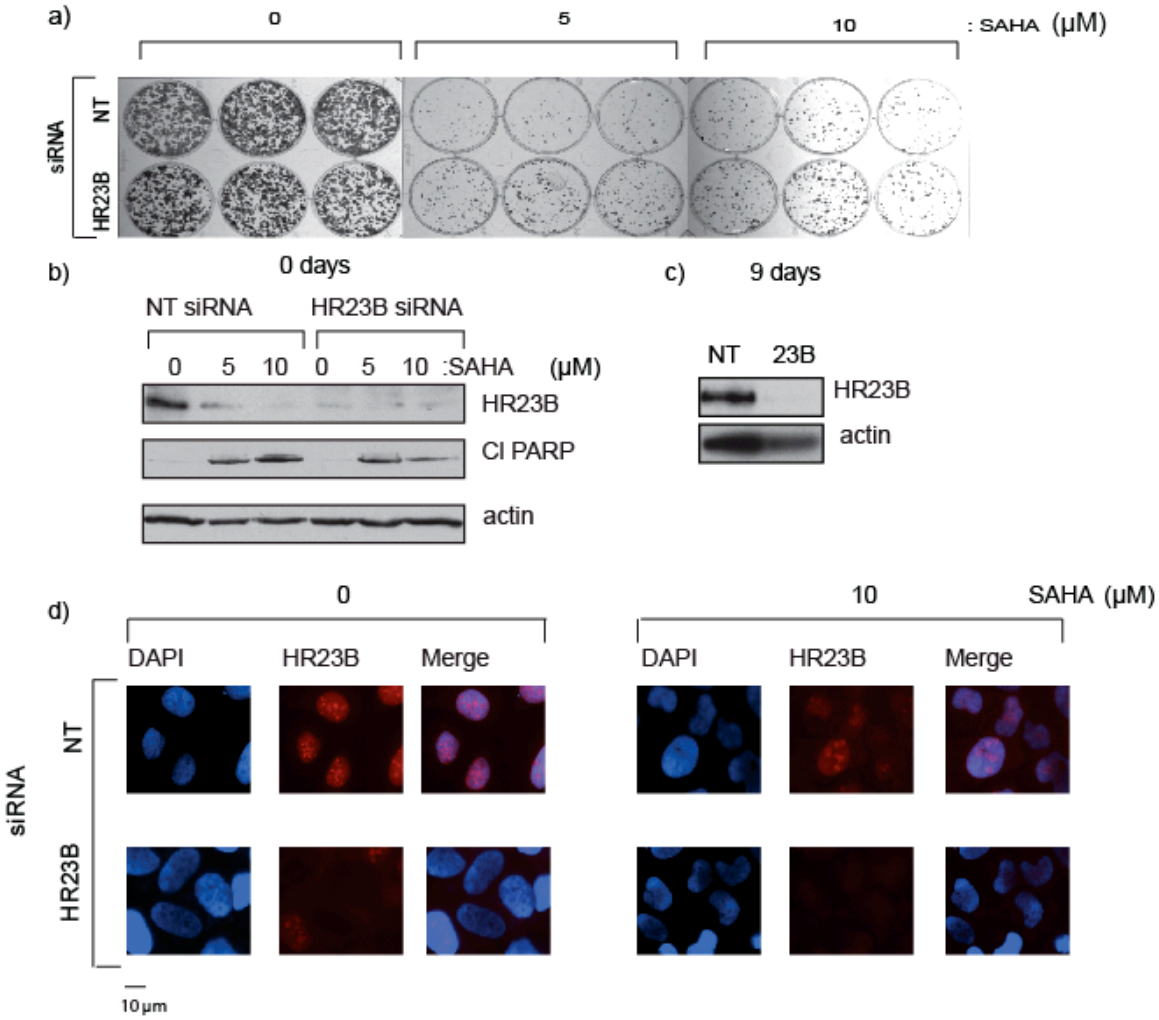

a) U2OS cells were transfected with control (NT) or HR23B siRNA for 48hr and seeded in triplicate for colony formation assay (CFA) for 9 days, with SAHA treatment for the first 24 hrs (indicated concentration in μM), after which number of viable cell colonies assessed by crystal violet staining. The DMSO-treated control cells are shown for comparison. The example shown is representative of three independent experiments.

b) U2OS cells used for CFA in a) were also used for immunoblot to confirm HR23B siRNA depletion at seeding the CFA (0 days). Western blot quantitation using Image J software shows a 22% decrease in cleaved parp levels on HR23B depletion at 5μM SAHA treatment, and a 55% decrease in cleaved parp levels on HR23B depletion at 10μM SAHA treatment The example shown is representative of three independent experiments.

c) U2OS cells used for CFA in a) were also harvested after 9 days and immunoblotted for HR23B levels to confirm siRNA still depletes HR23B after 9 days. Actin shown as loading control. The example shown is representative of three independent experiments.

d) U2OS cells used in transfected with control (NT) or HR23B siRNA for 48hr (the same as used in a)) where immunoflourescence was carried out with HR23B antibody (red). Merged images with nuclear DAPI (blue) are shown. The example shown is representative of three independent experiments.

3.5 HR23B depletion impacta on levels of SAHA-caused apoptosis

Pre-treatment levels of HR23B were modified by depletion using siRNA and a time-course of SAHA treatment was performed (Figure 3.5). Cells with high levels of HR23B levels displayed much greater sensitivity to apoptosis on HDI treatment compared to cells where HR23B levels were reduced by siRNA. For example, after 24 hrs of 10μM SAHA treatment, there was more apoptosis in cells with endogenous HR23B levels detected compared to those where HR23B is depleted by siRNA treatment (as shown by cleaved PARP levels). Note also the decrease in HR23B levels on SAHA treatment after 10 or more hours treatment (Figure 3.5). The correlation between increase in autophagy levels (as indicated by LC3-II increase), with reduction in HR23B levels suggests the possibility of a relationship between HR23B and susceptibility of cells to autophagy.

Figure 3.5

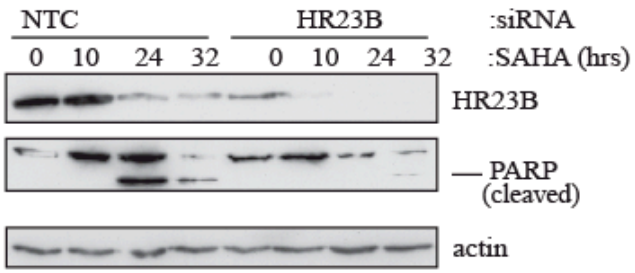

U2OS cells were treated with HR23B or control (NT) siRNA (50nM for 72hr) and 10μM SAHA for the indicated times, prior to immunoblotting to measure levels of HR23B, PARP and actin as loading control. The example shown is representative of three independent experiments.

3.6 HR23B and autophagy

Cell line treatment with increasing SAHA concentrations causes appearance of autophagocytic markers, specifically the cleaved form of LC3 as well as apoptosis (section 3.1). Increasing SAHA concentration frequently coincided with reduced levels of HR23B (Figure 3.1 b, c), as well as increased LC3 cleavage which suggests that there might be a relationship between HR23B and autophagy. To test whether this relationship occurs, HR23B levels were manipulated by depletion of endogenous HR23B with siRNA or ectopic overexpression in the Flag-HR23B inducible cell line, and the impact on autophagy after SAHA treatment was measured by assessing endogenous LC3 cleavage and ectopic GFP-LC3-Cherry cleavage.

Figure 3.6 a) shows HR23B siRNA treated cells to have a slight increase in autophagy levels, measured as cleaved LC3, compared to the control NT siRNA treated cells, when treated with SAHA. Unusually however, figure 3.6a) shows some LC3 cleavage in cells which were not SAHA treated, but only treated with HR23B siRNA. This could be due to experimental variation, cell stress or a non-specific effect of the HR23B siRNA.

To further clarify the impact HR23B levels have on autophagy in SAHA-treated cells, the same experiment as in figure 3.6a) was performed but cells were transfected with GFP-LC3-Cherry (see section 3.1 for background on this way of measuring autophagy) prior to siRNA treatment. Here also, the level of GFP-LC3-Cherry cleavage, which is indicative of autophagy levels, is slightly higher when HR23B levels are lower, coinciding with the decreased PARP cleavage. This suggests that cells may be undergoing autophagy and avoiding apoptosis. It

is important to note however, that GFP-LC3-Cherry cleavage does not show exactly the same effects on autophagy as endogenous LC3 cleavage, so although it is a useful tool to measure autophagy it needs to be considered in combination with other autophagy measures. For example, figure 3.6b shows some GFP produced as a result of GFP-LC3-Cherry cleavage even in cells which are not treated with SAHA, whereas the endogenous LC3 panel for this immunoblot shows LC3 cleavage to only take place on SAHA treatment.

The converse result is seen when HR23B levels are ectopically overexpressed (Figure 3.6c). Here higher levels of HR23B correspond to a decrease in LC3 cleavage on SAHA treatment, particularly at the higher concentration of 10μM SAHA. It appears therefore that high levels of HR23B sensitise cells to apoptosis, whereas lower HR23B levels lead to autophagy being a more likely cell fate in response to HDI treatment. Thus, HR23B has the ability to influence the biological outcome of SAHA treatment, specifically the level of apoptotic and autophagocytic cells.

Figure 3.6

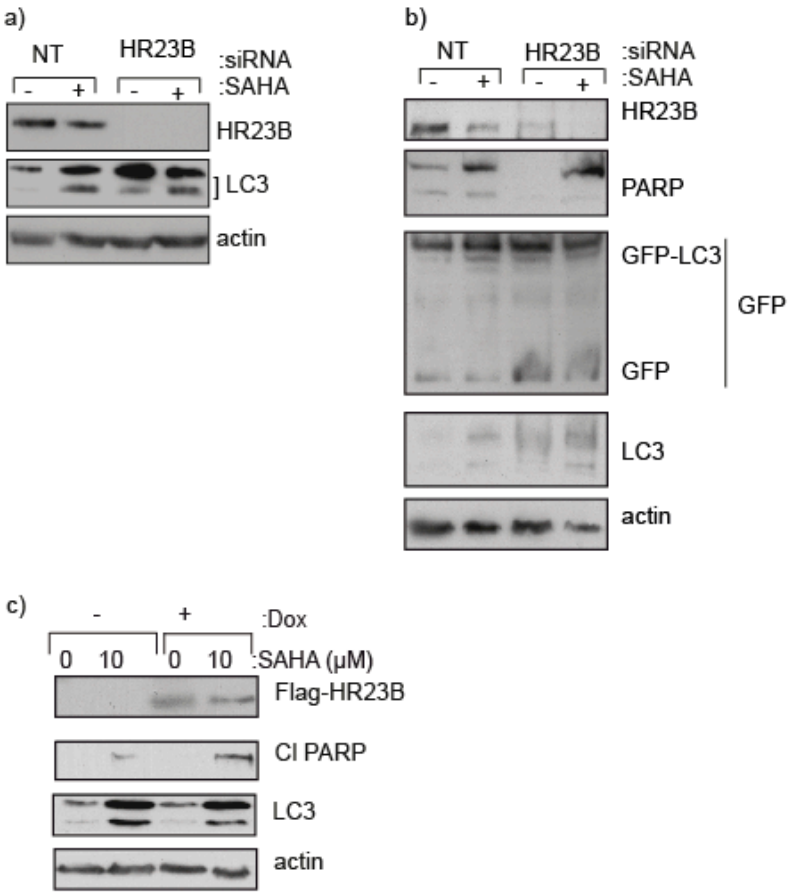

a) U2OS cells were treated with HR23B or control (NT) siRNA (50nM for 72hr) and 10μM SAHA for 24hrs The level of LC3 was measured by immunoblotting. The level of HR23B and actin is shown.

b) U2OS cells were transfected with GFP-LC3-Cherry for 24 hrs, then replated and treated with HR23B or control (NT) siRNA (50nM for 72hr) and 10μM SAHA for 24hrs. The level of HR23B, endogenous LC3, and ectopic GFP-LC3 and GFP was measured by immunoblotting.

c) HR23B- inducible cells were treated with 10μM SAHA for 24hrs and the level of autophagy analysed by immunoblotting for LC3 (cleaved and uncleaved) under non-induced (-) or induced (+) doxycycline treatment conditions as indicated. The level of ectopic HR23 and actin and cleaved PARP is shown.

3.7 IHC staining of human tumour tissue for levels of HR23B

Immunohistochemistry (IHC, see Chapter 2.11 for protocol) is the technique for determining the antigens present in a tissue though using specific antibodies that bind specifically to antigens in biological tissues, which can be visualised through staining [156]. The technique consists of two phases: slide preparation and staining followed by interpretation and quantification of the obtained expression. IHC is used both in the diagnosis of tumours as expression of specific proteins is characteristic of particular cellular events such as apoptosis or cell proliferation, as well as to understand the cellular and tissue localisation of potential biomarkers and other relevant biomolecules in the life sciences. It is the application of IHC in the detection of biomarker levels which was most relevant to my project.

The role of HR23B as a potential biomarkers for HDI treatment have been functionally validated in cell culture, and it has been shown that manipulation of their levels impacts on cell fate on HDI treatment. However these experiments were all performed in cell lines, so it was necessary to observe localisation of these proteins in human tumours and try to determine if there is any correlation between pre-treatment levels of HR23B and clinical outcome.

It was therefore interest to determine whether their pre-treatment levels vary in human tissue in haematological malignancy. To determine this, IHC was performed a subset of patients with the antibody for HR23B, alongside the relevant IgG control, in a number of different tumour types. A selection of images from these cancer types are shown in figures 3.7. The images form tumour tissue

from peripheral T-cell lymphoma tissue show some variations in HR23B levels, and the expected protein localisation (HR23B is predominantly nuclear).

Unfortunately, the availability of clinical samples was too low to carry out enough IHC staining for statistical analysis, and the information available on each patient was very limited – so it was usually only known what type of tumour was being stained rather than the treatment the patient received or the outcome of this treatment. In addition, the normal (non-tumour) tissue control was not available so it was not possible to determine whether levels of the proteins of interest change on tumourigenesis. Due to this, the IHC staining was focussed on determining the levels and localisation of HR23B in the available patient samples which included PTCL (peripheral T-cell lymphoma), Waldenstroms and colorectal tumour samples, and the relevant controls, whilst keeping in mind that it is not possible to make general conclusions in terms of clinical outcome and protein levels, but only determine cellular and tissue localisation and whether there is inter-patient variability.

Figure 3.7

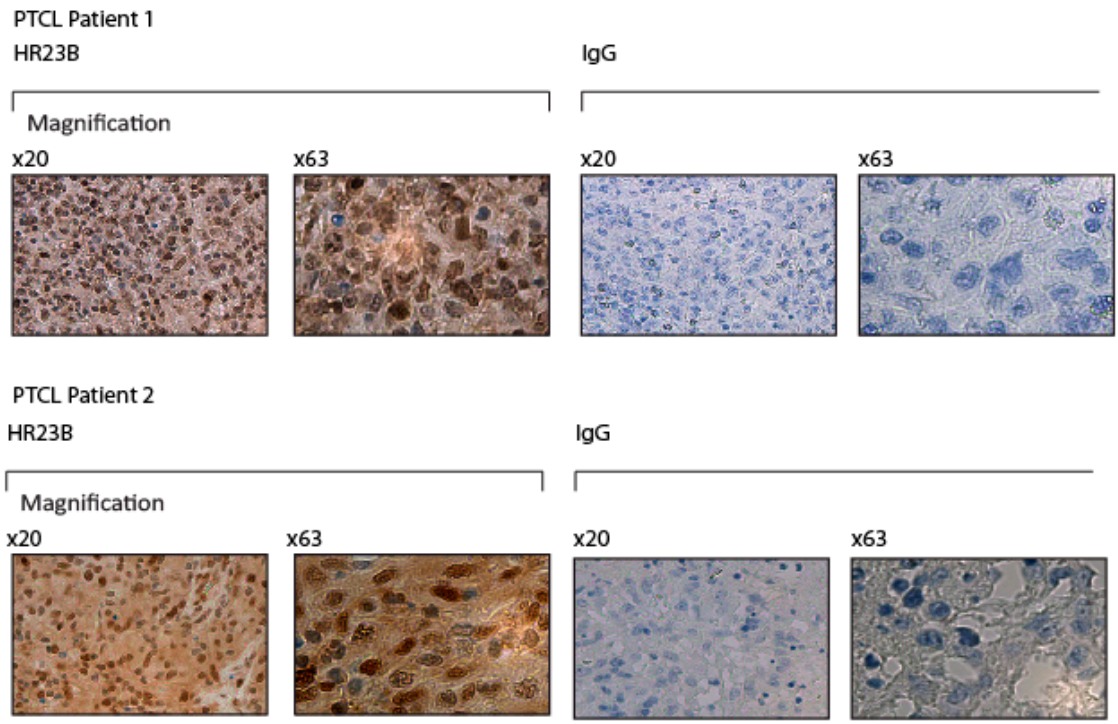

IHC staining with performed as described (Materials and Methods, Section 2.11) on 10 FFPE (formalin fixed paraffin embedded) patient sections with the HR23B and IgG antibodies. Images of slides from two patients shows, at 20x and 63x magnifications

3.8 CONCLUSIONS

HDI treatment causes cells to undergo a variety of cell fates, including apoptosis and autophagy, which is a means of evading apoptosis. HR23B has been shown previously to be necessary for cell death to occur during HDI treatment [15], and results presented above confirm these findings. Manipulation of levels of HR23B by siRNA depletion and ectopic overexpression impact on levels of cell death upon SAHA treatment at a variety of time-points and concentrations, and also affect the growth inhibitory effect of SAHA as shown by colony formation assay results.

The appearance of autophagocytic markers (LC3 cleavage) on SAHA treatment was seen to coincide with a reduction of the levels of HR23B, which lead to the hypothesis that HR23B may affect the cell fate choice between apoptosis and autophagy. This indication was tentatively confirmed through measuring LC3 cleavage on SAHA treatment after manipulating HR23B levels by siRNA depletion or ectopic overexpression, although the differences seen in autophagy levels are fairly subtle on HR23B depletion, but more convincing when HR23B is ectopically overexpressed.

As HDAC6 has been previously shown to promote autophagy, it was reasonable to suggest that it has a role in the mechanism of how HR23B influences the cellular outcome, which is the direction which futher investigation took place.

CHAPTER 4 HDAC6 plays a key role in autophagy and regulates HR23B levels

4.1 Introduction. HDAC6 and autophagy previous research

Autophagy, or cellular "self-eating" is a process required for degradation of proteins, protein complexes and organelles. As described in Introduction section 1.7, autophagy, there are three types of autophagy: microautophagy, macroautophagy and chaperone-mediated autophagy [8], and it macroautophagy is type hereafter referred to as autophagy. Autophagy can be triggered by nutrient starvation such as the depletion of certain amino acids and can be viewed as a process the function of which is to "recycle" resources. However, autophagy can also be induced by other extracellular stress, including hypoxia and oxidative stress, or intracellular stress such as accumulation of damaged organelles or protein aggregation. Although autophagy is a multi-step process (see Introduction section 1.7), these steps can be separated into two discrete stages: formation of double-membraned vesicles (autophagosomes) that sequester cytoplasmic components and the fusion of these autophagosomes with lysosomes to form an acidic compartment with enzymes that carry out degradation [77].

As discussed in chapter 3, autophagy can be seen as alternative outcome to apoptosis during HDAC inhibitor treatment, and one of the aims of my project has been to investigate why cells undergo a particular cell fate during HDI treatment. Of all the human cellular histone deacetylases, HDAC6 is the only HDAC which has been shown to have a direct role in autophagy, and it is one of the only predominantly cytoplasmic deacetylase. HDAC6 has previously been

shown to have a role in autophagy promotion, specifically by controlling autophagosome and lysosome fusion [14]. This takes place through HDAC6-mediated recruitment of cortactin, to cause F-actin network formation which is required for fusion of autophagosomes with lysosomes and subsequent protein aggregate clearance [14]. Interestingly however, HDAC6 is not required for starvation induced autophagy but only for QC (quality control) autophagy, which are differentially regulated processes [14]. Other cytoplasmic substrates of HDAC6 include α-tubulin and HSP-90 [35]. The α-tubulin deacetylation activity of HDAC6 could be important in HDAC6-mediated transport of protein aggregates to aggresomes as tubulin binding to kinesins and other molecular motors is acetylation dependent [157].

Because of the relevance of autophagy as potential alternative fate to apoptosis during HDI treatment, it was of interest to confirm the established role of HDAC6 in autophagy and investigate the role of HDAC6 in the cell fate outcome on HDI treatment. It was also interesting to determine whether HR23B has any potential interplay with HDAC6, or whether the levels of HR23B regulate levels of apoptosis on HDI treatment independently of HDAC6. It is important to note at this point, that HR23B has been shown to be acetylated [158], prior to my investigation, although HR23B acetylation levels do not change on SAHA treatment, which suggests that it is not deacetylated by HDAC6, or its acetylation is regulated in such a way that it remains present irrespective of HDI treatment.

4.2 The role of HDAC6 in autophagy.

Evidence for the role of HDAC6 in autophagy was provided by the comparison of levels of LC3 cleavage between the A549 HDAC6 wild-type (hereafter referred to as HDAC WT) and A549 HDAC6 knock-down (hereafter referred to as HDAC6 KD) cell lines, where the levels of HDAC6 are markedly different, as the HDAC6 KD cell line is stably expressing HDAC6 shRNA, which leads to HDAC6 being at such low levels that it is virtually undetectable by western blot. HDI (SAHA) treatment induced autophagy in an HDAC6-dependent way as observed by looking at levels of cleaved LC3-II in the A549 HDAC6 WT cell line compared with the A549 HDAC6 KD cell line on SAHA treatment (Figure 4.2a). Although cleaved LC3 levels increased on SAHA treatment in both cell lines these are much higher when HDAC6 levels are high in the HDAC6 WT cell line (Figure 4.2a).

In order to confirm that HDAC6 levels and activity impact on autophagy under the experimental conditions used i.e. in U2OS cells, in which the original genome-wide shRNA screen was performed [15], and under the SAHA concentrations and times of treatment which have been used to confirm that HR23B is a sensitivity determinant to SAHA treatment, a system was needed where levels of HDAC6 could be manipulated easily, and the effect on autophagy levels observed.

A cell line was created where expression of stable ectopic flag-tagged HDAC6 was under conditional control, specifically induction upon doxycycline treatment. Evidence for the role of HDAC6 in promoting autophagy was seen by performing immunofluorescence on the HDAC6 inducible cell line to observe the

approximate numbers of autophagosomes (seen as localised speckled LC3 staining in red in figure 4.2b). When HDAC6 levels were ectopically increased by doxycycline addition (see cytoplasmic HDAC6 in green, Figure 4.2b), the numbers of autophagosomes increased, confirming that HDAC6 has a role in autophagy promotion even in the absence of HDI treatment, particularly after 96hrs of HDAC6 over-expression. Ideally, quantification would have been helpful in determination of the exact number of autophagosomes to give a more accurate idea of how much autophagy levels increased on HDAC6 overexpression, but this was not practical to do by eye due to the numbers of cells and autophagosomes involved, and quantification software was not available. However, this immunofluorescence experiment was useful to perform, as it shows that Flag-HDAC6 (green in figure 4.2b) is expressed in a high proportion of cells upon doxycycline treatment, and its localisation is nuclear as expected and seen in previous publications [14].

Figure 4.2

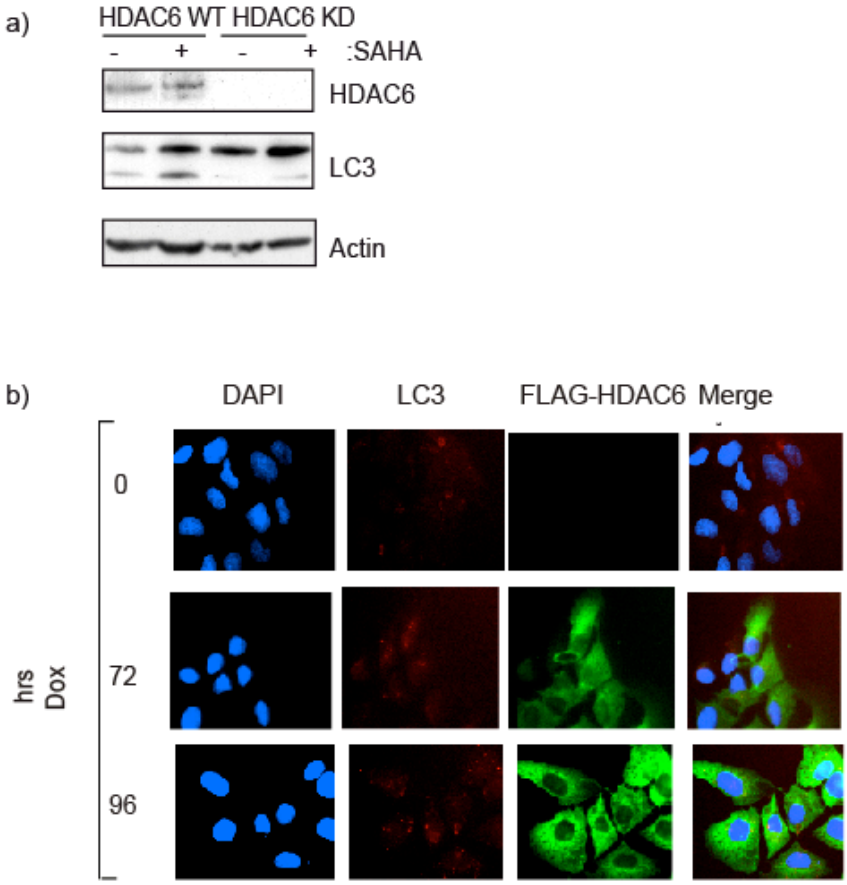

a) HDAC6 WT and KD cells were treated with 10μM SAHA for 24 hrs and analysed by immunoblotting for HDAC6 and LC3. Actin serves as loading control. The example shown is representative of three independent experiments.

b) Immunofluorescence to show endogenous LC3 (red) in the Flag-HDAC6 (green) in the HDAC6-inducible cell line at 72 and 96 hr post induction (Dox +). DAPI nuclear staining and the merged image is shown. The example shown is representative of three independent experiments.

The effects of SAHA treatment on autophagy in the HDAC6 KD and WT cell lines were also compared in a time-dependent manner. As shown in Figure 4.3a), there is an increase in LC3 cleavage in cells where HDAC6 is present, and this increase in dependent on the time of treatment with SAHA, i.e. autophagy levels, as measured by LC3 cleavage are higher at 36 hrs compared to 16 and 24. In the HDAC6 KD cell line, however, LC3 cleavage is nearly undetectable: again confirming that autophagy on SAHA treatment is dependent on the presence of HDAC6. It is interesting to note also the increase in cellular HDAC6 levels on SAHA treatment in the HDAC6 WT cell line (Figure 4.3 a). Since the majority of the replicates had the same outcome, a possible explanation for this could be a feedback mechanism – as more cellular HDAC6 becomes inhibited by SAHA treatment during the longer treatment timepoints in Figure 4.3a), there is up-regulation of synthesis of this protein to compensate for this.

Having established the need of HDAC6 for autophagy, it was important to compare the levels of cell death in response to SAHA in HDAC6 WT and HDAC6 KD cell lines, which is shown in the FACS analysis in Figure 4.3b) ii). SAHA treatment at the same concentration causes much higher levels of sub-G1 in the HDAC6 KD cell lines (18%), compared with the HDAC6 WT cell lines, where sub-G1 is about 12%. Autophagy, as measured by LC3 cleavage is at much higher levels in the HDAC6 WT cell line, and may be the alternative cell fate to apoptosis in these cells during SAHA treatment (Figure 4.3b i). Note also the increased levels of HR23B in the HDAC6 KD cell line compared to HDAC6 WT.

The relationship between autophagy and apoptosis has been discussed in Section 1.5 and there is evidence that SAHA-treated cells may undergo autophagy to escape

apoptosis. As HR23B levels seem to be influenced by HDAC6 presence and high HR23B levels sensitise cells to apoptosis (as discussed in chapter 2), it was a possibility that HDAC6 absence in the HDAC6 KD cell line may have an effect on cell sensitivity to HDAC inhibitors.

This is supported by figure 4.3bii) where higher levels of sub-G1 cells, as measured by FACS analysis, are present in SAHA-treated HDAC6 KD cells which have very low levels of autophagy compared to SAHA-treated HDAC6 WT cells (12% sub-G1 compared to 18%). However, it is important to note the higher basal levels of apoptosis in HDAC6 KD cell line (3% compared to 0.5% in HDAC6 WT), even in cells which are not treated with SAHA, which may be reflected sub-G1 levels on SAHA treated cells. These enhanced basal levels of apoptosis in the HDAC6 KD cell line correlate with the higher levels of HR23B in this cell line, and as the only difference between the HDAC6 KD and HDAC6 WT cell line is the levels of HDAC6, both the HR23B levels and apoptosis levels are a consequence of varying HDAC6 levels. As there is no HDI treatment in these conditions, it suggests that HDAC6 is required of cell survival and its absence leads to increased apoptosis even in the absence of HDI treatment. This is supported by the morphological appearance (light microscope 60 x magnification) of HDAC6 KD cells – they are less adherent and appear smaller with more floating cells present compared to HDAC WT cells. This could be due to the role of HDAC6 in promoting autophagy which allows cell survival during stress such as starvation (even in the absence of HDI treatment), but also due to other roles of HDAC6 in the cell such as microtubule dependent intracellular trafficking [35].

In conclusion, HDAC6 levels correlate with levels of autophagy in two different cell line systems: U2OS cells and A549 cells, so I have confirmed that HDAC6 does

seem to be promoting autophagy as shown by previous research [14]. As discussed in introduction section 1.3, HDAC6 has a number of cellular functions as well as autophagy promotion, and consists of two catalytic domains as well as a ubiquitin-binding BUZ domain. The next question was to dissect further the requirements of autophagy-promoting ability of HDAC6 and to determine whether HDAC6 catalytic activity is essential for its autophagy-promoting activity.

Figure 4.3.

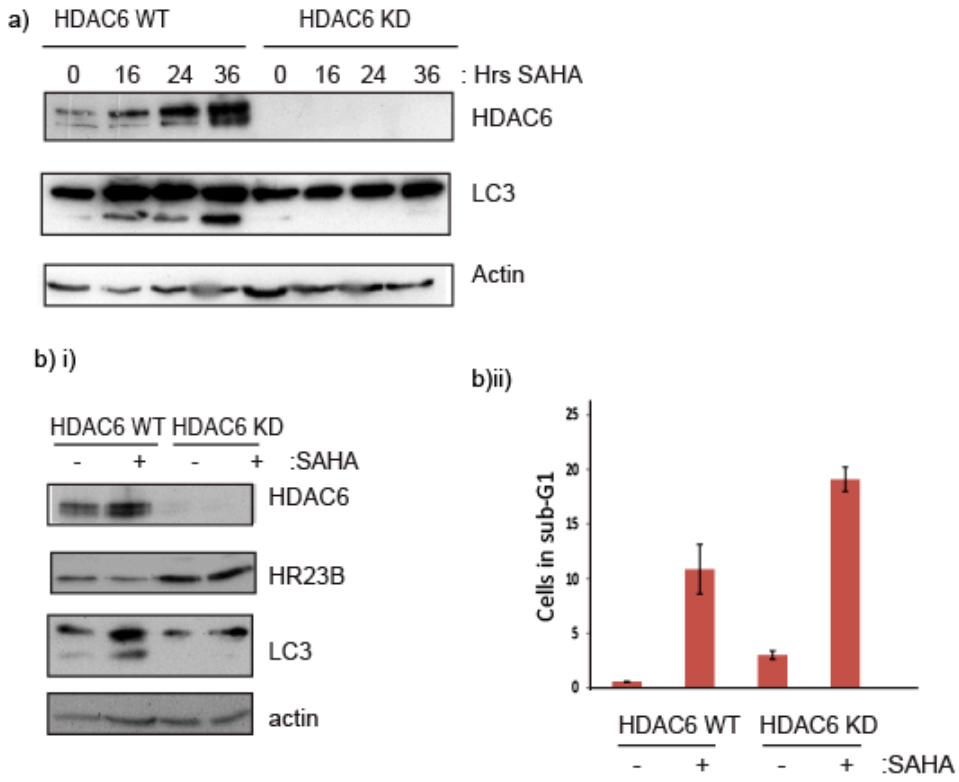

a) HDAC6 WT and KD cells were treated with 10μM SAHA for the indicated times and analysed by immunoblotting for HDAC6 and LC3. Actin serves as loading control. The example shown is representative of three independent experiments.

b) HDAC6 WT and KD cells were treated with SAHA (10 μM) for 24hrs, and analysed by immunoblotting for HDAC6, HR23B, LC3 and actin in i).FACS analysis was carried out on the same extracts and percentage of cells in sub-G1 is shown ii). The example shown is representative of three independent experiments.

4.3 HDAC6 catalytic activity is independent of autophagy

In order to determine whether the catalytic histone deacetylase activity of HDAC6 is required for its autophagy-inducing activity, U2OS cells were treated with tubastatin A, a specific small-molecule inhibitor of the deacetylase function of HDAC6 [48]. Initially a time-course of tubastatin treatment was performed with treatment times ranging from 1 to 24hrs (Figure 4.4a), in order to confirm that tubastatin is inhibiting HDAC6, by measuring the levels of acetylation of a known HDAC6 substrate, alpha-tubulin [159]. The catalytic deacetylase activity of HDAC6 was inhibited successfully in this cell type at the concentrations and time-points used, as shown by acetylation levels of alpha-tubulin, which show a steady increase as time treated with tubastatin increases (see Acetyl-Tubulin levels in Figure 4.4a).

Once the activity of tubastatin as an HDAC6 inhibitor was confirmed, U2OS cells were treated with a range of tubastatin concentrations, and the effect on autophagy was observed (Figure 4.4b). The inhibition of catalytic activity of HDAC6 caused a dose-dependent increase in autophagy as shown by increased levels of LC3-II. This suggests that the autophagy-inducing activity of HDAC6 is independent of (and possibly inhibited by) its catalytic activity. However, previous publications have shown HDAC6 catalytic activity to be required for autophagy, as microtubule acetylation is needed for intracellular trafficking [160].This means that it is important to interpret this result with caution. In addition, tubastatin is unlikely to be completely specific to HDAC6, but rather may cause autophagy through inhibition of other HDACs, in a similar way to SAHA and other general HDIs (see introduction section 1.3 for an explanation of how HDI treatment leads to autophagy).

FACS analysis was also performed on U2OS cells treated with a range of tubastatin concentrations to determine whether apoptosis as well as autophagy takes place on HDAC6 catalytic activity inhibition (Figure 4.4b). This analysis showed that the sub-G1 phase of the cell population (an indicator of apoptosis) to increase as the tubastatin concentration increases, which suggests that HDAC6 catalytic activity is required for cell survival, perhaps in an autophagy-independent way due to HDAC6 requirement for microtubule-mediated intracellular transport of substrates [161]. Other roles of HDAC6 which are independent of its enzymatic deacetylase activity include lymphocyte migration and chemotaxis [161], so it is conceivable that these or other processes may be required for cell survival also. Another potential explanation for the increase in sub-G1 on tubastatin treatment is that although tubastatin is said to be specific for HDAC6 [48], it may also inhibit the catalytic activity of other cellular HDACs at high concentrations, which leads to apoptosis in the same way as treatment with general HDIs (see Introduction 1.5).

To confirm that the increase in autophagy seen on tubastatin treatment is HDAC6 dependent, the HDAC6 KD and WT cell lines were treated with several concentrations of tubastatin (Figure 4.4c). LC3-II was very low in the HDAC6 KD cell line compared to WT at all tubastatin concentrations confirming that the increase in autophagy seen in cell-lines where HDAC6 is present (U20S in figure 4.3 a,b) and HDAC6 WT in figure 5c) is HDAC6 dependent. The levels of cleaved LC3 (LC3-II) increase in a dose-dependent manner on tubastatin treatment in the HDAC WT cell line, just as they do in U2OS cells, again suggesting that the role of HDAC6 in autophagy is independent of its catalytic activity, or that these two roles of HDAC6 may even be counteractive. However, this may also be an indirect effect, for example inhibition of the catalytic activity of HDAC6 may mean it is not able to play its usual

role in biological processes in the cells, such as cell morphology regulation and microtubule mediated intracellular transport [161] and this leads to cell stress and which consequently causes autophagy.

Figure 4.4

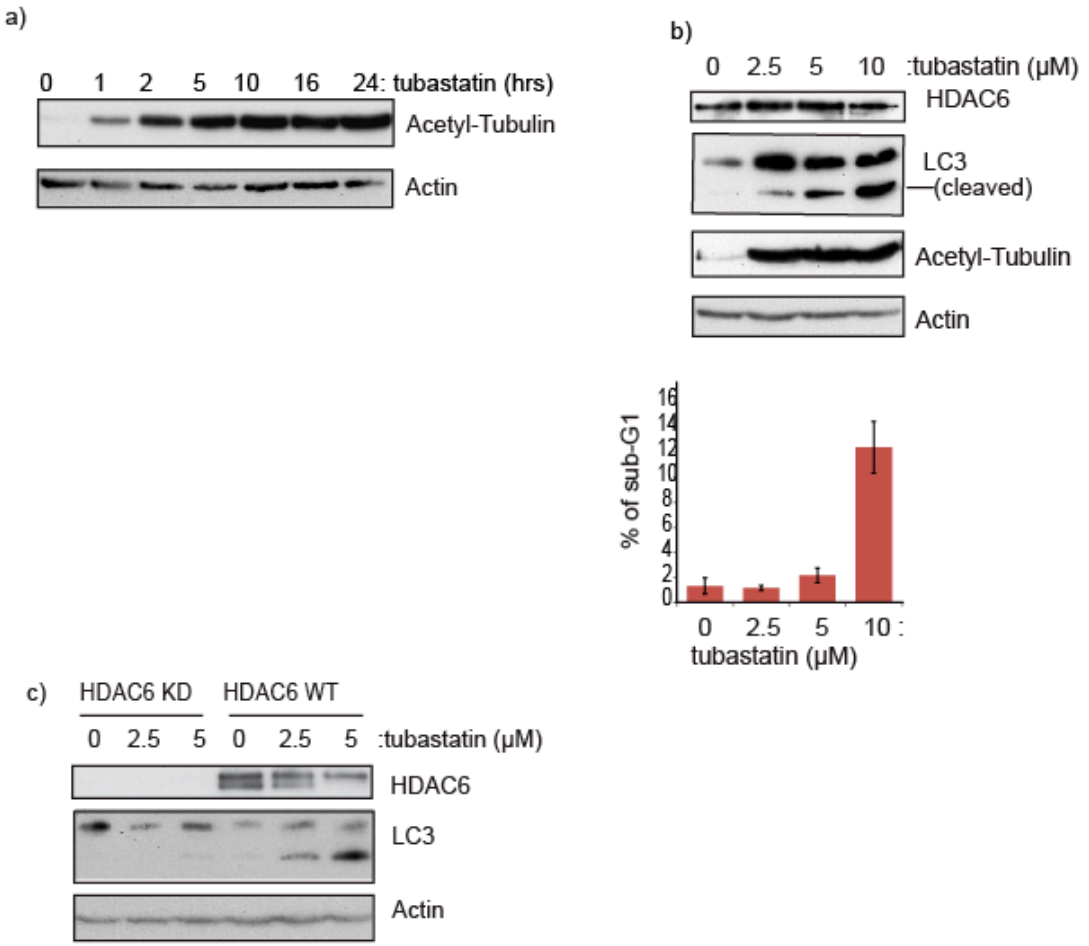

a) U2OS cells were treated with 5 μM tubastatin for the indicated time periods and analysed by immunoblotting for acetyl-tubulin and actin. The example shown is representative of three independent experiments.

b) U2OS cells were treated with tubastatin at the indicated concentrations for 24 hrs and analysed by immunoblotting for HDAC6, LC3, acetyl-tubulin and actin. These cell extracts were also analysed by FACS and the percentage of cells in sub-G1 is shown underneath the immunoblot. The example shown is representative of three independent experiments.

c) HDAC6 KD and WT cells were treated with Tubastatin at the indicated concentrations for 24 hrs and analysed by immunoblotting for HDAC6, LC3 and actin. The example shown is representative of three independent experiments.

4.4 HDAC6 regulates HR23B levels

Levels of endogenous HR23B decrease on HDI treatment, which coincides with increased levels of autophagocytic markers, specifically LC3 cleavage, as discussed in Chapter 3. Because of the prominent role of HDAC6 in autophagy, it was of interest to investigate any potential relationship between HDAC6 and HR23B, as part of the investigation of the mechanism through which HR23B levels impact on biological outcome of HDI treatment.

The potential interplay between HDAC6 and HR23B was investigated by the manipulation of HDAC6 levels by ectopic overexpression and transient siRNA depletion and observation of the effect on HR23B levels. The levels of endogenous HR23B upon induction of Flag-HDAC6 in the stable inducible cell line decreased as time of HDAC6 induction increased (Figure 4.5ai), which was achieved by doxycycline addition for increasing time periods. A minimum of 48hrs of HDAC6 overexpression is required to see a significant decrease in HR23B, but longer times of Flag-HDAC6 induction correlate with even lower levels of HR23B. The cellular localisation and levels of FLAG-HDAC6 (green in 4.5a ii) and endogenous HR23B (red in 4.5aii) were also observed in the FLAG-HDAC6 inducible cell line by immunofluorescence in cells from the same experiment as in Figure 4.5ai (0, 72 and 96 hr time-points shown). The localisation of HDAC6 was predominantly cytoplasmic, as seen in previous literature [159]. HR23B (red in 4.5aii) appears to be predominantly localised to the nucleus and its levels decreased after 72 hrs FLAG-HDAC6 induction, and even more so after 96hrs as observed immunofluorescence (4.5a ii). Although HDAC6 localisation is cytoplasmic, whereas HR23B appears

nuclear in immunofluorescence, HR23B is also found in the cytoplasm but at lower levels compared to the nucleus [15].

Depletion of HDAC6 by siRNA in U2OS cells caused a significant three-fold increase (as shown by immunoblot quantitation, not shown) in HR23B levels (Figure 4.5c), suggesting that HDAC6 negatively regulates HR23B levels. This is also supported by the observation that HR23B levels are higher in the HDAC6 KD cell line compared to the HDAC6 WT cell line (Figure 4.3bi). The mRNA levels of HR23B are not changed significantly on HDAC6 overexpression (Geng Liu, personal communication) indicating that HR23B down-regulation by HDAC6 takes place at a protein level, perhaps through regulation of HR23B degradation via the proteasome.

In order to determine which domain of HDAC6 was responsible for HR23B down regulation, a series of HDAC6 mutants (kind gift from Tso-Pang Yao et al) were expressed ectopically in HDAC6 WT and HDAC6 KD cells. The BUZ (ubiquitin binding) domain was required to down-regulate HR23B and reduces its levels by over 50% (immunoblot quantitation, not shown), whereas △BUZ failed to alter the level of HR23B (Figure 4.5 b). Because the BUZ domain is sufficient to affect HR23B levels, these results establish that the catalytic activity of HDAC6 is dispensable for the down-regulation of HR23B. Note that BUZ HDAC6 is poorly expressed compared to △BUZ in transfected cells (Figure 4.5 b), which makes the relative effect of the BUZ domain on HR23B more significant.

Figure 4.5

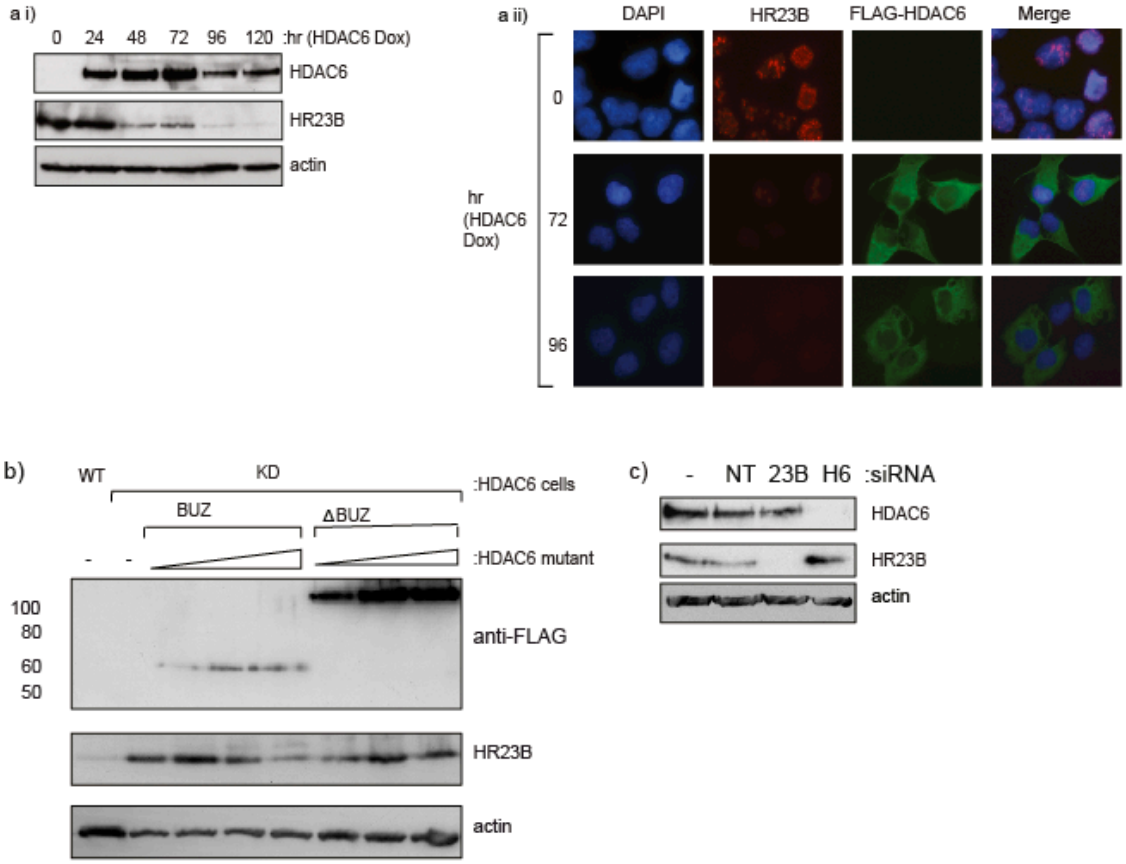

a) i) Immunoblot showing endogenous HR23B levels upon induction (Dox + treatment) of Flag-HDAC6 in the stable inducible cell line over the indicated time course. The example shown is representative of three independent experiments.

ii) Immunofluorescence to show endogenous HR23B (red) in the Flag-HDAC6 (green) stable cell line in the same conditions, as indicated at 72 and 96 hr post induction (Dox +). Nuclear DAPI (blue) and the merged image are shown. The example shown is representative of three independent experiments.

b) HDAC WT and HDAC6 KD cells were transfected with HDAC6 (WT) , BUZ (1, 2 and 3µg) or △BUZ (1,2 and 3µg) for 72h as indicated. Cell lysates were analysed by immunoblotting with indicated antibodies. Note that BUZ is poorly expressed compared to △BUZ in transfected cells. The example shown is representative of three independent experiments.

c) U2OS cells were treated with HR23B (23b), HDAC6 (H6), mock (-) or control (NT) siRNA (50nM for 72hr). The level of HR23B, HDAC6 and actin is shown. The example shown is representative of three independent experiments.

4.5 Mechanism of HDAC6 down-regulation of HR23B

Once the down-regulation of HR23B protein levels by HDAC6 was established it was of interest to determine the mechanism by which this down-regulation occurs. There are two major protein degradation systems in eukaryotic cells: the ubiquitin-proteasome system (Introduction section 1.5) which is responsible for selective degradation of many short-lived proteins, and the lysosomal system in which proteins are delivered to the lytic compartment [8]. Proteins can be delivered to the lysosome in a number of ways – through endocytosis which is responsible for extracellular and plasma membrane protein degradation, through macroautophagy (Introduction section 1.3), through microautophagy and through chaperone—mediated autophagy [8].

A common route for protein degradation as part of the cellular protein quality control mechanism is via the proteasome (section 1.5), so the initial investigation into the mechanism of HR23B down-regulation by HDAC6 was to inhibit proteasome activity in combination with HDAC6 overexpression and observe HR23B levels. Bortezomib (Velcade) is an FDA-approved ubiquitin-proteasome pathway inhibitor [162], so treatment with this drug was used in combination with HDAC6 induction (Figure 4.6a), to investigate how proteasome inhibition affects HR23B down-regulation by HDAC6. As figure 4.6a shows, increasing bortezomib concentrations do not counteract HR23B down-regulation by HDAC6. On the contrary, higher bortezomib concentrations of 150 nM cause a slight decrease in HR23B, further to the decrease in HR23B protein levels caused by HDAC6 induction alone. This suggests the down-regulation of HR23B by HDAC6 is unlikely to be via the proteasome. An alternative proteasome inhibitor

Mg-132 was also used (Figure 4.6b) in combination with flag-HDAC6 overexpression and again HR23B levels remained low under conditions of HDAC6 overexpression and proteasome inhibition. The mechanism of Mg-132 activity is through the binding of this compound to all β-subunits of the proteasome, whereas bortezomib is a dipeptide which functions by inhibiting the chymotrypsin-like activity of the β5 subunit of the proteasome, which is associated with the rate-limiting step of proteolysis [163]. In order to further extend this study, it would be of value to also use a proteasome inhibitor with a different mechanism of action, such as epoxomicin, which acts by covalently and irreversibly binding to catalytic subunits of the proteasome including LMP7, X, and MECL1 [164]. Another possibility would be to use siRNA mediated knockdown of the 20S proteasome, or cell lines where proteasome activity is impaired. In conclusion, it seems that down-regulation of HR23B by HDAC6 does not take place via the proteasome.

Figure 4.6

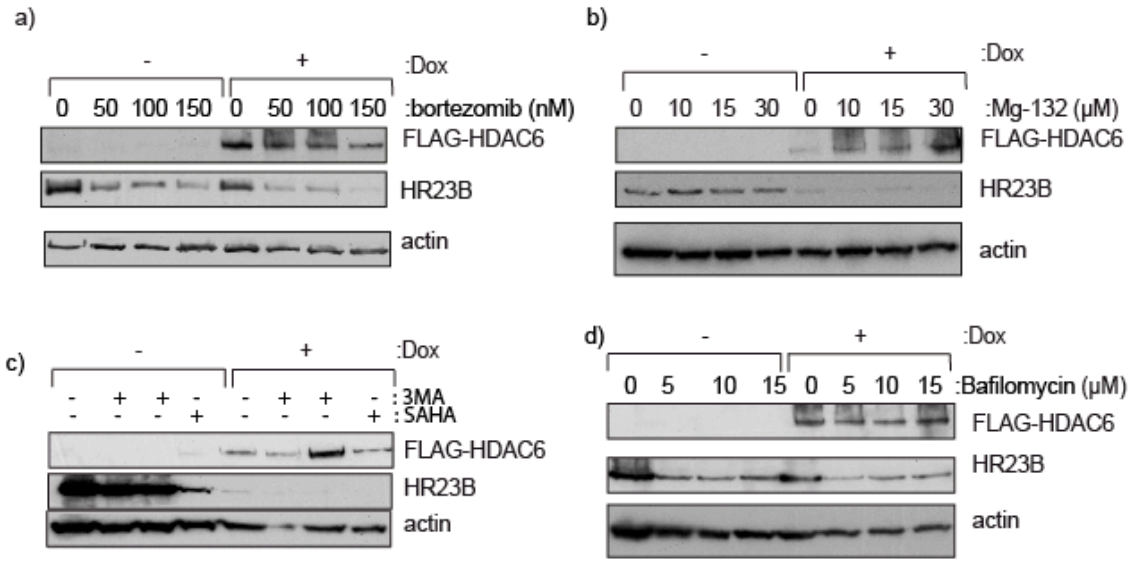

a) U2OS cells stably expressing inducible Flag-tagged HDAC6 were treated with bortezomib at the indicated concetrations for 24 hrs under non-induced (-) or induced (+) doxycycline treatment conditions (1μg/ml; induction for 72hr treatment). Cells were harvested and analysed by immunoblotting with anti-Flag (for ectopic HDAC6), HR23Band actin. The example shown is representative of three independent experiments.

b) Flag-tagged HDAC6 inducible cells were treated with Mg-132 at the indicated concetrations for 24 hrs) under non-induced (-) or induced (+) doxycycline treatment conditions as in a) Cells were harvested and analysed by immunoblotting with anti-Flag (for ectopic HDAC6), HR23B and actin. The example shown is representative of three independent experiments.

c) Flag-tagged HDAC6 inducible cells were treated with 3MA (10mM) and/or SAHA (10μM) at the for 24 hrs under non-induced (-) or induced (+) doxycycline treatment conditions (1μg/ml; induction for 72hr treatment). Cells were harvested and analysed by immunoblotting with anti-Flag (for ectopic HDAC6), HR23B and actin. The example shown is representative of three independent experiments.

d) Flag-tagged HDAC6 inducible cells were treated with bafilomycin at the indicated concetrations for 24 hrs under non-induced (-) or induced (+) doxycycline treatment conditions (1μg/ml; induction for 72hr treatment). Cells were harvested and analysed by immunoblotting with anti-Flag (for ectopic HDAC6), HR23B and actin. The example shown is representative of three independent experiments.

Because of the established role of HDAC6 in autophagy (see section 4.1) an alternative hypothesis was that HDAC6 may down-regulate HR23B via autophagosomal degradation. To test this hypothesis, two autophagy inhibitors, 3-MA and Bafilomycin were used in conjunction with HDAC6 ectopic overexpression to see if HR23B down-regulation still takes place if autophagy is inhibited (figure 4.6 c) and d)). Bafilomycin functions by specifically inhibiting the vacuolar H+ ATPase thus preventing acidification of the autophagosomal and lysosomal spaces which is important for their fusion [89]. 3-MA functions through inhibition of type III Phosphatidylinositol 3-kinases (PI-3K), which blocks autophagosome formation [165, 166]. Bafilomycin therefore inhibits autophagy at a late stage, whereas 3-MA inhibits early-stage autophagy [165]. Although a drawback of this experiment is the lack of control to test that autophagy inhibition is taking place, it gives an indication that HR23B down-regulation by HDAC6 continues to take place even when autophagy is inhibited, with two different inhibitors at various concentrations. This indicates that down-regulation of HR23B by HDAC6 is not via autophagy-mediated degradation. Treatment with autophagy inhibitors did not cause significant cell death in these cases (as observed by lack of floating cells on when cells were looked at prior to harvesting), perhaps because autophagy is required for cell survival only under specific conditions of stress and nutrient deficiency in tumours/in combination with other therapies.

In order to determine whether HDAC6 catalytic activity is required for its down-regulation of HR23B, a general HDAC inhibitor (SAHA) and an HDAC6 specific inhibitor (tubastatin [48]) were used in combination with HDAC6 overexpression

to see whether HR23B down-regulation still occurs (Figure 4.7 b) and c)). In both cases, HR23B levels were further reduced upon HDI treatment, suggesting that HDAC6 catalytic activity is not required for HR23B down-regulation.

Figure 4.7

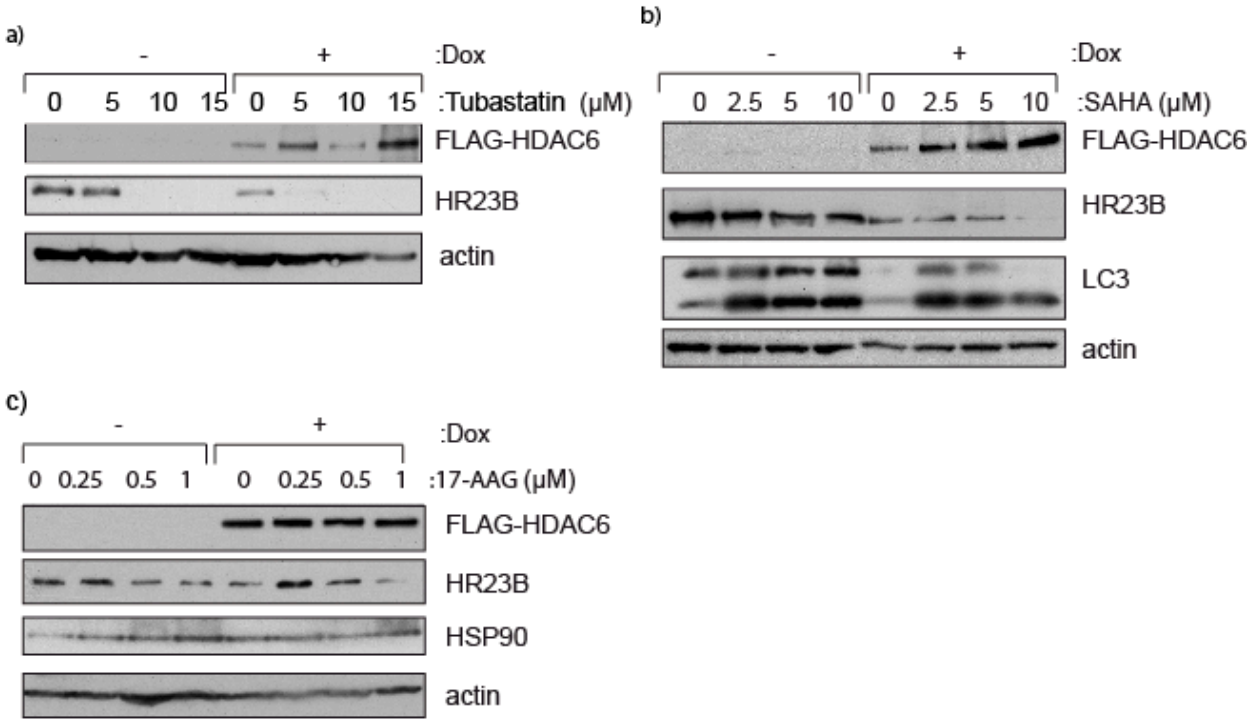

a) Flag-tagged HDAC6 inducible cells were treated with tubastatin at the indicated concetrations for 24 hrs under non-induced (-) or induced (+) doxycycline treatment conditions (1μg/ml; induction for 72hr treatment). Cells were harvested and analysed by immunoblotting with anti-Flag (for ectopic HDAC6), HR23B and actin. The example shown is representative of three independent experiments.

b) Flag-tagged HDAC6 inducible cells were treated with SAHA at the indicated concentrations for 24 hrs under non-induced (-) or induced (+) doxycycline treatment conditions (1μg/ml; induction for 72hr treatment). Cells were harvested and analysed by immunoblotting with anti-Flag (for ectopic HDAC6), HR23B, LC3 and actin. The example shown is representative of three independent experiments.

c) Flag-tagged HDAC6 inducible cells were treated with the HSP-90 inhibitor 17-AAG at the indicated concetrations for 24 hrs under non-induced (-) or induced (+) doxycycline treatment conditions (1μg/ml; induction for 72hr treatment). Cells were harvested and analysed by immunoblotting with anti-Flag (for ectopic HDAC6), HR23B, HSP90 and actin. The example shown is representative of three independent experiments.

In order to explore the mechanism through which HDAC6 downregulates HR23B, it was considered that HDAC6 may mediate this effect through interacting with additional proteins. To address this possibility, Flag-tagged HDAC6 was immunoprecipitated and the interacting proteins were analysed by mass spectrometry (performed by Dr Heidi Olzscha in collaboration with Dr Benedikt Kessler). A variety of interacting proteins came out of this analysis, including some that had been previously shown to interact with HDAC6, such as GRP78 and β-tubulin. An HDAC6 interacting protein of particular interest which was identified using this mass spectrometry analysis and previous studies was HSP90 [30]. This suggested the alternative possibility that HDAC6 may influence HR23B through the HSP90 chaperone network. It is known that heat-shock protein 90 (HSP-90) is a substrate of HDAC6 and the deacetylation of HSP-90 enhances ATP binding and thus promotes assembly of functional HSP-90 chaperone complexes [30]. The role of HSP-90 in the HDAC6-dependent down-regulation of HR23B was evaluated using the HSP90 inhibitor 17-AAG, historically the first HSP90 inhibitor that is being evaluated in clinical trials. [167]. HDAC6 fails to down-regulated HR23B when HSP90 activity is inhibited by 17-AAG (Figure 4.7c), which means that the HSP90 chaperone network is likely to be important in HR23B down-regulation by HDAC6. Interestingly, if HSP90 inhibition by 17-AAG is combined with tubastatin treatment (Dr Heidi Olzscha, personal communication and published in [168]), there is no longer an increase in HR23B on 17-AAG treatment.,.This suggests that that the catalytic activity of HDAC6 has a role in reactivation of HR23B under 17-AAG treatment. An interesting direction for further investigation from these results would be to

determine how exactly HDAC6 prompts down-regulation of HR23B through the HSP90 chaperone network, a line of investigation currently ongoing in the group.

In addition, immunoprecipitation using the stable FLAG-HR23B inducible cell line showed that endogenous HDAC6 interacts with ectopic FLAG-tagged HR23B (Dr Geng Liu, personal communication). This interaction may explain the negative regulation of HR23B protein levels by HDAC6; or it may assist the transport roles of HR23B in transporting ubiquitinated proteins to the proteasome, and HDAC6 in transporting proteins for autophagy [37].

HR23B is made up of one ubiquitin-like domain (UbL) and two ubiquitin-associated domains (UbA1 and UbA2), whereas HDAC6 consists of two catalytic domain and a ubiquitin-binding BUZ domain. It is possible that it is the ubiquitin-binding BUZ domain interacting with the ubiquitin-like UbL domain which is responsible for the direct interaction. While this is a likely interpretation of the experimental results above, other possibilities include the binding of ubiquitinated regions of HR23B to the BUZ domain, or a ubiquitinated region of HDAC6 binding to the UbA domain of HR23B.

4.6 Conclusion. HDAC6 and HR23B interplay are responsible for autophagy/apoptosis choice on HDI treatment

Autophagy has been shown to be initiated by forms of treatment including chemotherapy and radiation during cancer treatment where it is thought to represent tumour cell survival against apoptosis [169]. HDI treatment also causes autophagy, which could be a tumour cell survival mechanism and an alternative cell fate to apoptosis. Both previous studies and my experiments have shown HDAC6 to have an important role in autophagy progression [14], whereas HR23B appears to influence the biological outcome of HDI treatment, with higher levels of HR23B correlating to lower levels of autophagy and higher levels of apoptosis (Chapter 3). This lead to the hypothesis that HDAC6 and HR23B may act together to determine whether cells undergo apoptosis or survive through autophagy on HDI treatment. It was subsequently determined that HDAC6 interacts with and down-regulates HR23B through the HSP90 chaperone network (Chapter 4), and it seems reasonable to suggest that the cell fate choice between autophagy and apoptosis on HDI treatment may depend on the relative levels of HDAC6 and HR23B – if HDAC6 levels are high and HR23B is down-regulated, cells are more likely to undergo autophagy and survive, whereas if HDAC6 is low and HR23B is high cells are likely to undergo apoptosis on HDI treatment.

Having investigated several avenues by which HDAC6 may down-regulate HR23B, we have shown that the down-regulation of HR23B by HDAC6 requires HSP90 activity and can be overcome by treatment with the HSP-90 inhibitor 17-AAG. The role of HDAC6 in control of HSP90 chaperone activity is already established. HDAC6 interacts with HSP90 and deacetylates it, which is required

for the interaction of HSP-90 with the critical cochaperone p23 [30]. In the absence of HDAC6, or when its catalytic activity is inhibited, stable client protein complexes are not formed and key HSP-90 client signalling proteins such as the glucocorticoid receptor cannot undergo maturation and transport to the nucleus [30]. My results suggest that the regulation may also function in reverse, i.e. Hsp90 activity is required to ensure HDAC6 can act to down-regulate of HR23B, although further investigation is needed to confirm this hypothesis. For example, HDAC6 could be acting on Hsp90, which in turn binds HR23B which causes its degradation. A remaining question is how HR23B degradation is carried out, if it is not via the proteasome or autophagosome.

HDAC6 is a microtubule-associated deacetylase and regulated microtubule-dependent protein transport [37], and there has been evidence that Hsp90 is also associated with microtubules [170], which facilitates client protein transport to the correct compartments by way of microtubules. It is possible therefore, that HR23B down-regulation by HDAC6 also takes place via this route and requires the microtubule-associated Hsp90. It is important to note, however, that inhibition of HDAC6 catalytic activity by tubastatin treatment did not affect HR23B down-regulation, so it is possible that there is an alternative type of non-acetylation dependent interplay between HDAC6 and HSP90, different to the one which is already established in which HDAC6 regulates HSP90 by deacetylating it. It may be that HDAC6 acts as a link between proteasome and chaperone activity, which allows it to down-regulate HR23B. Further investigation of the specific mechanisms involved needs to be carried out in order to determine the role HSP90 plays in the down-regulation of HR23B by HDAC6.

Interestingly, there has been evidence that inhibition of HSP-90 with compounds like 17-AAG, or siRNA mediated depletion of HSP90 or HDAC6 can inhibit tumour progression by destabilising the macrophagy migration inhibitory factor, a client of HSP90 which correlates with poor prognosis [171]. Findings such as these highlight the potential clinical applications of this study, as there is a possibility that HR23B in combination with HDAC6 and HSP90 catalytic activity could provide a biomarker signature which may allow clinicians to differentiate between tumours with different prognosis on HDI treatment. Tumours in which HR23B levels are high and HDAC6 is low are likely to respond to HDI treatment, whereas tumours where HDAC6 is high, and HR23B is down-regulated, and HSP90 is inactive are more likely to survive via autophagy than undergo apoptosis. However, extensive validation of these ideas through patient sample analysis is required to find a statistically significant correlation between levels of the proteins investigated and HDI treatment response.

CHAPTER 5.Myd88 as an HDI sensitivity determinant and effect of Myd88-mediated inflammatory cytokine release on cell fate during HDAC inhibition

5.1 Myd88 inHDI response and Toll-like receptor signalling

Myd88 has been identified as a potential biomarker for HDI treatment in the same shRNA screen as HR23B [15], and and its primary known role is as an adaptor in Toll-like receptor (TLR) signalling as part of the inflammatory response [128] and as a component of Ras signalling [10], both processes which are especially interesting given the increasing understanding of the important role of inflammation in carcinogenesis [149]. The initial goal of this part of study is to confirm Myd88 as a sensitivity determinant to HDI treatment, by varying its levels and observing to impact on cell apoptosis and cell proliferation ability on HDI treatment.

Myd88 was initially discovered in 1990 as a myeloid differentiation primary response gene [172], after which the homology between Myd88 and cytoplasmic Toll like receptors in Drosophila was noticed, suggesting Myd88 may play a part in signal transduction during immune system activation [173]. The best current known role of Myd88 is as an adaptor protein in Toll-like receptor (TLR) signalling. The mammalian TLR family consists of at least 11 members, of which some are located on the cell membrane and others in lysosomes. TLRs stimulate essential signalling pathways as part of innate immunity on recognition of patterns which are conserved in microbes, but not present in mammals [174]. These activated signalling pathways result in expression of genes which are required for further development and control of the immune response [174].

Regulation of the TLR signalling pathway is carried out by a number of adaptor proteins containing toll-like receptor interacting (TIR) domains, such as TRIF, TRAM and Myd88 [174]. All TRLs, except TLR3 have been shown to be activated in a Myd88-dependent manner [175] (see introduction section 1.13 for more detail). Myd88 has shown to be required for phagocytosis of bacteria including *Escherichia coli* and *Staphylococcus aureus* as this process is impaired in its absence due to impaired phagosome maturation [176]. Patients deficient in Myd88 suffer a predisposition to severe bacterial infection, produce low levels of IL-6, and have a decreased ability to increase concentration of plasma C-reactive protein [177].

TLR-receptor signalling results in production of a number of cytokines. IL-6 is an NF-κB-regulated cytokine that acts as a tumour promoter by enhancing proliferation of tumour-initiating cells, effects which are mediated by the transcription factor Stat3 [133, 178]. Interestingly, there has been evidence that abolishing Myd88-related IL-6 production reduces risk of liver cancer in men where it is more prevalent compared to women [179].

The next aim of my study at this stage has been to investigate the mechanisms by which pre-treatment Myd88 levels impact on the cell fate outcome of histone deacetylase treatment. To achieve this, I have investigated the role of Myd88 as a TLR protein adaptor and determined how this role is important in governing the Myd88-mediated cell fate outcome on SAHA treatment.

5.2 Myd88 levels impact on apoptosis and colony formation ability on HDI treatment

Myd88 was identified alongside HR23B in the genome-wide loss-of function screen as a sensitivity determinant for HDI-based therapy [41], and few subsequent experiments were performed to confirm whether its levels are indeed important in cell fate determination on HDI treatment. It was therefore of interest to determine whether its levels also impacts on cell death and proliferation ability on HDI treatment.

To investigate this, a U2OS cell line was created in which expression of stable ectopic Flag-tagged Myd88 was under conditional control (induction upon doxycycline treatment), in a Tet-on system identical to the one used by Susan Fotheringham to create the Flag-HR23B inducible cell line. This system was then used to determine the correlation between cellular Myd88 levels and apoptosis on HDI treatment. Similarly to ectopic HR23B overexpression (see section 3.2) increased levels of Myd88 correspond to increased PARP cleavage at 2.5 and 5μM SAHA (Figure 5.1a), although this is not seen at 10 μM SAHA and increased cleaved caspase 3 levels at 2.5, 5 and 10 μM SAHA. Myd88-overexpression alone however does not seem to lead to apoptosis as measured by PARP cleavage (Figures 5.1a), b), c), suggesting that Myd88 levels impact on whether cells undergo apoptosis or not specifically on SAHA treatment. In addition to the inducible cell line, a stable cell line was created where PCMV-Flag-Myd88 (subsequently referred to as Flag-Myd88) was continuously expressed at high level in G418-enriched media, alongside a control PCMV-expressing cell line (Figure 5.1b). Treatment of these cell lines with SAHA also results in much higher levels of apoptosis as shown by cleaved PARP levels in the cells where Flag-Myd88 is overexpressed (Figure 5.1b)

To analyse the role of Myd88 in cell survival in real time, the real-time xCELLigence cell monitoring system was used to assess the number of viable adherent cells, represented by cell index. Cells were plated at 1000 cells/well into E-plate 16 and analysed by an xCELLigence RTCA DP instrument. Electronic sensors provide quantative measurement of the cell index every 15 mins for up to 72 hrs, which is an indication of the number of cells attached to the electrodes and thus their viability. Following the continuous xCELLigence cell monitoring, the slope (which represents the rate of change of the cell index) was calculated from time 12–66 h (i.e., when changes in cell viability were apparent) and presented graphically. In cells with higher levels of Myd88, the cell index decreases nearly twice as fast as in cells with low Myd88 levels on SAHA treatment, suggesting Myd88 levels are important in cell survival (Figure 5.1 c) i). The batch of cells used for the assays were harvested and the levels of Flag-Myd88 protein is shown by immunoblot, with actin loading control and cleaved PARP to indicate apoptosis levels.

Figure 5.1

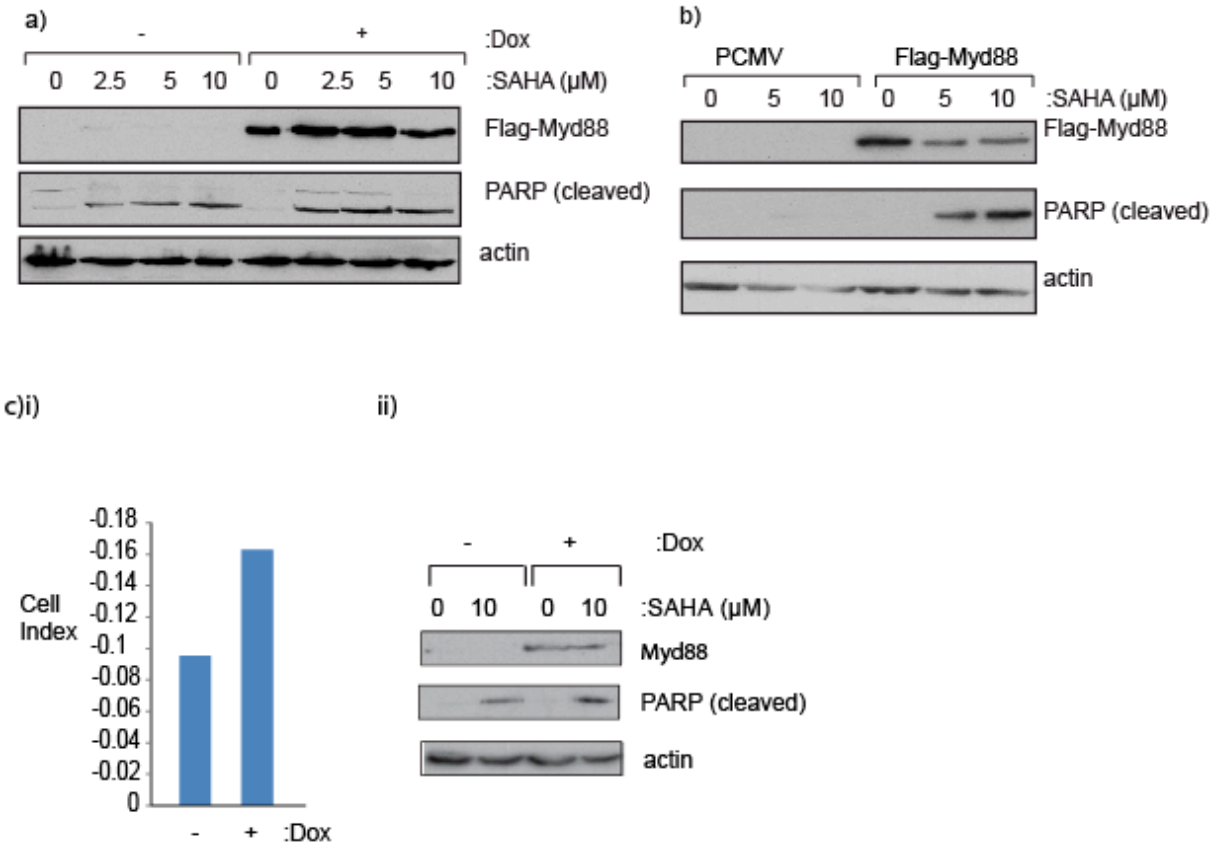

a) U2OS cells stably expressing inducible Flag-tagged Myd88 were treated with SAHA at indicated concetrations for 24 hrs under non-induced (-) or induced (+) doxycycline treatment conditions, prior to immunoblotting with anti-Flag (for ectopic Myd88), cleaved PARP and actin as indicated. The example shown is representative of three independent experiments.
b)U2OS stable Flag-Myd88 or PCMV expressing cells were treated with SAHA at the indicated concetrations for 24hrs and immunoblotted as indicated. The example shown is representative of three independent experiments.
c) U2OS cells stably expressing inducible Flag-tagged Myd88 were treated with SAHA (10μM) under non-induced (-) or induced (+) doxycycline treatment conditions and plated 1,000 cells/well into E-plate 16 and analyzed using a xCELLigence RTCA DP instrument. Following the continuous xCELLigence cell monitoring, the slope (which represents the rate of change of the cell index) was calculated from time 12–66 h (i.e., when changes in cell viability were apparent) and presented graphically (i). The levels of Flag-Myd88 protein is shown by immunoblot, with actin loading control and cleaved PARP to indicate apoptosis levels at 24hrs (ii). The example shown is representative of three independent experiments.

The role of Myd88 was further evaluated by measuring the effect of increasing its levels in CFAs, in the presence and absence of two SAHA concentrations. The expression of ectopic Myd88 (+ Dox in figure 5.2a) caused a markedly enhanced growth inhibitory effect of the drug compared to uninduced (- Dox) cells, reflected as a reduction in cell colony formation number. This reduced number of colonies is seen both at 5, 10 and 20 μM SAHA treatment (for 24hrs) under conditions of Myd88 overexpression, but the doxocyclin addition alone does not have an effect on colony number. It was important to consider effect of doxocyclin addition alone as a control both here and in other experiments with the Myd88-inducible cell line, as doxocyclin is an antibiotic and may cause a slower rate of proliferation, as well as changes of metabolism at high enough doses [155], and that CFA assays do not give a direct measure of cell death (as discussed in section 3.3).

Myd88 siRNA depletion also results in a reduced sensitivity to SAHA treatment, as shown by sub-G1 levels on FACS analysis (see figure 5.2 c)ii). The depletion of Myd88 was confirmed by immunoblotting (Figure 5.2c))i). To summarise so far Myd88 has not been previously shown to be a potential sensitivity determinant, but this is a conclusion I can make from my data, as Myd88 overexpression leads to increased apoptosis levels on SAHA treatment, and Myd88 depletion coincides with decreased apoptosis on SAHA treatment.

Figure 5.2

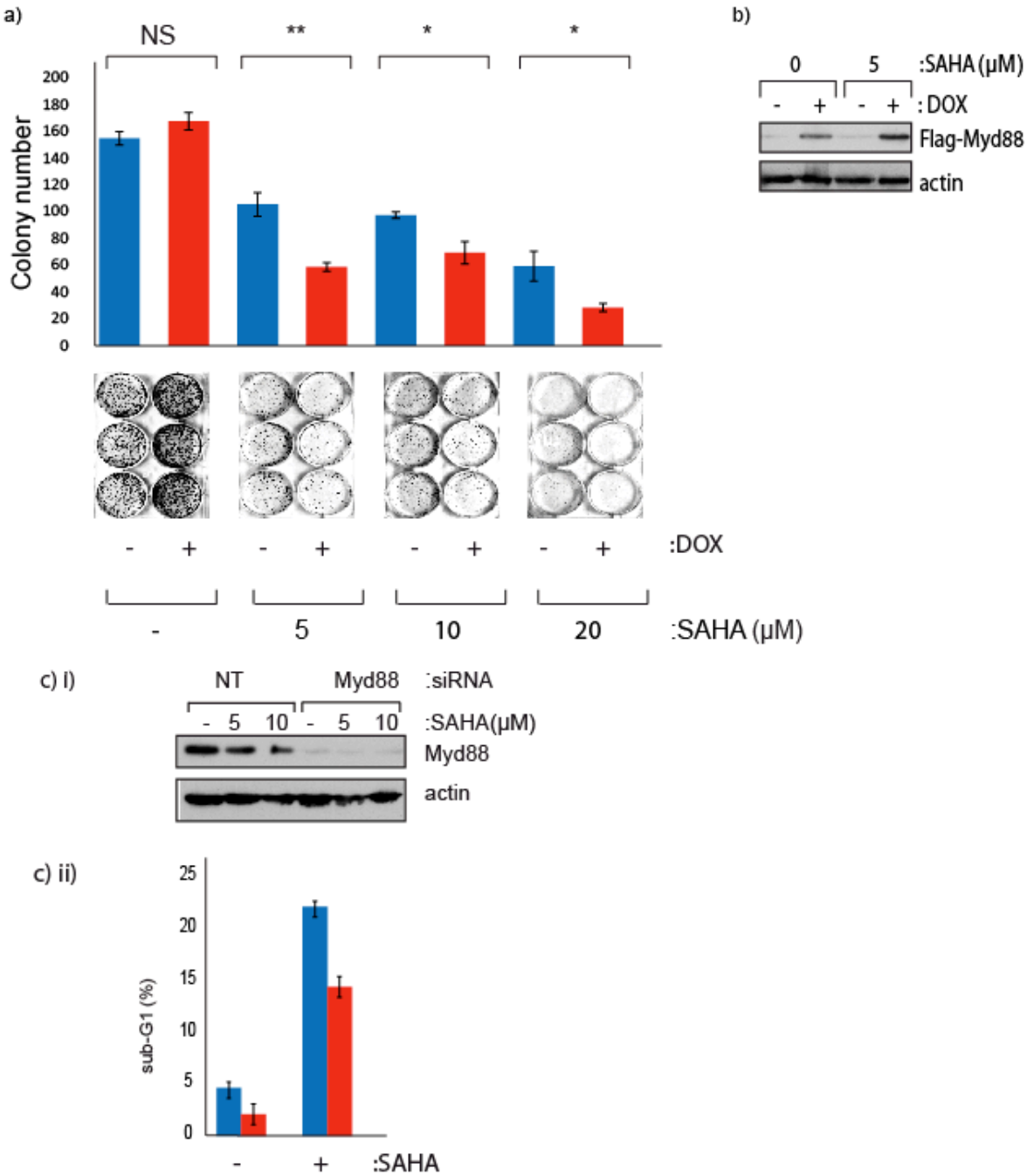

a) U2OS cells stably expressing inducible Myd88 were grown in triplicate in the absence (-) or presence (+) of doxycycline together with SAHA (indicated concentration in μM) and, after 9 days, the number of viable cell colonies assessed by crystal violet staining. The untreated control cells are shown for comparison. Qunatification of colony numbers is shown above the colony assay plate photographs as a bar chart. Statistical analysis was performed on the colony numbers by using the student t-test. Ns: non-significant difference P≥0.05 (P=0.7 in this case). * P≤0.05 difference is statistically significant ** P≤ 0.01difference is very statistically significant. The example shown is representative of three independent experiments.

b) Immunoblot showing levels of ectopic Flag-Myd88 in the same batch of cells as used in the CFA.

c) i) U2OS cells were treated with Myd88 or non-targeting control (NT) siRNA (50nM for 72 hrs in the presence (+) or absence (-) of SAHA (5 and 10μM for 24hrs) and immunoblotted with ani-Myd88, and anti-actin antibody. ii) The levels of sub-G1 cells as an apoptosis indicator was determined by FACS analysis for the 5μM SAH concentration. The example shown is representative of three independent experiments.

For a potential biomarker, it is of interest to investigate protein presence and variation in levels in tumour tissue (as discussed for HR23B in section 3.7), so IHC was performed on a limited number of available tumour tissue (images for two peripheral T-cell patients shown in figure 5.3 a). Myd88 is a cytoplasmic protein, so it's localisation in Patient 1 is cytoplasmic as expected, although Patient 2 appears to have Myd88 both in cell cytoplasm and nucleus, suggesting there may be non-specificity in staining (although the same antibody concentration and conditions were used for both patients. In order to optimise the antibody used in IHC and verify it's specificity for Myd88, FFPE embedded cell pellets were made from cells treated with non-targeting and Myd88 siRNA, and stained with the Myd88 antibody at several concetrations, as well as an IgG control (Figure 5.3b). This showed that the optimal antibody dilution to use is 1:800, as this is when a clear difference in staining can be seen between the cells which are non-targeting siRNA treated and those which are Myd88 siRNA treated. However, nuclear Myd88 staining can be seen even at the lowest concentration of antibody used, which indicates further optimisation of the IHC with Myd88 is needed before commencing a large-scale study with relevant human tissue to confirm it's role as a biomaker.

Figure 5.3

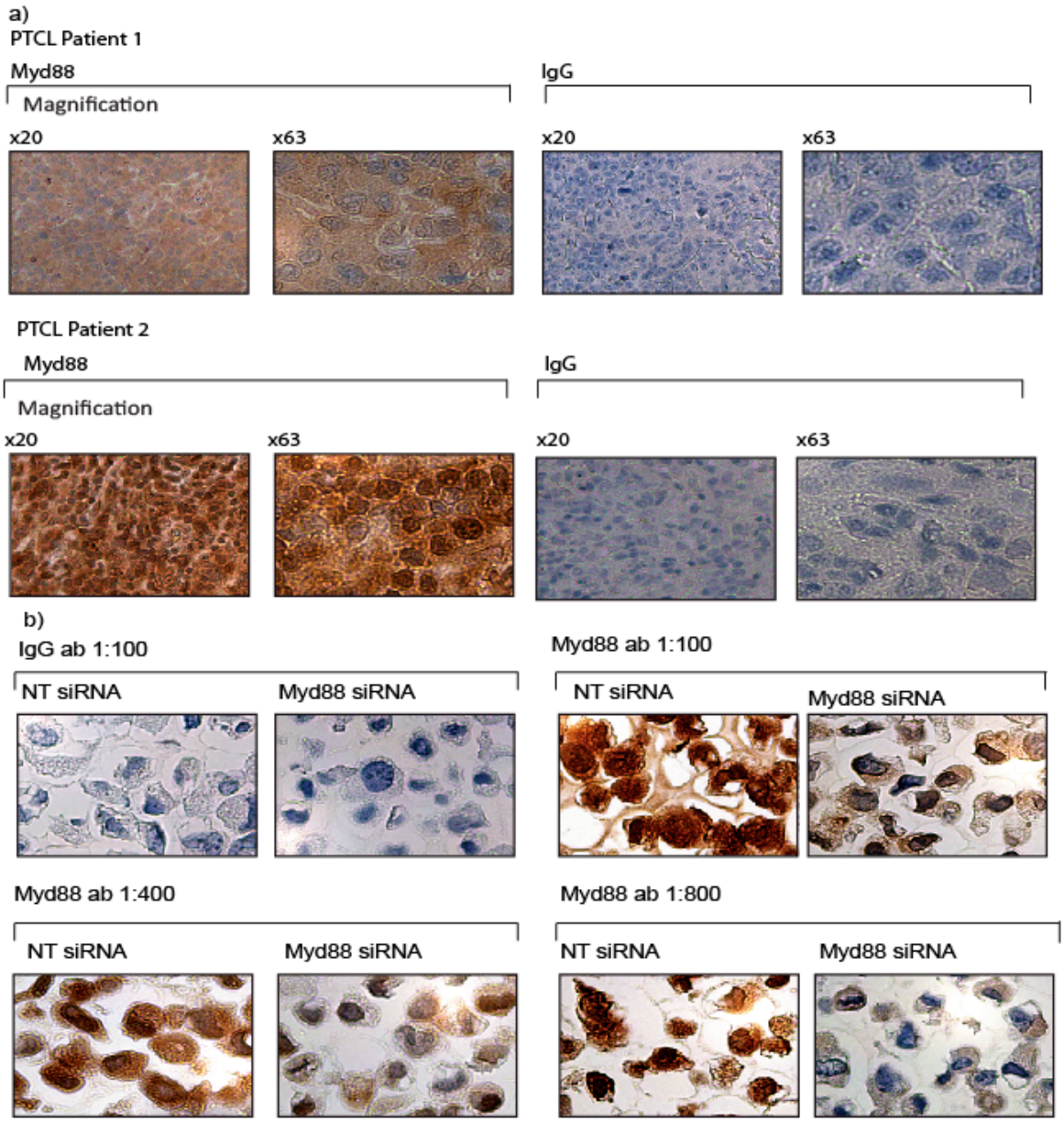

a) IHC staining with performed as described (Materials and Methods, Section 2.11) on 10 FFPE (formalin fixed paraffin embedded) patient sections with the Myd88 and IgG antibodies. Images of slides from two patients shows, at 20x and 63x magnifications
b) U2OS cells were transfected with control (NT) or Myd88 siRNA (both at 50nM) for 48hr, cells harvested by trypsinisation and cell pellets embedded in paraffin prior to sectioning. IHC was then carried out at indicated Myd88 antibody concentrations as part of antibody optimization.

5.3 Myd88 in TLR activation through Bcl-xl

Nuclear factor of kappa light polypeptide gene enhancer in B cells (NF-κB) activation is an outcome of the activation of all TRL signalling pathways, which in turn results in up-regulation of B-cell lymphoma apoptosis regulator xL (Bcl-xl) [180] [181].

In order to show that in the experimental system used Myd88 does function as a component of TLR signalling, reporter assays were performed with the Bcl-xl reporter plasmid (kind gift of Neil Perkins, as used in [182]), which gave a measure of Bcl-xl transcription activation as a function of relative luciferase activity. Transfection of Flag-tagged wild-type Myd88 resulted in a significant increase in relative luciferase activity compared to PCMV transfection alone, suggesting that the NF-κB pathway and therefore Bcl-xl transcription activation takes place when Myd88 levels are increased (Figure 5.4 a) i), consistent with the established role of Myd88 in TLR signalling [175]. This gives evidence that ectopic Myd88 expressed as a result of transfection with the Myd88 plasmid used for this study is functional, and gives further validity to the investigation. When cells expressing high and low levels of Myd88 are also treated with the general HDI SAHA, relative luciferase activity decreases both in PCMV and Flag-Myd88 transfected cells, possibly to reflect the increase in cell death and cell cycle arrest which takes place as a result of HDI treatment (Figure 5.4ai). However, in SAHA-treated cells there is also a significant difference in levels of relative luciferase activity between PCMV and Flag-Myd88 transfected cells – luciferase activity is higher if Myd88 levels are higher, which is to be expected considering

the established role of Myd88 as a TLR signalling adaptor. This reporter assay was performed in triplicate plates for each condition and the corresponding immunoblot for the cells used is shown in Figure 5.4a) ii). This is a necessary control to ensure transfection of Flag-Myd88 with similar levels being expressed in the triplicate plates, which is shown by the immunoblot (Flag-Myd88 in Figure 5.1a ii), although there is a slight decrease in Flag-Myd88 levels in SAHA treated compared to untreated cells. Note also the higher levels of PARP cleavage (PARP (Cl) in Figure 5.4a ii) and therefore apoptosis in Flag-Myd88 transfected cells compared to the PCMV control again confirming that Myd88 levels impact cell fate on HDI treatment (as shown in section 5.2).

Figure 5.4

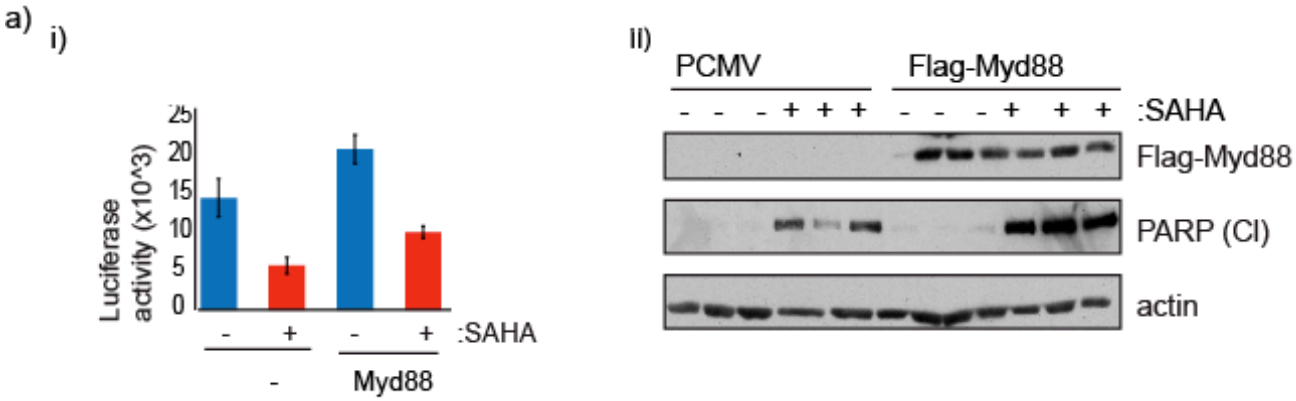

a) i)U2OS cells were plated and transfected with the bcl-xl reporter plasmid at 200ng (a kind gift from Neil Perkins), along side PCMV (-) and Flag-Myd88 (Myd88) expression vectors (1µg) for 48hrs, and treated with 10µM SAHA for another 24 hrs. The effect on Bcl-xl-luciferase was measured. The luciferase activity is shown relative to co-transfected pCMV-βgal expression (i), together with the level of ectopic proteins for each plate (ii). Example shown is representative of three independent experiments.

5.4 Myd88 in inflammatory cytokine release

Myd88 is essential for inflammatory cytokine release mediated by TLR signalling for most members of the TLR family [128]. The next stage of the investigation into why Myd88 levels affect cell outcome on SAHA treatment, was to determine whether and how manipulation of Myd88 levels affects cytokine release, both in untreated cells and in cells treated with HDIs. For this purpose a kit (Human inflammatory cytokine kit BD™ Cytometric Bead Array (CBA)) was used to monitor levels of six inflammatory cytokines: IL-10, IL-8, IL-6, TNF-α, IL-12P70 and IL-1β in the media of the cells after SAHA treatment both with and without Myd88 induction (Figure 5.5). The experiment was performed to include triplicate plates per condition in which the Flag-Myd88 inducible cell line was treated with DMSO, and SAHA for 24hrs in the presence and absence of doxycycline to induce ectopic Myd88 expression, after which media was collected from the cells and the levels of 6 inflammatory cytokines were measured. The BD™ Cytometric Bead Array (CBA) works by providing 6 specific antibodies against each of the six inflammatory cytokines to be measured, each of which is conjugated to a capture bead with a distinct fluorescence intensity. The six bead populations are mixed and incubated with the fluid to be analysed (cell media in this case), during which complexes are formed between the capture bead, the analyte (inflammatory cytokine) and the detection reagent, which provides a fluorescent signal that can be measured using flow cytometry. The signal produced is proportional to the amount of inflammatory cytokine present, and subsequently levels of all inflammatory cytokines were plotted relative to the DMSO-treated Myd88-uninduced cells (Figure 5.5).

The relative levels of the six inflammatory cytokines measured are shown in Figure 5.2, where cytokine levels in cells with Myd88 levels induced through doxycycline addition are in represented by red bars, and those in uninduced cells by blue bars. A media alone control was used alongside the supernatants from tissue culture plates (green bar in Figure 5.5), as inflammatory cytokines may have been present in the fetal calf serum added to the media in which cells are grown. Levels of TNF-α, IL-12P70, IL-10, and IL-1ß levels in the media alone were relatively similar to their levels in the media removed from the cells (Figure 5.5 c) d) e) f)), and no differences are seen on Myd88 induction or SAHA treatment, so assays involving investigation of these cytokines were not pursued further. The cytokines which change in a significant way on Myd88 induction are IL-6 (Figure 5.5a)) and IL-8 (Figure 5.5b)). In addition, the levels of these cytokines are significantly different in the cell media compared to the media alone control. A six-fold increase in IL-6 levels is seen on Myd88 induction (Figure 5.5a), and a 3-fold increase in IL-8. This is consistent with published literature, where Myd88 has been shown to be required for NF-κB activation and IL-6 and IL-8 production, although this is cell type dependent: for example it is the case in fibroblasts and endothelial cells, but not macrophages [185]. IL-6 levels reduce dramatically on SAHA treatment, in particular in Myd88-induced cells (Figure 5.5a), where the level of IL-6 in DMSO-treated cells in 12-fold that of SAHA treated cells. This is also consistent with published literature, where treatment with the general HDAC inhibitor TSA as an anti-inflammatory drug in mouse studies has been shown to correlate with a decreased expression of both IL-6 protein and it's mRNA [186] [187]. However, if a comparison is made between

SAHA treated cells where Myd88 levels in induced, and those where it is uninduced, IL-6 levels are about twice as high in Myd88 induced cells.

On the contrary, SAHA treatment correlates with a 4-fold increase in IL-8 expression in Myd88 uninduced cells, and also a slight increase in Myd88 induced cells. This observation is also consistent with published literature, as it has been seen that treatment of MCF-7 (breast cancer) cells with the general HDAC inhibitor TSA has caused an upregulation of IL-8 mRNA and protein levels, which is thought to be due to a role for HDACs in the control of IL-8 promoter [188]. However, studies in U2OS cells of IL-6 and IL-8 expression on SAHA treatment have not been performed to my knowledge at the time of writing.

Figure 5.5

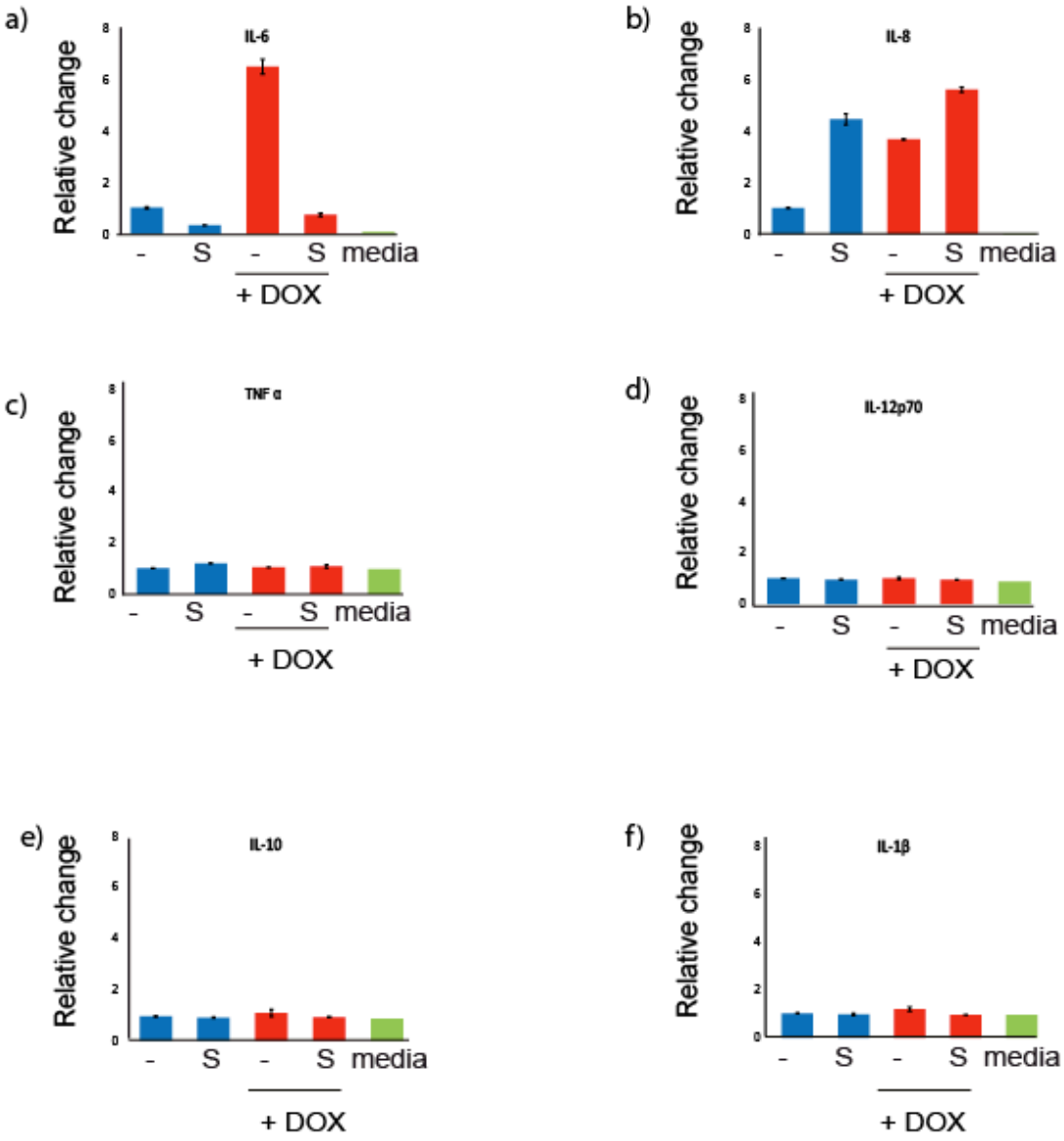

U2OS cells expressing inducible Flag-tagged Myd88 were treated with SAHA (10μM) for 24hr under non-induced (-) or induced (+) doxycycline treatment conditions (1μg/ml; induction for 72hr treatment), and relative levels of the indicated cytokines (IL6, IL8, THF, IL12, IL10 and IL1) in the tissue culture media were measured using BD™ Cytometric Bead Array (CBA) human inflammatory cytokine measurement kit. Mean values from triplicate plates are shown. Example shown are representative of three independent experiments.

Absolute concentrations in pg/ml of IL-6 in cell media for a similar experiment as that in Figure 5.5 are shown in figure 5.6 and show a similar pattern to the fold-changes in Figure 5.5a). Absolute concentrations were obtained by plotting a standard curve of known cytokine concentrations using different concentrations of recombinant cytokines supplied with the CBA inflammatory cytokine measurement kit (not shown). The corresponding immunoblot from these cells which shows Flag-Myd88 induction is shown in figure 5.6b). Velcade treatment was used in addition to SAHA treatment for this particular experiment, because Myd88 was considered as a potential biomarker to proteasome inhibition as well as HDI treatment, although this line of investigation was not pursued further.

Figure 5.6

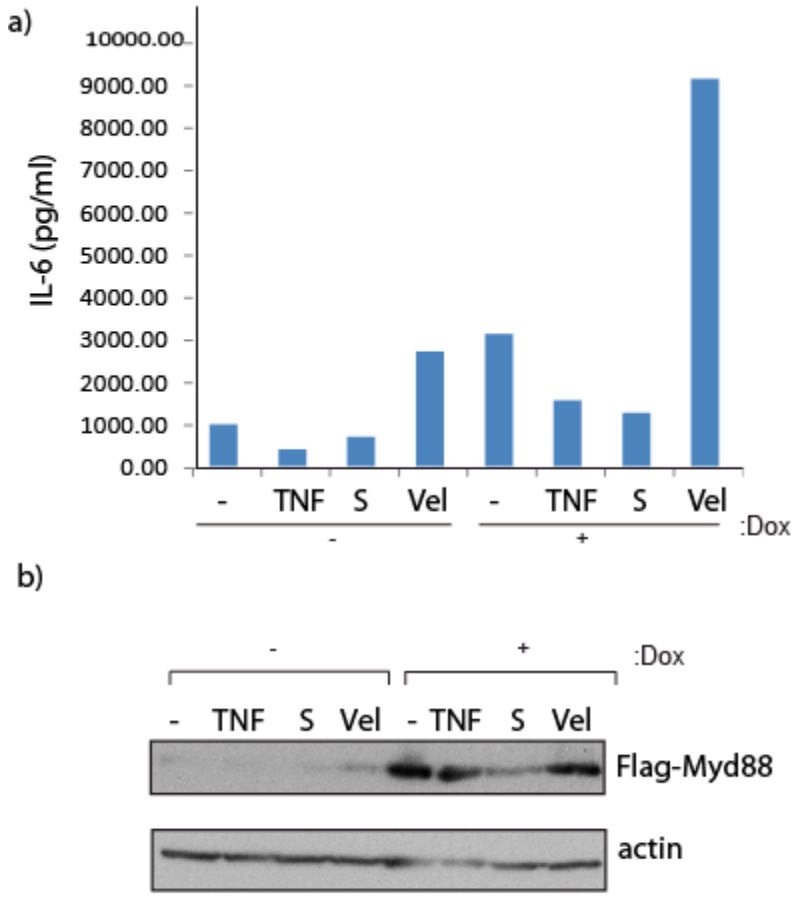

a) U2OS cells expressing inducible Flag-tagged Myd88 were treated with SAHA (10μM), TNF-α or velcade (100nM) for 24hr under non-induced (-) or induced (+) doxycycline treatment conditions (1μg/ml; induction for 72hr treatment), and relative levels of the indicated cytokines (IL6, IL8, THF, IL12, IL10 and IL1) in the tissue culture media were measured using BD™ Cytometric Bead Array (CBA) human inflammatory cytokine measurement kit. Concentrations of interleukin-6 in pg-ml are shown. Concentrations obtained from plotting a standard curve with known cytokine concentrations and FCAP_v3 CBA software analysis. Example shown are representative of three independent experiments.

b) Levels of ectopic protein from the plates of stably expressing inducible Flag-tagged Myd88 shown in a).

Having confirmed that cellular Myd88 levels impact on cell fate upon SAHA treatment (section 5.2) and gained evidence that Myd88 levels impact inflammatory cytokine release both in the presence and absence of SAHA (section 5.4) the next stage of the project was to test whether this cytokine release is necessary for Myd88 to play its role in the determination of cell fate on HDI treatment, specifically apoptosis.

5.5 Interleukin-6 and Myd88

The most interesting changes on Myd88 overexpression are seen in levels of IL-6 and IL-8 (Figure 5.5, 5.6). In order to investigate specifically whether Myd88-dependent high levels of these cytokines are needed for the higher levels of apoptosis seen in SAHA-treated Myd88 induced cells, compared to uninduced, specific antibodies were acquired with have previously been used to effectively deplete IL-6 and IL-8 in cell culture ([189] for IL-6 and [190, 191] for IL8).

Treatment with IL-6 neutralising antibody reduced Myd88-dependent apoptosis as measured by cleaved PARP and cleaved caspase levels in SAHA-treated cells where levels of Myd88 are induced by doxycycline addition (Figure 5.7a), which suggests that the impact Myd88 has on SAHA-treated cells may be connected to IL-6 release. Recombinant IL-6 was used to test whether its addition has an impact on apoptosis levels in SAHA treated cells, in order to see whether it is possible that an increase in concentration of this cytokine could lead to cell death as well as it's already established role in cell proliferation [133]. However, there were no differences seen in apoptosis levels on SAHA treatment in Myd88 induced or uninduced cells (data not shown), which may be due to the recombinant IL-6 not being active or at a suitable concentration. Media addition from DLBCL cells producing high levels of IL-6 to cells where IL-6 production is naturally low caused an increase in apoptosis on SAHA treatment (personal communication with Dr Semira Sheikh, Laboratory of Cancer Biology, Department of Oncology). These results support the model of high Myd88-dependent IL-6 release contributing to cell death on SAHA treatment, although

pro-apoptotic factors may be present in such conditioned cell media, so these observations may not be due to IL-6 addition.

Interestingly, IL-6 neutralisation in cells where Myd88 levels are low (no induction through doxycycline addition), leads to an increase in PARP cleavage on SAHA treatment compared to cells where SAHA treatment alone is carried out. It is difficult to provide an explanation for this observation, as IL-6 levels are relatively low in Myd88 uninduced cells (Figure 5.5). One possibility may be that the IL-6 neutralising antibody is exerting a non-IL-6 specific effect such as non-specific binding to other cytokines, the levels of which have not been investigated or even other extracellular proteins.

IL-8 neutralisation did not cause any changes in apoptosis on SAHA treatment in Myd88-induced cells, as measured by cleaved caspase 3 levels in Figure 5.7 b). This suggests that it is IL-6, rather than IL-8 with is the cytokine important in the sensitivity determinant role of Myd88. Note also the higher levels of PARP and cleaved caspase 3 in SAHA-treated cells which are Myd88 induced, compared to uninduced cells, in both Figure 5.7a) and b), in the absence of any cytokine neutralisation. This provides further evidence for the sensitivity determinant function of Myd88 in the case of SAHA treatment.

Figure 5.7

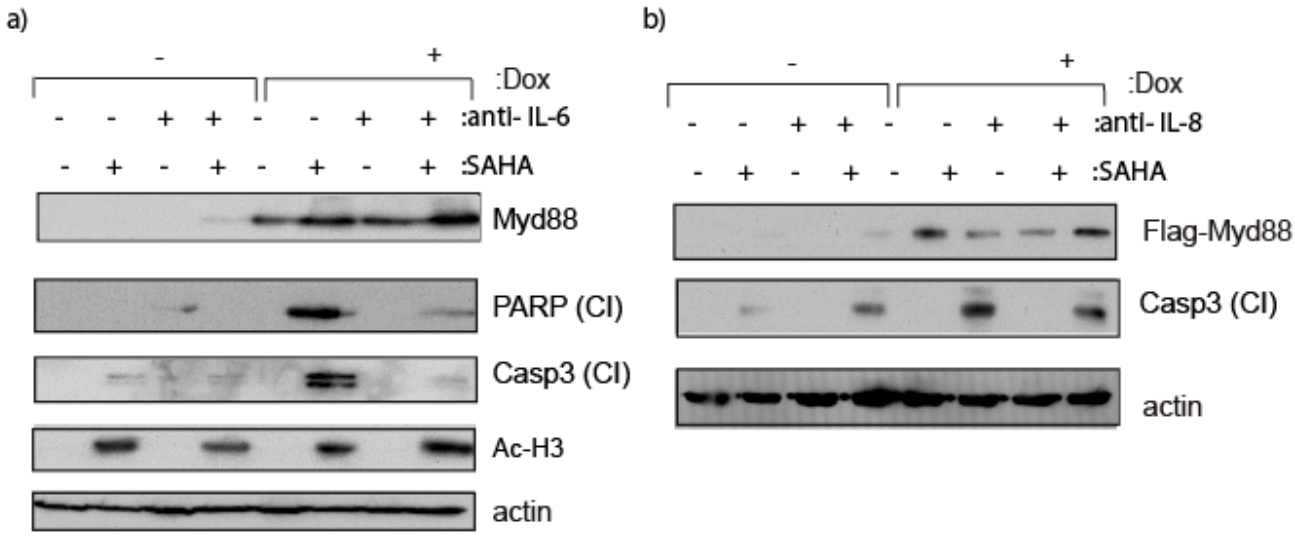

U2OS cells expressing inducible Flag-tagged Myd88 were treated with SAHA (10μM; +) and IL-6 (a) or IL-8 (b) neutralising antibody (2μg/ml) for 24hr under non-induced (-) or induced (+) doxycycline treatment conditions (1μg/ml; induction for 2hr treatment). Cells were harvested and immunoblotted with anti-Flag (for ectopic Myd88), cleaved PARP, cleaved caspase 3 and actin antibodies as indicated. Example shown is representative of three independent experiments.

5.6 Effect of Myd88 levels on S-phase

Chemotherapeutic drugs frequently induce tumour cell death in a cell cycle-dependent manner [192], and S-phase in particular. For example, camptothecin is an inhibitor of topoisomerase I which is required for DNA unwinding during replication, and cells in S-phase are 100-1000 times more sensitive to camptothecin than those in G1 or G2 phases of the cell cycle [192].

As discussed in introduction section 1.5, HDAC inhibitor treatment affects cells in S-phase though disruption of the spindle assembly checkpoint and chromosomal passenger proteins such as BubR1, CENP-F and CENP-E [65]. In addition, there has been evidence showing that various HDACs are essential for S-phase to take place, for example HDACs1 and 2 are recruited to the replication fork and are needed for its progression and maintenance of nascent chromatin structure as they maintain the correct balance of histone deacetylation [193]. Similarly, deletion of HDAC3 caused changes in epigenetic modifications including altered H3 K9/K14 methylation, changes in chromatin structure and changes in apoptosis, which revealed that this histone deacetylase is also important in S-phase progression [194].

The requirement of HDACs for S-phase regulation and progression lead to the hypothesis that cells in S-phase may be particularly sensitive to HDI treatment. As Myd88 has been has been shown to be required for proliferation [195] and NF-κB activation has been shown to have a role in proliferation ranging from T- and B-cell differentiation to limb development, it seemed reasonable to suggest that Myd88 may alter sensitivity to SAHA by altering the percentage of cells

undergoing cell division. In order to test this hypothesis, incorporation of the nucleoside analogue bromodeoxyuridine (BrdU) into cells was used as a measure of the percentage of cells in S-phase (Figure 5.8a). However, overexpression of Myd88 alone did not cause any significant changes in the percentage of cells undergoing S-phase. Similarly, there were no clear differences between SAHA-treated cells where Myd88 was induced and uninduced. As expected, the number of cells in S-phase decreased significantly on SAHA treatment from 55% in untreated cells to 15% in treated cells (Figure 5.8b), but this decrease took place both in cells with low and high Myd88 levels. HDI treatment reduces the number of cells in S-phase due to a greater percentage of cells in sub-G1, (as discussed in Introduction 1.5), and due to the importance of various HDACs such as 1,2 and 3 in S-phase progression and chromatin structure maintenance. However the drawbacks of this part of the investigation include it was not investigated whether cells in S-phase are more sensitive to SAHA than in other phases of the cell cycle, which could have been achieved by carrying out a cell synchronisation experiment. In addition, BrdU incorporation is higher than expected, for example typically in untreated cells the percentage of cells in S-phase is about 20%, rather than 55% as in my experiment (Figure 5.8b). This is due to some non-specific BrdU incorporation into cells in G1, and could have been reduced by altering and optimising experimental conditions such as BrdU concentration or time of incubation of cells in BrdU. The conclusion at this stage therefore treatment is significantly reduces the number of dividing cells and previous investigations have shown that HDACs are required for S-phase progression and thus HDI sensitivity is likely to depend on the percentage of cells in S-phase, it seems that Myd88 levels in these conditions do not significantly affect the proportion of cells

undergoing S-phase. This lead to an investigation of other possibilities which may explain the mechanisms by which Myd88 levels and IL-6 release may be affecting cell fate.

Figure 5.8

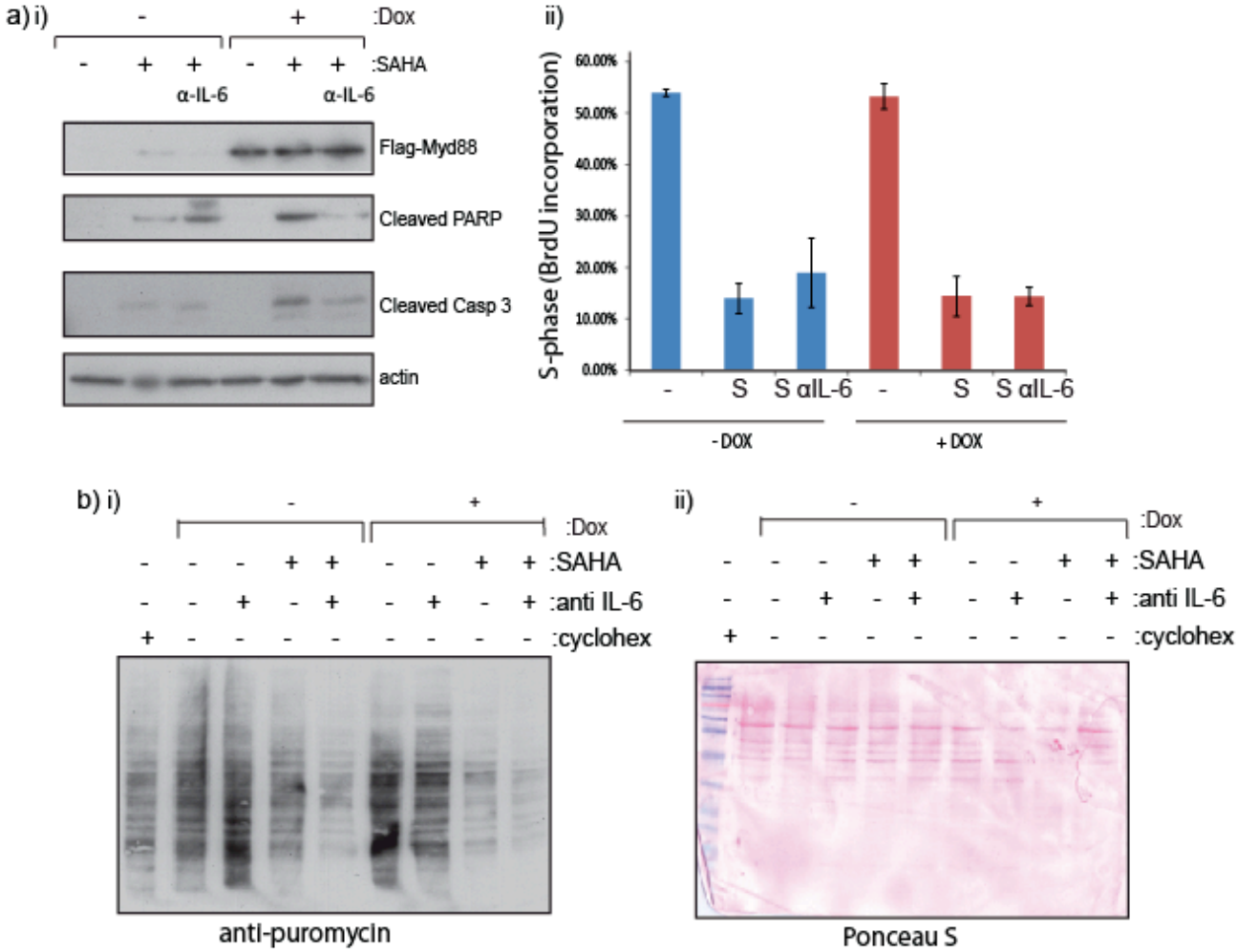

a)i) U2OS cells expressing inducible Flag-tagged Myd88 were treated with SAHA (10μM) and IL-6 neutralising antibody (2μg/ml) for 24hrs under non-induced (-) or induced (+) doxycycline treatment conditions (1μg/ml; induction for 72hr treatment). Cells were harvested and immunoblotted with Flag (for ectopic Myd88), Cleaved PARP, cleaved caspase 3, acetylated histone H3 (Ac-H3) and actin antibodies as indicated. Example shown is representative of three independent experiments.
ii) BrdU (5-bromodeoxyuridine) incorporation into cells used in a)i) and cell cycle analysis was performed using standard techniques. Briefly, cells were pulse labelled with BrdU, fixed, and stained for BrdU incorporation and with propidium iodide. The proportion of cells in phase of the cell cycle was determined by flow cytometry. Myd88 overexpression does not affect BrdU incorporation. Example shown is representative of three independent experiments.
b) U2OS cells expressing inducible Flag-tagged Myd88 were treated with SAHA (10μM) and/or IL-6 neutralising antibody (2μg/ml) for 24 hrs, or cyclohexamide (50μg/ml) for 30 minutes under non-induced (-) or induced (+) doxycycline treatment conditions (1μg/ml; induction for 72hr treatment). Cells were pulsed with puromycin (10μg/ml), for a period of 5 min prior to harvesting, and immunoblotting with puromycin antibodies (i). The cells counted and loaded by cell number, and the Ponceau is shown in ii) to indicate equal protein loading. Example shown is representative of three independent experiments.

5.7 Effect of Myd88 levels on cellular translation.

Translation is ribosome mediated protein synthesis from mRNA. Cellular protein synthesis is subject to regulation upon cellular stresses such as starvation and conditions which cause cell death. Anti-cancer drugs such as etoposide kill cells by inhibiting translation [196].

The overall levels of cellular translation were measured by allowing cells to incorporate the amino-acid analogue puromycin for a period of 5 minutes prior to harvesting (Figure 5.8 b) i), after which cells were lysed as usual, loaded on an SDS gel according to cell number in each condition, and probed with an anti-puromycin antibody [197]. The ponceau-S scan of the nitrocellulose membrane probed for puromycin is provided in 5.8 b) ii) as a control for protein loading. The translation inhibitor cycloxehamide was used as a negative control. This method of cellular translation measurement was designed by Dr Heidi Olzsha (personal communication). The aim of this experiment was to see what effects Myd88 induction has on translation both in the presence and absence of SAHA treatment, and now these vary if IL-6 secretion is neutralised.

The highest levels of translation are seen in cells which are untreated with SAHA or IL-6 neutralising antibody (Figure 5.8 b) i), and Myd88 induction does not appear to affect translation levels. There is no change in translation on IL-6 neutralisation. As expected, translation levels decreased in the presence of SAHA treatment. It not possible to conclude from this experiment, however, whether the decrease in translation is simply a consequence of induction of early-stage apoptosis caused by SAHA, or whether one of the ways in which SAHA causes

apoptosis is by reducing translation levels, although the former is more likely. In addition, there has been evidence that protein synthesis and protein degradation by the proteasome may be processes that are coordinated in such a way that their rates coincide [198]; so a decrease in proteasome activity, could lead to a decrease in translation machinery synthesis and thus translation rate. As SAHA treatment has been shown to decrease proteasome activity [42], partially due to increased transport of ubiquitinylated proteins to the proteasome by HR23B [41], it could be that this compromised proteasome activity causes reduction in translation rate.

5.8 Effect of Myd88 mediated IL-6 on cell cycle progression

A number of hypotheses have been tested for the mechanism through which extracellular IL-6 may sensitize cells to SAHA treatment, including measurement of cellular translation, which did not show significant difference on IL-6 neutralisation and Myd88 levels (Figure 5.8b), and measurement of cells in S-phase, which did not give conclusive results, although this may have been due to non-specific Brd-U accumulation (Figure 5.8a).

Another hypothesis to test was how IL-6 neutralisation affects cell cycle progression in all phases of the cell cycle (not only S-phase). In order to measure cell cycle progression, FACS analysis was carried out under conditions of Myd88 induction and/or IL-6 neutralisation (Figure 5.9a). Flow cytometry identified an increased population of cells in the G2 phase of the cell cycle upon IL-6 neutralisation (coinciding with a decrease in S-phase and G1), but only under conditions of Myd88 induction. When Myd88 is uninduced, there is no visible effect of IL-6 neutralisation on cell cycle progression, probably because IL-6 levels are very low under these conditions (Figure 5.5). This experiment was performed in triplicate and the average percentages of cells in the G2 phase of the cell cycle are shown in Figure 5.9b), which shows a significant increase in the percentage of cells in the G2 phase of the cell cycle from 28% to 40% on IL-6 neutralisation. This suggests there is a degree of cell cycle arrest in G2 on IL-6 neutralisation under conditions of Myd88 induction.

Cell cycle progression was also measured by immunoblotting to observe levels of Chk-1 phosphorylation on serine 317 under conditions of Myd88 induction,

SAHA treatment and IL-6 neutralisation (Figure 5.9 c). Chk1 is phosphorylated on serines 317 and 345 by the ATR (ataxia telangiectasia mutated- and rad3-related) kinase, which leads to cell cycle arrest during DNA damage during the G2/M phases of the cell cycle [199]. There is also evidence that Chk1 is required for normal cell growth in the absence of DNA damage [200].

As SAHA has been shown to cause DNA damage in normal and cancer human cells [201], it would be reasonable to expect an increase in P-Chk1 on SAHA treatment, however this is not seen in figure 5.9c) in the absence of IL-6 neutralisation. The explanation for this may be that the levels of double-strand breaks caused by SAHA treatment [201] are relatively low and cannot be seen by this method of detection. However, IL-6 neutralisation causes significant up regulation of P-Chk1, which is even higher in Myd88 induced cells, whereas protein levels of Chk1 remain constant throughout (Figure 5.9c). This suggests that extracellular IL-6 release through Myd88-dependent TLR signalling is involved with augmenting the cellular proliferation rate. HDAC inhibition is likely to affect proliferating cells more than arrested cells which are not actively going through the cell cycle, which may explain why IL-6 neutralisation reduces Myd88-dependent cell death, as a greater proportion of cells are arrested in G2 when IL-6 is neutralised. Note the decrease in cleaved PARP and cleaved caspase 3 in SAHA-treated Myd88-induced cells where IL-6 neutralised compared to cells in which IL-6 production is high (Figure 5.9 c).

Figure 5.9

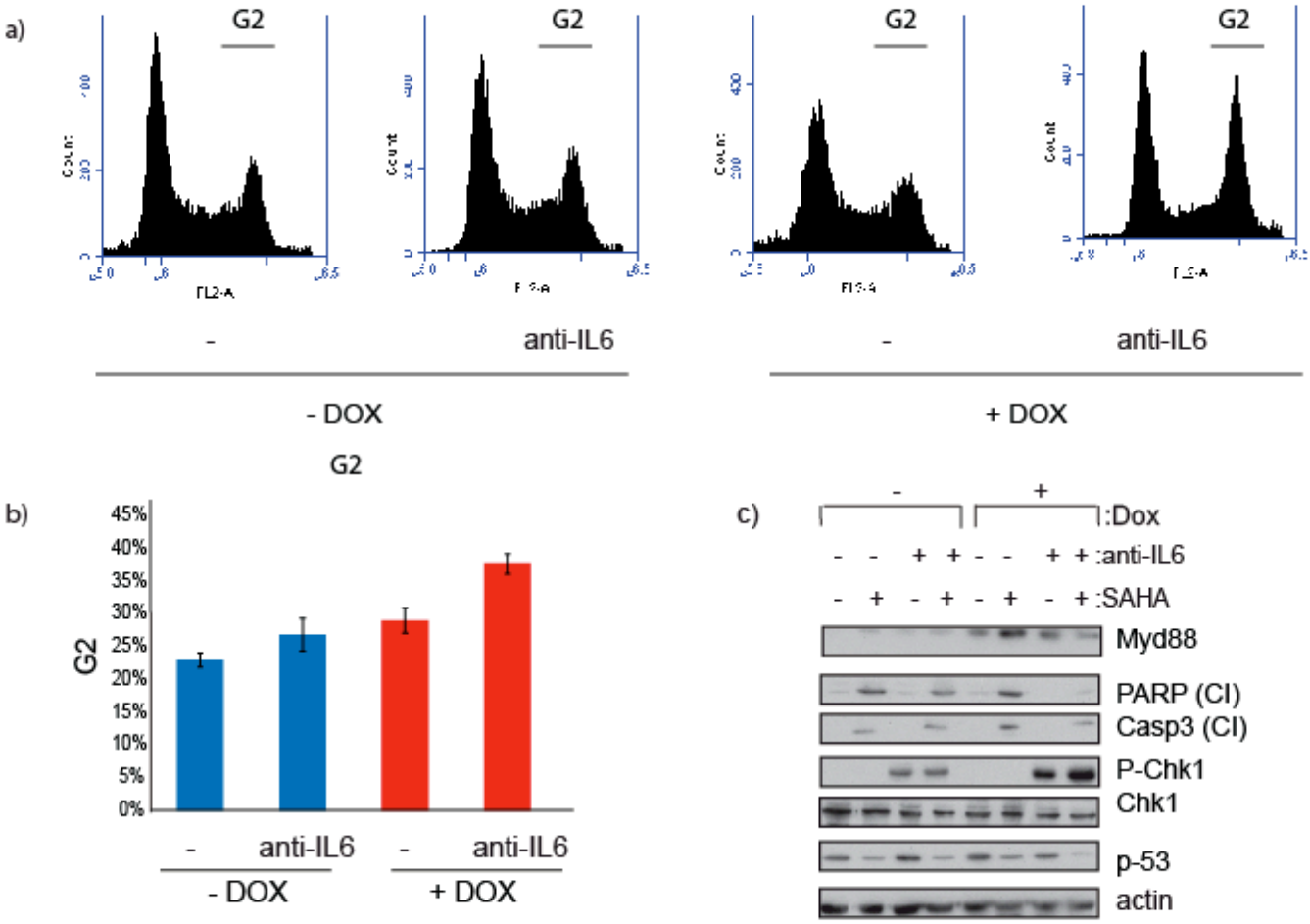

a) U2OS cells stably expressing inducible Flag-tagged Myd88 were treated with IL-6 neutralising antibody (2µg/ml) for 24hrs under non-induced (-) or induced (+) doxycycline treatment conditions (1µg/ml; induction for 72hr treatment). Cells were harvested by trypsinisation, fixed for 16hrs in 70% ethanol/30% PBS and FACS analysed on the C6 Accuri machine. The cell cycle profile of one of three triplicate plates is shown. Example shown is representative of three independent experiments.

b) Quantification of the G2 phase of the cell cycle from a). Means of triplicate plates are shown.

c) Cells from a) were harvested and immunoblotted with Flag (for ectopic Myd88), Cleaved PARP, cleaved caspase 3, Phospho-Chk1 (Serine 317), total Chk1, p53 and actin antibodies as indicated. Example shown is representative of three independent experiments.

5.9 Conclusions

The role of Myd88 as an adaptor protein in NF-κB pathway activation has been confirmed, both by Bcl-xl reporter gene activation and detection of inflammatory cytokine levels in cell media from cells with low and high levels of Myd88. The changes in the extracellular levels of the inflammatory cytokines IL-6 and IL-8 were most striking on Myd88 overexpression, but only IL-6 neutralisation affected the ability of Myd88 to increase apoptosis levels on SAHA treatment.

It seems counterintuitive that high Myd88 levels cause more apoptosis in SAHA treated cells through increased IL-6 release, as IL-6 has been predominantly implicated in pro-tumorigenic proliferation and cell survival [133]. Due to the established roles of IL-6 in proliferation [133], it was reasonable to form a hypothesis whereby the increased apoptosis due to SAHA treatment when Myd88 levels are higher is due to an increased rate of cell division, or protein synthesis. However, having tested both of these, it seems as though Myd88 levels do not have an impact on the proportion of cells in S-phase of the cell cycle, or on the rate of cellular translation. Cellular transcription levels have not been investigated by this study. Both the proportion of cells in S-phase and translation levels were seen to decrease on SAHA treatment, as expected from the variety of effects on HDAC inhibition (see Introduction section 1.5).

However, there is a possibility that IL-6 release as a consequence of Myd88-dependent signalling leads to cells dividing faster and thus being more vulnerable to HDI treatment, which impacts on gene transcription – IL-6 is a known positive regulator of proliferation [133]. On the contrary, when IL-6 is neutralised, cells

become delayed in their progression through the cell cycle and arrest in G2, which may cause them to be less sensitive to SAHA compared to actively cycling cells.

CHAPTER 6 Myd88 acetylation and relationship with HDAC6

Myd88 has been identified as a potential biomarker for HDI treatment in the same shRNA loss-of function screen for genes that impact on cell sensitivity to HDAC inhibitors as HR23B [15]. This screen utilised gene-specific shRNA to silence genes that are functionally relevant for HDAC inhibitor sensitivity, thus allowing cells to survive in the presence of a lethal SAHA concentration [15]. Myd88 levels have subsequently been manipulated both through overexpression and siRNA depletion and been shown to impact on cell apoptosis and cell proliferation ability on HDI treatment (Chapter 3). The best-known role of Myd88 is as an adaptor protein in TLR signalling [128], and the activity of Myd88 in this role under the experimental conditions used for this investigation was verified through reporter assays to measure NF-κB pathway activation and inflammatory cytokine release (Chapter 5). Interestingly, the investigation has shown that Myd88-driven IL-6 release impacts on cell cycle progression, and increases cell death on HDAC inhibition (Chapter 5).

However, elucidating the pathway between Myd88 and IL-6 does not explain how inhibition of deacetylation of cellular proteins through SAHA treatment, and thus increased acetylation affects Myd88. SAHA treatment has been shown to induce lysine acetylation not only in chromatin-associated proteins such as histones, but in addition a variety of non-histone proteins including cell structure proteins, chaperones, and glycolytic enzymes, as identified by use of a mass spectrometric approach [92]. This acetylation may be important in regulating the function of these proteins, for example through affecting enzyme activity, or protein function

in signal transduction, and there is a possibility that sustained lysine acetylation may be required for the therapeutic effect of SAHA [92].

It was reasonable to suggest that HDAC inhibition may regulate Myd88, for example through the acetylation status of Myd88, or acetylation of proteins which interplay with Myd88. It was of interest to investigate whether Myd88 is directly acetylated, and how this acetylation affects its functionality, as well as which HDAC may be responsible for deacetylation of Myd88. Myd88 acetylation has not been reported in the literature at the time of writing (1st july, 2014), so the identification of an acetylation site, particularly if such a modification was to have functional relevance would present a novel and exciting finding. Because of the investigation of the role of HDAC6 in cell survival (chapter 4) and previous publications which have shown HDAC6 is required for Myd88 aggregation together with sequestosome 1 (SQSTM1) [124], it was of interest to determine whether Myd88 and HDAC6 interact and whether HDAC6 impacts on Myd88 levels, functionality and post-translational modification status.

6.1 Myd88 is acetylated

As Myd88 levels have an effect on cell fate outcome during treatment with histone deacetylase inhibitors, which lead to higher cellular protein acetylation levels, it was a relevant question to determine whether Myd88 itself is acetylated, which could have an impact on its biological function.

In order to determine whether Myd88 is acetylated, U2OS cells were treated with SAHA (to increase the acetylation levels of cellular proteins), after which an immunoprecipitation with the Flag antibody which pulls down Flag-tagged Myd88 was performed, and the resulting immunoblot with the Ac-K antibody (figure 6.1a), followed by reprobing with Flag antibody. This approach gave a band at 33kDa, which overlapped exactly with the Flag-Myd88 band upon stripping and reprobing the membrane with Flag. This approach showed ectopic flag-tagged Myd88 to be acetylated, giving convincing evidence that the acetylation takes place. However, there is still a possibility of another acetylated protein with exactly the same molecular weight as Myd88 being pulled down, which may be the reason for the Ac-K band at 33kDa. The control for these immunoprecipitations is a pull-down with the IgG antibody of the same species as the specific antibody, which is labelled as “NS” (non-specific) in Figure 6.1.

Figure 6.1

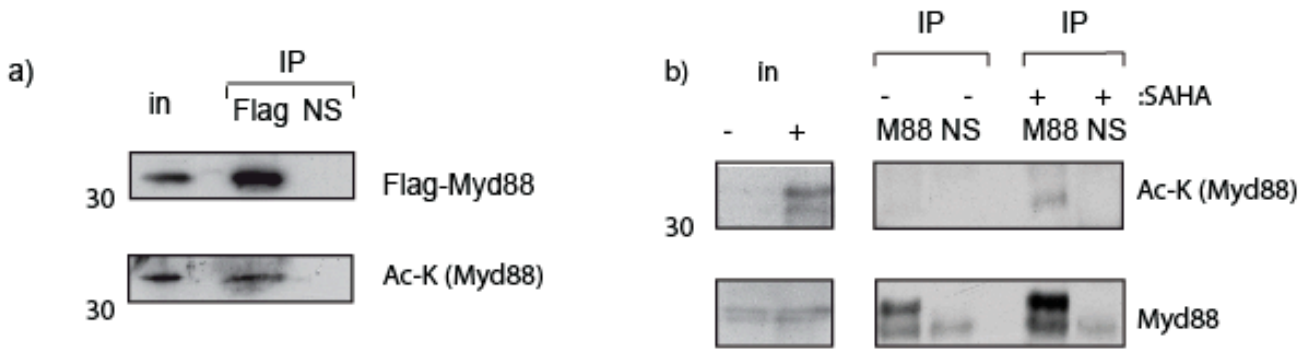

a) U2OS cells expressing inducible Flag-tagged Myd88 were treated with SAHA (10 μM) for 16 hours, harvested, immunoprecipitated with the anti-Flag antibody and IgG (mouse) antibodies and subsequently immunoblotted with Flag and anti-acetyl-lysine (Ac-K) antibodies. Input levels are shown. Experiment shown is representative of three independent experiments.

b) U2OS cells expressing inducible Flag-tagged Myd88 were treated with SAHA or DMSO and SAHA (10 μM) for 16 hours, harvested, immunoprecipitated with the anti-acetyl-lysine antibody and IgG (rabbit) antibodies and subsequently immunoblotted with Myd88 anti-acetyl-lysine (Ac-K) antibodies. Input levels are shown. Experiment shown is representative of three independent experiments.

In order to gain evidence of acetylation of the endogenous form of Myd88, rather than the Flag-tagged overexpressed version, an immunoprecipitation was performed with the endogenous Myd88 antibody in U2OS cells with and without SAHA treatment (Figure 6.1b), where it can be seen clearly that the band corresponding to acetylated Myd88 is much stronger upon SAHA treatment. This band overlaps with the Myd88 band after the membrane is stripped and reprobed with the endogenous Myd88 antibody. This gives further evidence that Myd88 is acetylated, and acetylation on SAHA treatment could play a role in the way Myd88 determines cell fate during HDI treatment.

Once substantial evidence of Myd88 acetylation had been accumulated through immunoprecipitation of the ectopic and endogenous protein, it was necessary to determine which of the possible 10 lysines within Myd88 is acetylated, so that the residue of interest could then be mutated to one which cannot be acetylated to check if there is an impact of acetylation on biological function. This was achieved by mass spectrometry analysis in collaboration with Benedikt Kesslers group (Figure 6.2a)). The cell line expressing inducible Flag-tagged Myd88 cell line was treated with SAHA, prior to Flag pull-down and digestion with elastase – mass spectrometry analysis was subsequently performed by Rebecca Konietzny in Benedikt Kesslers group, to identify lysine (K) 119 as an acetylated residue (Figure 6.2aii). A small fraction (5%) of the sample to be submitted for mass spectrometry was run on an immunoblot to verify Flag-Myd88 presence and successful immunoprecipitation (Figure 6.2 a) iii)). Lysine 119 (K119) is located in the intermediate domain of the protein (http://www.uniprot.org/uniprot/Q99836), the structure of which has not been determined to date. The presence of intrinsically unstructured regions (IURs) has been noted in a number of proteins, particularly those involved in signalling [202].

These regions may serve simply as linkers between structural domains, but their presence may also allow binding with high specificity and reversibility [202], with a large surface are of interaction, reminiscent of the “induced fit” model of enzyme-substrate binding, which is particularly useful in the case of a protein with many binding partners, such as p53, which may use such disordered regions to bind to several partners [203].

As Myd88 is a sensitivity determinant to histone deacetylase inhibitor treatment (Chapter 3), it was relevant to investigate the possibility that Myd88 acetylation status could be important in determining cell fate in response to HDI treatment. In order to determine whether Myd88 acetylation is relevant in this context, site-directed mutagenesis was used to create a mutant of Myd88 where lysine 119 (K119) is replaced by arginine 119 (R119) which mimics the unacetylated lysine residue and cannot be acetylated. An inducible cell line where flag-tagged K119R Myd88 could be induced upon doxycycline addition was then created alongside another wild type Flag-Myd88 cell (for the same batch of parental U2OS cells), in order to make comparison between properties of the wild-type and R119K mutant possible.

When the ectopic R119K protein was expressed in cells alongside wild-type Myd88 there was no acetylation seen in the R119K mutant, although immunoprecipitated Myd88 had a significant level of acetylation (Figure 6.2b). The levels of K119R Myd88 are approximately four-fold higher than wild-type Myd88 in this immunoprecipitation (Figure 6.2b), and yet no Ac-K signal is seen at 33kDa in the K119R mutant but significant signal is seen for wild-type Myd88. This gives confirmation that the lysine residue identified by mass spectrometry to be acetylated is the correct residue.

Figure 6.2

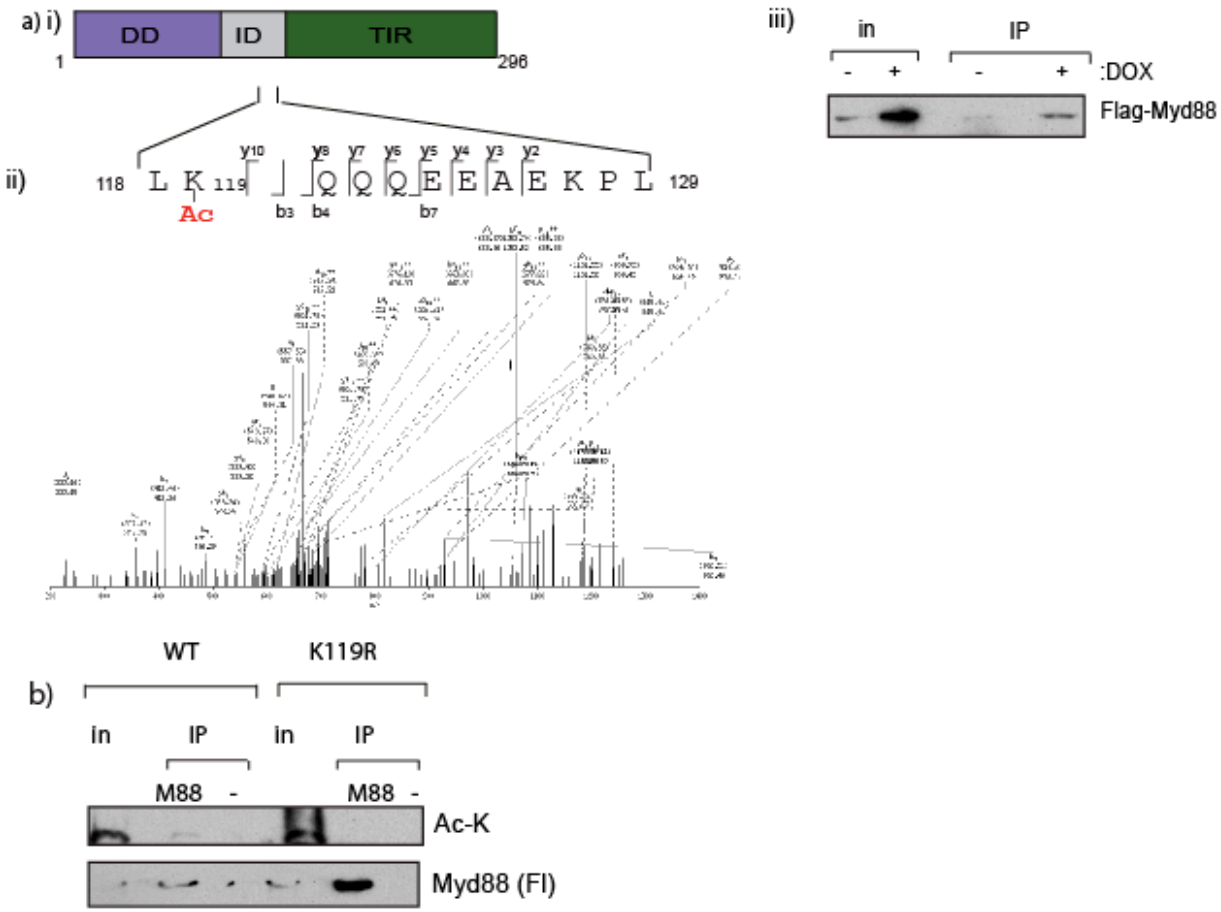

a) i) Domain structure of Myd88, where DD indicated death domain, IR indicates intermediate domain, and TIR is the Toll-like receptor interacting domain.ii) U2OS cells expressing inducible Flag-tagged Myd88 were treated with SAHA (10 μM) for 16 hours, harvested, immunoprecipitated with the anti-acetyl-lysine (Ac-K) and IgG (rabbit) antibodies. In-solution elastase digestion was subsequently performed (see Materials and Methods section 2.14) and samples were analysed by mass-spectrometry by Benedikt Kessler and Rebecca Konietzny. The spectrogram shows Myd88 acetylation on residue lysine 119.ii) Cells were prepared as described in i), and a small fraction (5%) of the immunoprecipirated extract was run on an immunoblot to verify Flag-Myd88 pulldown, through immunoblotting with Flag antibody

b) U2OS cells expressing inducible WT or K119R Flag- Myd88 were treated with SAHA (10 μM) for 16 hours, harvested, immunoprecipitated with the anti Flag and IgG (mouse) antibodies and subsequently immunoblotted with Flag and anti-acetyl-lysine (Ac-K) antibodies. Input levels are shown. Experiment shown is representative of three independent experiments.

6.2. Myd88 acetylation on lysine K119

Once the lysine residue of Myd88 on which acetylation takes place had been identified, and the mutant made which cannot be acetylated, it was of interest to compare the properties of wild-type and K119R Myd88, particularly in terms of response to HDAC inhibition. The response to SAHA of cells overexpressing wild-type and K119R Myd88 was compared by measuring cleaved PARP and cleaved caspase as apoptosis markers (Figure 6.3a), which showed that the K119R mutant had different properties to wild-type Myd88. Whereas overexpression of wild-type Myd88 leads to greater levels of cell death on SAHA treatment compared to uninduced cells (Figure 6.3a) and seen previously in Chapter 3), overexpression of K119R Myd88 does not significantly change levels of cleaved caspase 3 or cleaved PARP on SAHA treatment (Figure 6.3a). However, it is noteworthy that even low levels of K119R Myd88 due to "leakage" of the inducible cell line sensitise cells to a higher level of apoptosis (both cleaved PARP and cleaved caspase 3) upon HDAC inhibitor treatment (Figure 6.3a) compared to low levels of WT Myd88 (levels of the two flag-tagged proteins are similar in lanes two and six of Figure 6.3a). Another important property of Myd88 connected to its sensitivity determinant role is the enhanced release of the inflammatory cytokine IL-6 on Myd88 overexpression (Chapter 5), so it was relevant to measure IL-6 release on overexpression of K119R Myd88 and compare these to levels of IL-6 release on overexpression of WT Myd88 (Figure 6.3b). At a first glance, it appears that IL-6 release on overexpression of K119R is much higher than when wild-type Myd88 is overexpressed, however, the fold increase on overexpression of each protein is similar compared to the uninduced cells (approximately 3-fold in each case). The levels of extracellular IL-6 are also

slightly higher in uninduced K119R-Myd88 cells compared to uninduced WT-Myd88 cells. This difference should not be apparent if the inducible cell lines only express flag-tagged protein on doxycycline induction, however, in this case, unfortunately, there is a degree of "leakage" in both cell lines, where WT and K119R Myd88 become expressed even in absence of doxycycline (Figure 6.3a). This is one of the limitations to this part of the study, alongside the difficulties of making a direct comparison between two difference cell lines (albeit created simultaneously), as growth rates may be slightly different, and the presence of endogenous WT Myd88 in the K119R inducible cell line which is likely to contribute to IL-6 release and SAHA response.

Having established that IL-6 release on expression of K119R Myd88 is higher compared to WT, the next step was to determine whether this IL-6 release contributes to cell death upon SAHA treatment, as was shown to be the case for WT Myd88 (Chapter 5). IL-6 neutralisation in combination with SAHA treatment and K119R Myd88 induction coincides with a reduction in levels of cleaved PARP and cleaved caspase 3 (Figure 6.3c). This indicates that IL-6 release plays a similar pro-apoptotic role when Myd88 cannot be acetylated, compared to the wild-type and potentially acetylated version of the protein. In addition, Phospho-chk1 (ser317) becomes upregulated on IL-6 neutralisation (Figure 5.9c), suggesting that the mechanism in which IL-6 release impacts on SAHA-response in Myd88-induced cells may be similar for the K119R mutant and the wild-type. The question which remains, therefore, is to establish why K119R My88 has different properties to the WT protein in terms of higher IL-6 release and higher apoptosis levels even when low protein levels are expressed.

Figure 6.3

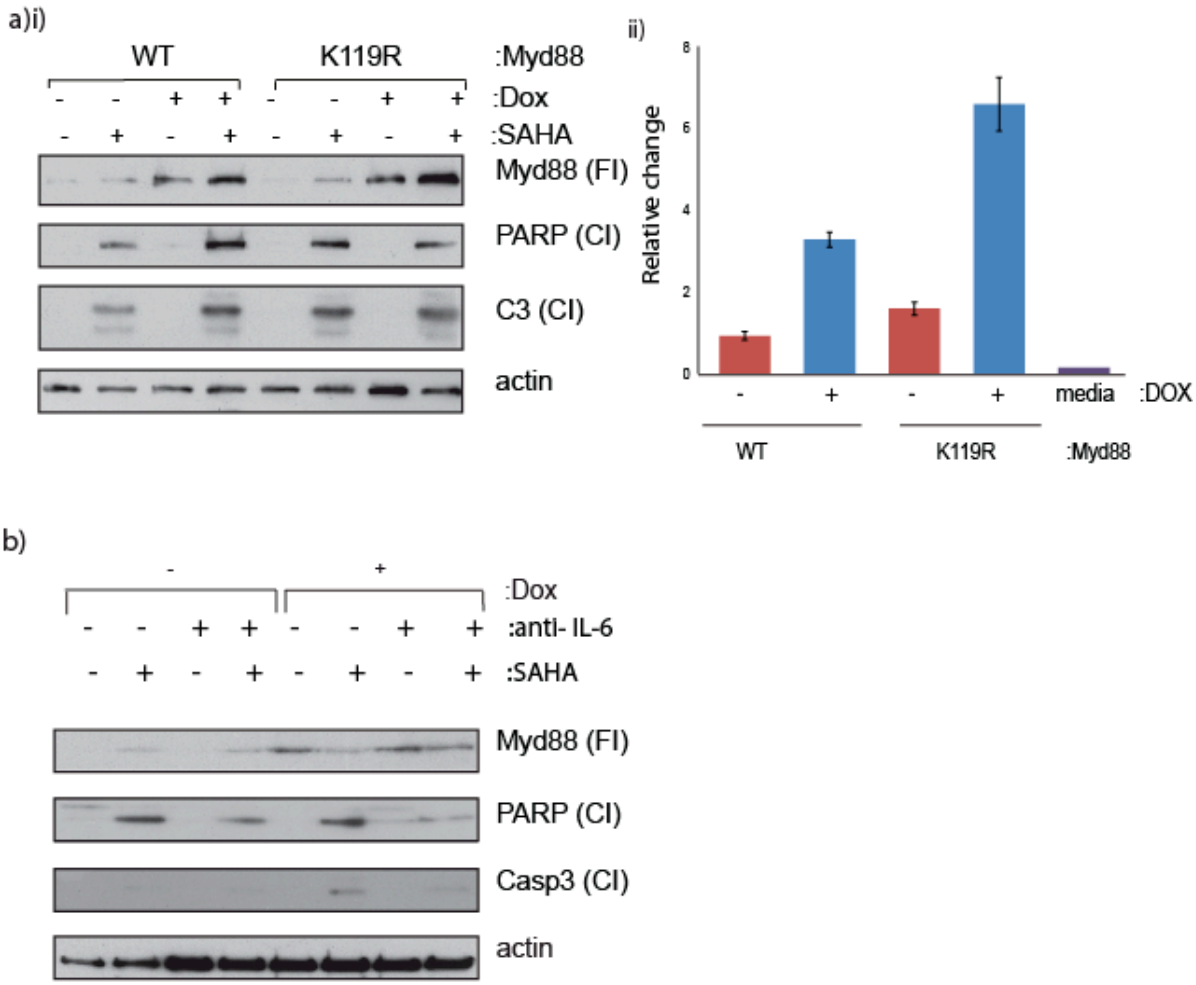

a) U2OS cells expressing inducible Flag-tagged Myd88 or K119R Flag-Myd88 were treated with SAHA (10 μM) for 24 hours under non-induced (-) or induced (+) doxycycline treatment conditions (1μg/ml; induction for 72hr treatment). Cells were harvested and immunoblotted with anti-Flag, cleaved PARP, cleaved caspase 3 and actin as loading control. Example shown is representative of three independent experiments.

b) Relative levels of IL-6 in the tissue culture media of cells in a) was measured using BD™ Cytometric Bead Array (CBA) human inflammatory cytokine measurement kit. Mean values from triplicate plates are shown alongside a media-alone control. Example shown is representative of three independent experiments.

c) U2OS cells expressing inducible K119R Flag-tagged Myd88 were treated with SAHA (10μM; +) and IL-6 neutralising antibody (2μg/ml) for 24hr under non-induced (-) or induced (+) doxycycline treatment conditions (1μg/ml; induction for 2hr treatment). Cells were harvested and immunoblotted with anti-Flag (for ectopic Myd88), cleaved PARP, cleaved caspase 3 and actin antibodies as indicated. Example shown is representative of three independent experiments.

6.3 Relative stability of acetylated Myd88 compared to K119R Myd88

As levels of K119R Myd88 were seen to be higher than WT Myd88 (Figure 6.3 a) i)), which corresponds to higher levels of IL-6 release (Figure 6.3 b), it was relevant to compare the protein stability levels of Myd88 which can be acetylated (WT) and Myd88 which cannot be acetylated (K119R). The prediction was that acetylated Myd88 is less stable, and the lower protein levels are the cause for lower IL-6 secretion in the case of the WT acetylated protein. The stability levels of the two proteins were compared by a cycloheximide assay (Figure 6.4). Cycloheximide treatment inhibits protein synthesis and the decrease in levels of the target protein over time is determined by immunoblot analysis [204]. As indicated by the immunoblot and its quantitation (Figure 6.4), WT Myd88 has a much lower half-life (of about 2 hours) compared to the K119R mutant which cannot be acetylated, although there is a degree of variability in protein levels over time in both cases rather than a simple decrease with time. For example, there is a more intense band after 2 hrs of cycloheximide treatment in the WT-Flag-Myd88 cell line compared to 1 and 4hrs of treatment, which is likely to be due to experimental variation, rather than a biological phenomenon, as it has not been seen reproducibly in other repeats of this experiment.

In order to increase the validity of this comparison, an alternative measurement of protein stability could have been used, such as pulse-chase analysis, where the protein of interest is labelled with a radioactive precursor for a short period of time, after which an excess of non-radioactive precursor molecules are added, and cells are lysed at various time periods and immunoprecipitated with an antibody against the

target protein [204]. This approach is commonly used because it causes minimal disruption to cell metabolism and growth [204].

Figure 6.4

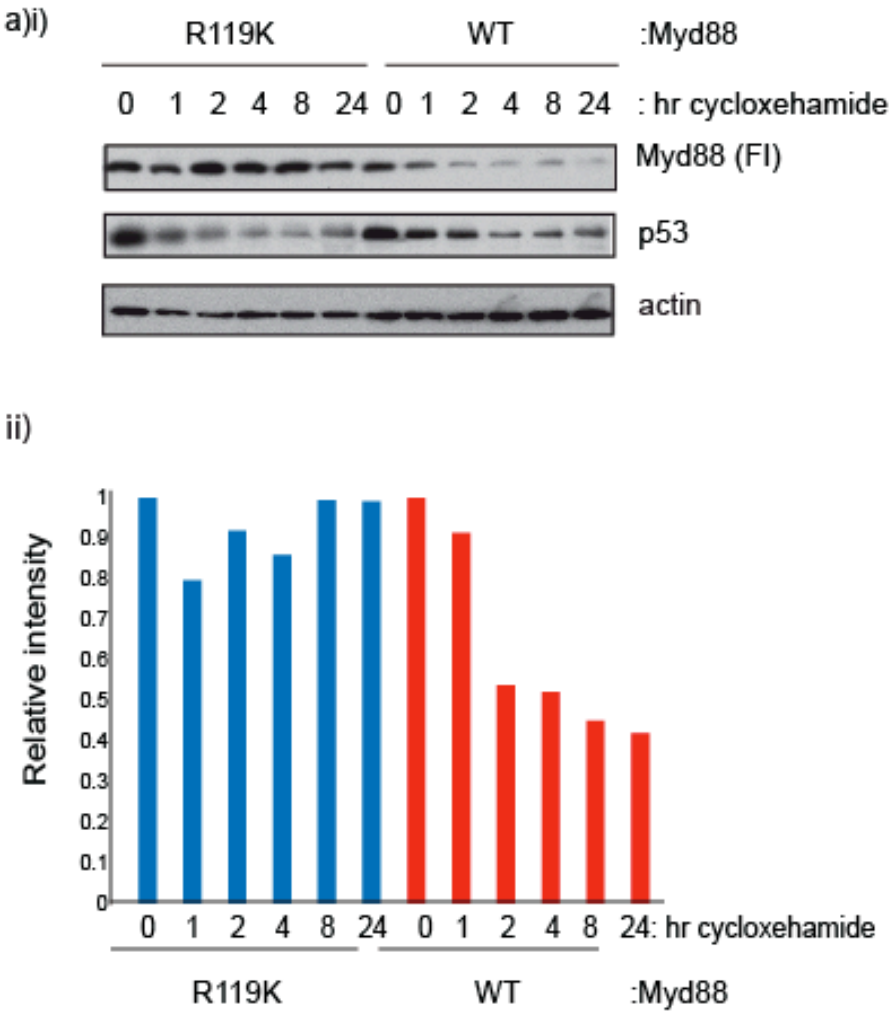

a) U2OS cells expressing inducible Flag-tagged Myd88 or K119R Flag-Myd88 were treated with cyclohexamide (100 μM) for the time-periods indicated and immunoblotted with Flag (to indicate levels of ectopic Myd88), p53 and actin as loading control (i). Immunoblot quantitation of Flag-Myd88 levels relative to actin was subsequently performed using ImageJ software (ii). Example shown is representative of three independent experiments.

6.4 HDAC6 and Myd88

As Myd88 is a cytoplasmic protein associated with the TLR complex, it was reasonable to suggest that Myd88 acetylation is regulated by a HDAC also present in the cytoplasm.

HDAC6 was considered as a possibility, due to its localisation in the cytoplasm and established role in the deacetylation of cytoplasmic proteins [35], as well as the known role of HDAC6 in Myd88 signalling ([124] and below for more detail). As the acetylated form of Myd88 has been found to be less stable (Figure 6.4), the initial stage of investigation of the relationship between HDAC6 and Myd88 was simply to observe Myd88 protein levels on silencing of HDAC6 (Figure 6.5a). A549 HDAC6 WT and KD cells were used for this purpose (cell lines discussed in Chapter 4), and it was seen that Myd88 is absent from the HDAC6 KD cell line (Figure 6.5a), perhaps because in the absence of HDAC6, Myd88 is no longer deacetylated, and the acetylated form becomes degraded.

In addition, Myd88 levels were seen to decrease on SAHA treatment, which may be due to decreased levels of HDAC6 activity and consequently higher levels of the less stable acetylated form of Myd88 (Figure 6.5a). To test this hypothesis, the HDAC6-specific inhibitor tubastatin [48] was used at a range of concentrations in the HDAC6 KD and WT cell lines. Acetylated tubulin levels were measured by immunoblotting as a control of HDAC6 activity (tubulin is a known HDAC6 substrate [205]), and were seen to increase with increasing tubastatin concentrations in the HDAC6 WT cell line (Figure 6.5b). This increased level of

HDAC6 inhibition correlated with a decrease in Myd88 levels, indicating that it is HDAC6 responsible for governing Myd88 stability.

It was then of relevance to test whether there is a direct interaction between HDAC6 and Myd88, as such an interaction may indicate that Myd88 is a substrate for HDAC deacetylation. A clear endogenous interaction can be seen between HDAC6 and Myd88 in the U2OS cell line (Figure 6.5 c) upon immunoprecipitation of Myd88. The interaction can also see if the immunoprecipitation is set up in the opposite way, i.e. if HDAC6 is pulled down, an interaction can also be seen with Myd88 (data not shown). These experiments give convincing evidence that HDAC6 and Myd88 interact which is supported by previous findings of endogenous Myd88 coprecipitation with HDAC6 [124]. There have also been indications of HDAC6 being required for Myd88 aggregation along with sequestosome 1 (SQSTM1) [124].

The interaction between HDAC6 and Myd88 was compromised in the K119R mutant of Myd88 (Figure 6.5 d). This comparison was made by carrying out an immunoprecipitation in both WT and K119R Myd88 inducible cell lines with the Flag antibody to pull down Myd88, and observing the amount of HDAC6 which was pulled down. Although slightly higher levels of K119R Myd88 were pulled down than WT (perhaps reflecting the relative stability of the two proteins), HDAC6 levels were higher in the WT Myd88 immunoprecipitation (Figure 6.5d). This indicates an interaction between Myd88 and HDAC6, although this interaction may not be direct, i.e. a complex of proteins may be involved. The presence of the interaction (albeit at low levels) between HDAC6 and K119R Myd88 suggests that HDAC6 may interact with other regions of Myd88 in addition to its acetylation site.

Figure 6.5

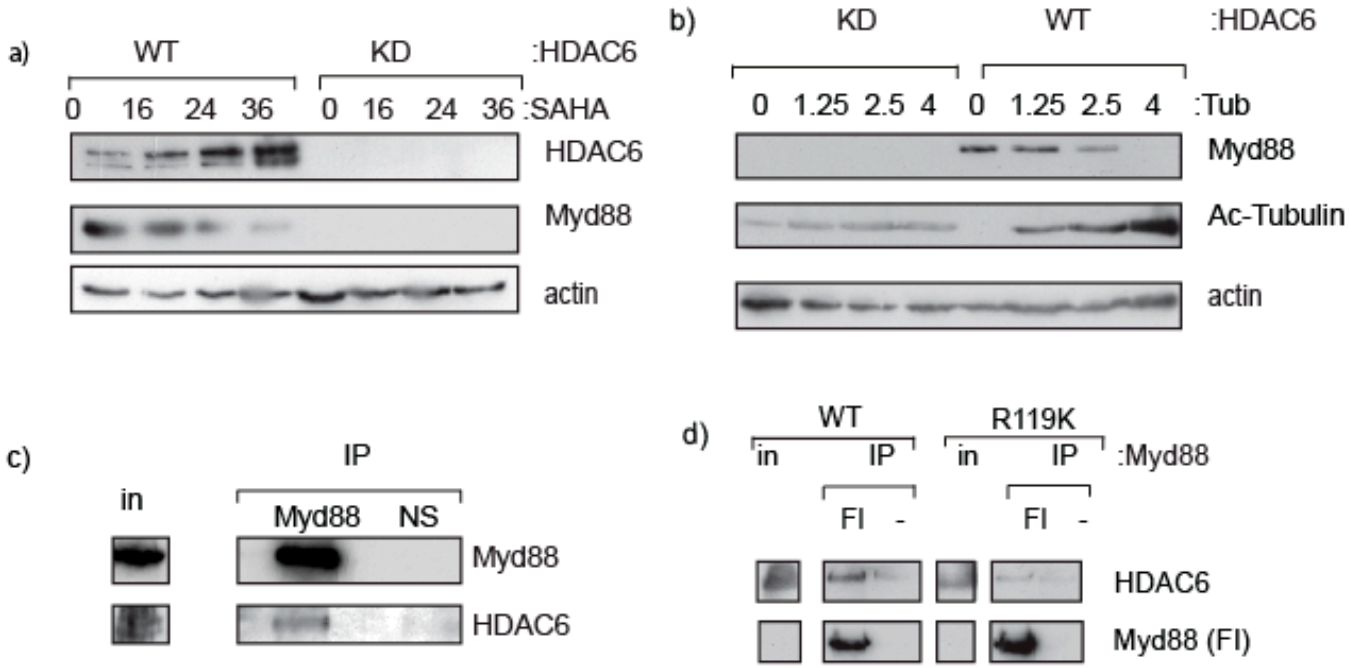

a) A549 HDAC6 WT (WT) and KD (KD) cells were treated with 10 μM SAHA for the indicated times and analysed by immunoblotting for HDAC6 and Myd88. Actin serves as loading control. Example shown is representative of three independent experiments.

b) A549 HDAC6 WT (WT) and KD (KD) cells were treated with the indicated tubastatin concentrations for 24hrs and analysed by immunoblotting for Myd88 and acetylated tubulin (Ac-Tubulin) as a control for tubastatin activity. Actin serves as loading control. Example shown is representative of three independent experiments.

c) U2OS cells were harvested, immunoprecipitated with Myd88 antibody and subsequently immunoblotted with Myd88 and HDAC6 antibodies. Input (2% of total lysate) Myd88 and HDAC6 levels are shown. Example shown is representative of three independent experiments.

d) U2OS cells stably expressing inducible WT or K119R Flag- Myd88 were treated with SAHA (10 μM) for 16 hours, harvested, immunoprecipitated with the anti Flag and IgG (mouse) antibodies and subsequently immunoblotted with HDAC6 and Flag antibodies. Input levels are shown. Example shown is representative of three independent experiments.

6.5 Pan-bromodomain inhibition effect on SAHA response in cells with high Myd88 levels

In order to distinguish whether recognition K119 acetylation of Myd88 recognition is required for the sensitivity determinant role of Myd88, a broad-spectrum bromodomain inhibitor, bromosporine was used. Bromosporine binds to a deep, hydrophobic acetyl-lysine binding site in the conserved BRD fold of bromodomain-containing proteins, which in turn prevents such proteins binding to their normal cellular targets (http://www.thesgc.org/chemical-probes/bromosporine).

As shown in figure 6.6a), bromosporine addition to cells where Myd88 levels are have been induced by doxycycline addition, significantly diminishes cell death upon SAHA treatment. In contrast, bromosporine does not significantly affect apoptosis as measured by PARP cleavage in cells where no doxocyline has been added and Myd88 levels are low. Bromosporine alone, used at this concentration (3μM), does not cause any PARP cleavage (Figure 6.6a). However, the broad-spectrum bromodomain inhibiting effects of bromosporine may lead to non-specific and complex effects on the cells, which may not have any connection with Myd88 levels and activity. This is why one of the next stages of the investigation was to attempt to establish which bromodomain protein is important for recognition of acetylated Myd88.

Figure 6.6

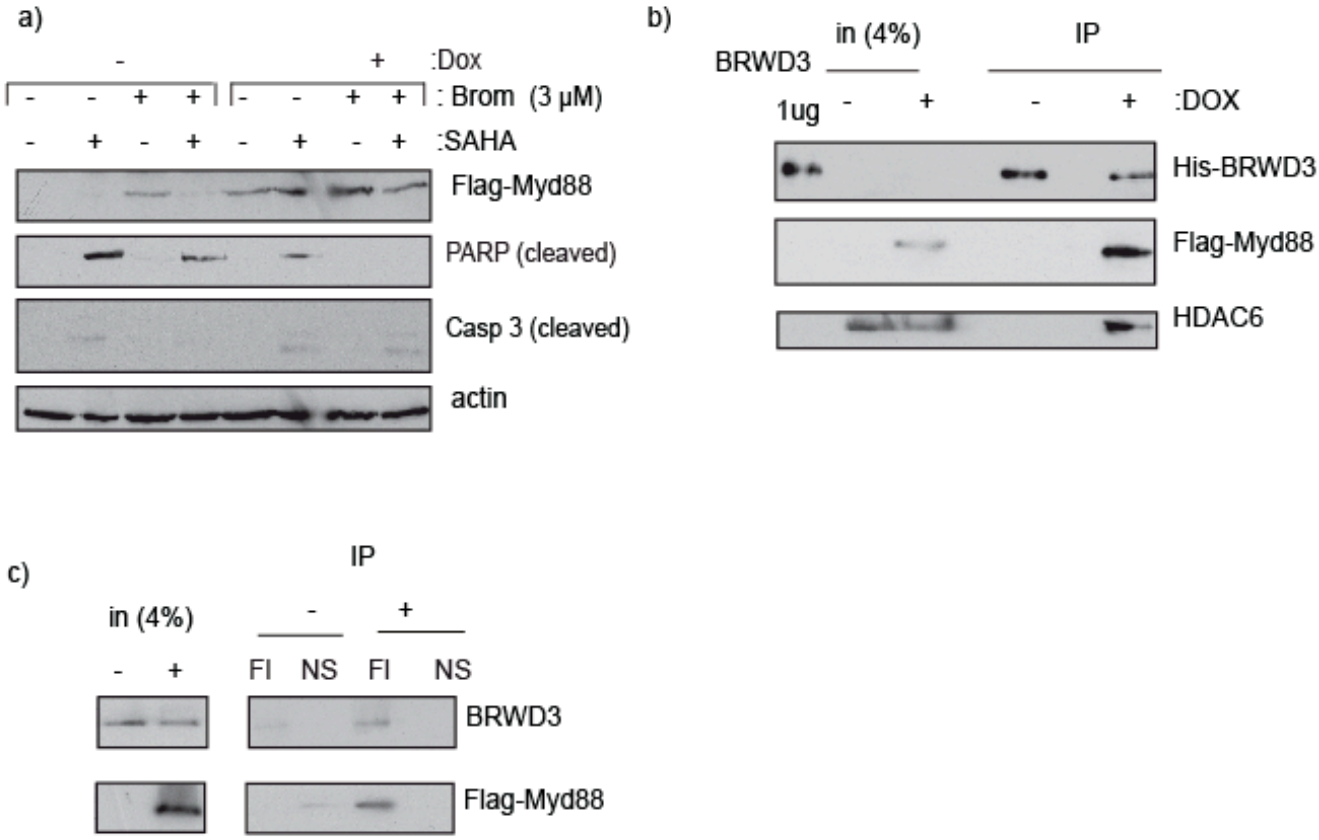

a) U2OS cells stably expressing inducible Flag-tagged Myd88 were treated with SAHA (10 μM) and bromosporine (3μM) for 24 hours under non-induced (-) or induced (+) doxycycline treatment conditions (1μg/ml; induction for 72hr prior to treatment). Cells were harvested and immunoblotted with anti-Flag, cleaved PARP, cleaved caspase 3 and actin as loading control. Example shown is reproducible of three independent experiments.

b) U2OS cells stably expressing inducible Flag-tagged Myd88 were treated with SAHA (10 μM) for 16 hrs under non-induced (-) or induced (+) doxycycline treatment conditions (1μg/ml) were harvested, lysed and incubated for 1 hour with 1 μg of BRWD3 peptide (kind gift from Panagis Filippakopoulos, prior to immunoprecipitation with His antibody, and immunoblotting with His, Flag and HDAC6 antibodies. BRWD3 peptide is loaded alone (lane 1 from left), followed by input (4% of total lysate) levels of Flag-Myd88 and HDAC6.

c) U2OS cells stably expressing inducible Flag-tagged Myd88 were treated with SAHA (10 μM) for 16 hrs under non-induced (-) or induced (+) doxycycline treatment conditions (1μg/ml) were harvested and immunoprecipitated with Flag and IgG (mouse) antibodies, prior to immunoblotting for endogenous BRWD3 and Flag-Myd88

6.6 Recognition of acetylated Myd88 by bromodomain proteins

Having shown that Myd88 acetylation on residue K119 affects Myd88 stability, which may be important in its role as a sensitivity determinant to HDI treatment, the next question was to establish a "reader" for this acetylation site, i.e. a protein which recognises the acetylation which leads to a sequence of events such as a signalling pathway which may lead to a particular cell fate, or degradation of the protein recognised.

Bromodomains are protein modules that specifically recognise ε-N-lysine acetylation, and there are 61 bromodomains, and 46 bromodomain containing proteins in the human genome [93]. Of these, most are located in the nucleus where they recognise acetylated histones, but there are also 11 cytoplasmic bromodomain proteins [93]. As Myd88 is a predominantly cytoplasmic protein, only these were of interest as potentially recognising its K119 acetylation. Of these 11 bromodomain-containing cytoplasmic proteins [93] bromodomain and WD repeat domain containing 3 (hereafter referred to as BRWD3) seemed to be the most likely protein to recognise Myd88, because of its established role in JAK/STAT signalling as established by RNA interference [206]. The connection between TLR signalling, in which Myd88 plays a key role, and JAK/STAT signalling is that, upon viral infection, TLR activation causes release of interferon and pro-inflammatory cytokines as part of the innate response, after which interferon activates the JAK/STAT signalling pathway, to result in gene activation and virus inhibition [207]. In addition, analysis of gene expression signatures showed that JAK kinase signaling in ABC DLBCL overlapped significantly with the MYD88 signature [137]. The BRWD3 gene has also been found to be disrupted in B-cell chronic lymphocytic

leukaemia in patients with particularly poor survival [181]. As chronic lymphocytic leukaemia is a type of B-cell lymphoma (www.lymphoma.org), and diffuse large B-cell lymphoma has been found to be dependent on Myd88 expression [208], it seemed reasonably likely that BRWD3 may be a protein connected with Myd88 in its mechanism of action.

Therefore, it was considered worthwhile to establish whether Myd88 interacts with BRWD3. To achieve this, his-tagged BRWD3 peptide (kind gift from Panagis Flippapopolous, Structural Genome Consortium, University of Oxford was incubated with cell lysates containing Flag-Myd88 from the inducible cell line, with extract from uninduced Myd88 cells as a control, prior to pull-down with anti-His antibody (Figure 6.6b). An interaction was seen between His-BRWD3 and Flag-Myd88, but an interaction between a peptide and a cellular protein may not be physiologically relevant as the synthetic peptide may not be folded in the same way as its cellular counterpart, and only a small part of the protein (second domain of BRWD3 in this case) may be expressed. Therefore, this interaction was subsequently verified with an antibody against the endogenous BRWD3 protein (Figure 6.6c).

The results above give a clear indication of an interaction between Myd88 and BRWD3. However, more experiments need to be performed to verify that BRWD3 recognizes the acetylation site of Myd88, for example through comparison of the interaction levels in WT and K119R Myd88, as well as to provide insight into the functional importance of this interaction. The important remaining question is to determine the consequences of recognition of acetylated Myd88 by BRWD3 – this may lead to a signaling cascade, perhaps through the JAK/STAT signaling. An alternative possibility is that BRWD3 recognition of Myd88 may lead to its

degradation, which would therefore explain the lower stability of WT acetylated Myd88 compared to its K119R mutant which cannot be acetylated.

6.7 Conclusions

In this final chapter of my investigation, a number of interesting insights into the function of Myd88 have been unveiled. It has been identified that Myd88 is directly acetylated through immunoprecipitations of both the ectopic and endogenous protein, after which the specific site of this post-translational modification was determined to be at lysine 119, in collaboration with Dr Benedikt Kesslers proteomics group. Site-directed mutagenesis was used to make a mutant of Myd88 where lysine 119 is replaced with an arginine, which mimics the non-acetylated lysine group and cannot be acetylated, after which the properties of WT and mutant Myd88 were compared. Acetylated Myd88 appeared to be less stable than the K119R mutant and there is some evidence that HDAC6 is responsible for the deacetylation of Myd88. A potential model for the mechanism of the positive regulation of Myd88 by HDAC6 could be that Myd88 acts as a substrate for the deacetylase activity of HDAC6. The deacetylated form of Myd88 may be more stable, which means when HDAC6 is present a greater proportion of Myd88 is in its deacetylated state and is not degraded. In contrast, in the HDAC shRNA A549 cell line, where HDAC6 is virtually absent (cannot be detected in an immunoblot), Myd88 is also absent, perhaps because it is in its acetylated form which is subject to degradation.

Having identified the acetylation site of Myd88, it was of interest to investigate which bromodomain protein recognises this site. From the list of established bromodomain proteins [93] BRWD3 seemed like the most likely candidate, due to its established role in JAK/STAT signalling as established by RNA interference [206], which Myd88 is also implicated in [207] [137]. An interaction

between the endogenous BRWD3 protein and Myd88 was seen by immunoprecipitation, and some tentative evidence that bromodomain recognition was necessary for the sensitivity determinant function of Myd88 was obtained using the broad-spectrum bromodomain inhibitor, bromosporine. However, further investigation is needed to confirm that BRWD3 recognizes lysine 119 in Myd88, and to elucidate what consequences this recognition has for Myd88 stability and cell fate.

Interestingly, although the above investigation shows that inhibition of bromodomain proteins leads to a reduction in apoptosis under the conditions of SAHA treatment and Myd88 induction, there have been studies where bromodomain inhibition has been used to suppress tumourigenesis [209]. For example, sustained NF-κB signalling and expression of NF-κB target genes due to infection by the viral oncoprotein Tax is one of the causes of human T cell leukaemia virus 1 (HTLV-1) the expression of many NF-κB target genes. The bromodomain inhibitor JQ1 prevents interaction of the acetylated RelA subunit of NF-κB with BRD4, which leads to Tax-mediated transcriptional NF-κB signalling activation [209].

Chapter 7 DISCUSSION

CONCLUSIONS

7.1 Alterations in HR23B and Myd88 levels alter cell line sensitivity to apoptosis on HDI treatment

One of the aims of this project has been to validate HR23B and Myd88 as sensitivity determinants to HDI treatment, as they were both discovered in the shRNA library screen of human genes involved in cancer for genes required for U2OS cell death on HDI treatment [15]. HR23B and Myd88 have been confirmed as sensitivity determinants for HDI treatment in functional assays by manipulation of levels of HR23B and Myd88 in the U2OS cell line, which resulted in altered sensitivity to HDI treatment, as shown both by differing levels of apoptosis (as measured by levels of cleaved PARP, cleaved caspase 3 and sub-G1) and different colony formation ability of cells, which is an indication of cell growth (Chapter 3). This means that pre-treatment levels of HR23B and Myd88 could act as potential prognostic biomarkers of sensitivity to HDIs.

Due to the potential of HR23B and Myd88 as future biomarkers, it was of interest to look at the localisation of their expression in human tumour tissue (Sections 3.7 and 5.2). There has been little previous examination of these proteins using IHC. In this investigation, it has been seen that HR23B expression is predominantly nuclear although some protein is seen in the cytoplasm and there is variability between different tumours. This is similar to the HR23B pattern of expression seen by immunofluorescence. Myd88 expression appeared both nuclear and cytoplasmic, contrary to cytoplasmic expression of Myd88 that has been seen in previous studies, which may reflect tissue variability or simply an artefact/non-

specificity of the IHC staining [210]. Unfortunately, only small numbers of patient samples were available to be analysed by IHC and limited information was available about treatment received by each patient, so it is not possible to draw conclusions at this stage about impact of treatment on levels of proteins or correlation between pre-treatment protein levels and clinical outcome.

7.2. Interplay of HDAC6 and HR23B dictates cell fate on HDI treatment

The observation that HR23B decrease as levels of autophagy markers increased in HDI treatment and the established role of HDAC6 in autophagy suggested that there may be a relationship between these two proteins. Further evidence for this was obtained by comparing cell lines in which HDAC6 levels are very low through shRNA protein expression (A549 HDAC6 KD and A549 HDAC6 WT) and through creation of a new inducible HDAC6 cell like where it was possible to induce Flag-tagged HDAC6 expression through doxycycline treatment. These systems were used to show that HDAC6 down-regulates HR23B and subsequently it was shown that the domain required for this is the HDAC6 BUZ domain using a number of HDAC6 deletion mutants. It was subsequently shown that this is the domain which interacts with the UbL domain of HR23B [168]. A proteomic approach was used to demonstrate that a number of other proteins interact with HDAC6, which can be grouped into protein networks involved in various cellular proteins [168] (proteomics performed by Dr. Heidi Olzscha). These include proteins involved in DNA repair, cell metabolism, tubulins, HSP90 chaperone proteins and others [168]. It seems as though it is HSP90 which is required for HR23B down-regulation, as HR23B is no longer down-regulated when HSP90 activity is inhibited. This fits with previous findings, which have shown that HDAC6 controls and activates HSP90 activity through deacetylation [30]. It is therefore conceivable that HDAC6 could be a link between chaperone activity and proteasome activity, and it is HSP90 which mediates HR23B degradation (see section 7.12 for potential further work in this direction). In

summary, it has been identified that HDAC6 down-regulates HR23B levels, and the relative levels of these proteins dictate the cell fate choice between cell survival through autophagy and cell death through apoptosis, as summarised in Figure 7.1. These findings suggest the relative levels of HR23B and HDAC6 may act as a promising biomarker signature for HDI treatment.

7.3 Inflammatory cytokine IL-6 release through Myd88-dependent signalling causes apoptosis

Once the role of Myd88 as a sensitivity determinant had been established (Chapter 5), it was of interest to determine which functions of Myd88 are necessary for SAHA-mediated cell death. Myd88 is a known mediator of inflammatory cytokine secretion [211], so the involvement of this process in cell death was tested (Chapter 5), and extracellular IL-6 was identified as responsible for the enhanced cell sensitivity to HDI treatment, through autocrine signalling. IL-6 neutralisation caused a reduction in HDAC inhibitor sensitivity under conditions of Myd88 induction, and also a delay in cell cycle progression, which was observed both through FACS analysis of cell cycle phases and checkpoint protein activation. These findings are summarised diagrammatically in Figure 8.1b). IL-6 has been shown to increase cellular proliferation rate [133], which supports the finding that IL-6 neutralisation leads to delayed cell cycle progression (section 5.7). HDAC inhibition is likely to increase the proportion of cell death in actively proliferating cells due to the effects of these compounds on DNA repair and protein quality control (see introduction section 1.6), which may explain how IL-6 neutralisation reduces cell death on SAHA treatment, as it increases the proportion of cells in the G2 phase of the cell cycle.

An alternative explanation for this observation is that IL-6 released as during Myd88-mediated signalling may act to lead to apoptosis directly and there has been previous evidence of a pro-apoptotic role for IL-6. For example, in a bone-marrow derived stromal cell line, exposure to IL-6 lead to down-regulation of BCL2, stimulation of BCL-XL and induction of apoptosis, which could be

blocked by Bcl-2 expression [212]. There has also been evidence that exposure of cells to IL-6 increases Fas-ligand induced apoptosis in normal lung fibroblasts, (although the opposite was seen in lung fibroblasts from patients with idiopathic pulmonary fibrosis) [12]. This pro-apoptotic effect of IL-6 was thought to be through a STAT-3 dependent mechanism, which causes a low Bcl2-Bax ratio [12].

Figure 7.1

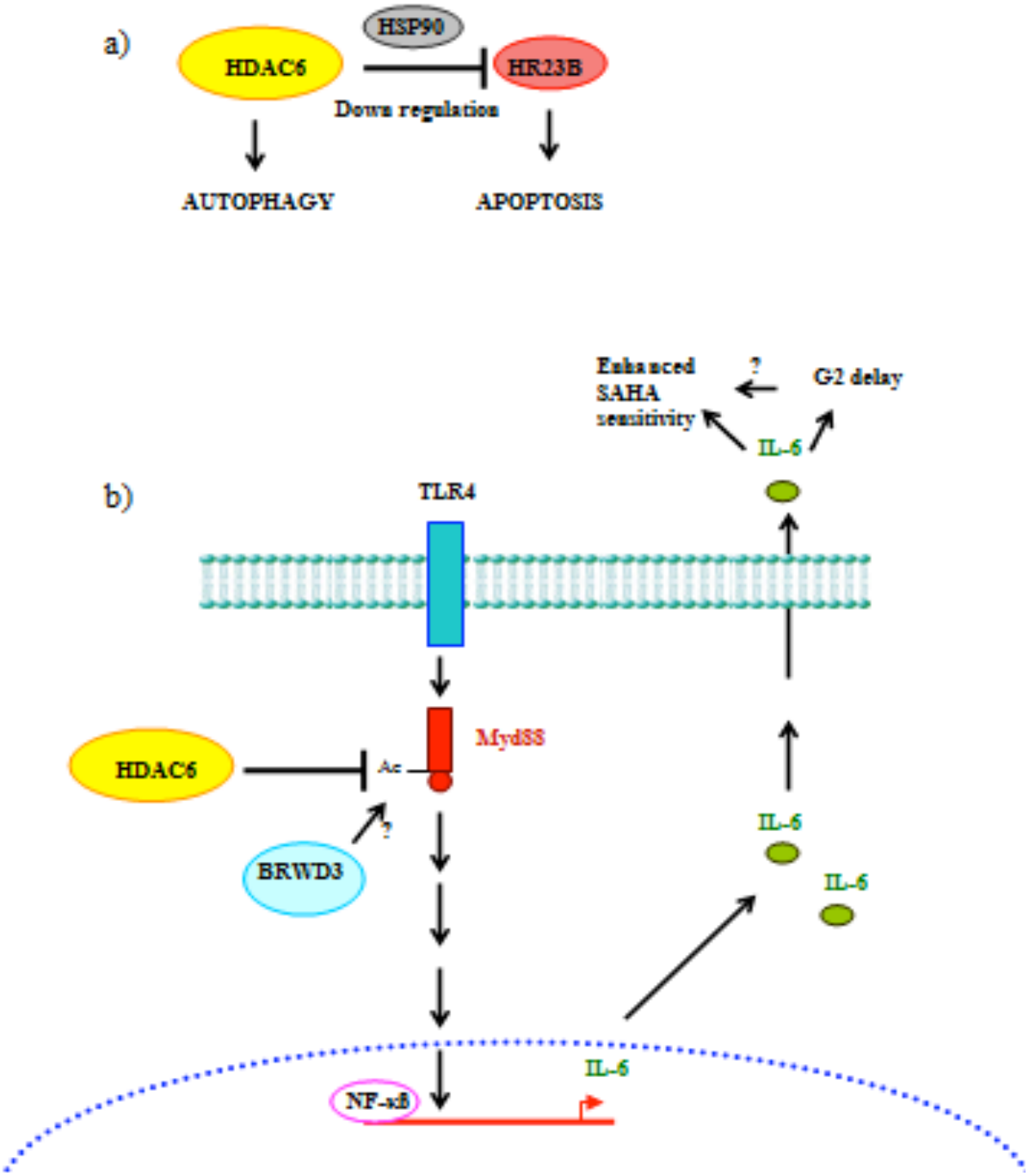

a) Interplay between HDAC6 and HR23B govern cellular response to histone deacetylase inhibitor treatment. HDAC6 down regulates HR23B through HSP90, and in cells where HDAC6 is high and HR23B is low, autophagy is likely to be the cellular outcome on HDI treatment, where as in the converse scenario, apoptosis is more likely

b) Summary diagram of how in cells with high Myd88 levels Myd88-mediated signalling leads to increase IL-6 release which in turn causes cells to be more sensitive to SAHA. HDAC6 mediated Myd88 deacetylation is shown, as well as the possibility (uncertainty indicated by "?") that BRWD3 recognises acetylated Myd88 and that IL-6 mediated cell cycle arrest in G2 may be reason for increased SAHA sensitivity.

7.4. Myd88 acetylation status determines stability and role in response to HDI treatment

There is increasing evidence for the role of acetylation of important non-histone proteins, such as p53, c-Myc, HSP-90 and many others in regulating protein function, by altering protein stability, localization and interactions [213]. Many of these cellular proteins are relevant to cancer cell proliferation and tumourigenesis, and targeting of such acetylation can be a viable cancer therapy approach [213].

Therefore, it was of interest to determine whether Myd88 is directly acetylated, which was achieved through immunoprecipitation and mass spectrometry. A novel Myd88 acetylation site at lysine K119 was identified, and established to regulate Myd88 protein stability (Chapter 6). The K119R mutant was shown to be more stable than wild-type Myd88, suggesting that Myd88 acetylation may reduce the stability of this protein. The more stable K119R mutant of Myd88 was also involved in secreting more IL-6, establishing a connection between Myd88 acetylation status and inflammatory cytokine signalling. Previous publications have shown HDI treatment to reduce inflammatory cytokine release, including that which is part of the TLR-driven immune response [214, 215] and this investigation suggests that one of the mechanisms for this reduction may be through the acetylation status of Myd88. HDI treatment causes increased acetylation levels of cellular proteins, including Myd88, which cause it to be less stable and therefore less active in TLR signalling, which leads to less inflammatory cytokine release (see Figure 8.1b). The reasons for stability changes have not been investigated due to time constraints and could include altered recognition of K119 acetylation by a bromodomain protein which causes Myd88

degradation (see section 7.13, 7.14 in future directions). It is worthy of note that HDAC6 is involved in regulating Myd88 acetylation status and therefore it's stability. Evidence for this includes the interaction between HDAC6 and Myd88 (but not K119R Myd88, which cannot be acetylated), and the regulation of Myd88 levels by HDAC6 (Chapter 6). It is likely that in cells where HDAC6 is absent or at very low levels, Myd88 acetylation is high and protein stability is low which is why it cannot be detected by immunoblotting (Chapter 6).

In summary, a connection has been identified between Myd88 mediated cytokine release, in particular IL-6, and cell death on HDI treatment, as well as a role for HDAC6 in control of Myd88 acetylation levels, and therefore the stability of this protein.

PROJECT LIMITATIONS

7.5. Cell fate measurement

As discussed in the introduction section 1.6, HDI treatment leads to a number of cellular outcomes other than apoptosis and autophagy, such as senescence. In the assays above typically only apoptosis and autophagy were assessed. One of the limitations was the measurement of cell death only by immunoblotting for cleaved PARP and FACS analysis to look at sub-G1. Other analysis methods such as Annexin V staining could be implemented to give a more complete understanding of cell death levels, including being able to differentiate between apoptotic and necrotic cell death [216], and MTT assays to measure drug effect on cell metabolism and therefore viability [217].

Autophagy measurement can also be carried out in a variety of ways as discussed in the introduction 1.9, such as the use of electron microscopy to count autophagic vesicles and determine the ration of their volume to the volume of the whole cytoplasm. Of these potential methods, autophagy was only measured by observing LC3 I and LC3 II levels by immunoblotting as techniques such as electron microscopy were not available. This has limitations however, as it does not measure autophagic flux, but rather only the levels of autophagy at one particular moment in time. This is an issue as the use of static measurement to observe a dynamic process can be misleading, and, in addition, even if autophagy is detected it does not necessarily mean it is performing an important function at that particular moment in time. Measurement of autophagy by observation of autophagosomes in immunofluorescence was also attempted but quantitive measurement of autophagy was not possible by this method due to the

numerousness of the autophagosomes. An additional limitation of this method is that the number of autophagosomes is not the only important factor in identifying autophagy levels, but the size of autophagosomes is also important [85].

7.6. Cell system relevance

The HDAC inhibitors which have been received approval from the FDA are Vorinostat (SAHA, Zolinza) for the treatment of CTCL, Depsipeptide (for the treatment of CTCL and PTCL) [218] and, very recently, Belinostat for the treatment of PTCL (www.fda.gov). However, the shRNA screen for potential HDI treatment sensitivity determinants and subsequent experiments to validate these were conducted in U2OS cells [15], and this was the system used for all the experiments in the current investigation (Chapters 3, 4, 5, 6). U2OS cells were used during the investigation, because this was the cell type used during the screen where HR23B and Myd88 were initially identified as potential sensitivity determinants to HDAC inhibitor treatment [15], and because of the ease of use of this particular adherent cell line, which is an established cancer model cell line (www.ATCC.org).

The cell lines in which the levels of inflammatory cytokines, including IL-6, were measured and their effects investigated were primarily U2OS cells. This has both advantages and disadvantages. Although there has been evidence of IL-6 receptor presence in U2OS cells [219], there is a relatively low amount of IL-6 in these cells compared to other cell types. This can be considered an advantage as there is a lower base level of IL-6 presence, so the increase in IL-6 on Flag-Myd88 induction is more apparent. On the other hand, the low numbers of IL-6 receptors can be considered a limitation as the effects of IL-6 may not be as clear as in other cell lines derived from cancer types where IL-6 is a known key regulator, such as colorectal cell lines [220]. The use of U2OS cells may be the explanation for low levels of cytokines such as IL-10 and IL-1B seen even during Myd88

induction, which is not consistent with existing literature, where high Myd88 levels correlate with increased secretion of those cytokines [221].

More clinically relevant diffuse large B-cell lymphoma cell lines (DLBCL) cell lines, such as RIVA and HBL-1 were used alongside U2OS cells and gave similar results to those in the investigation above (Dr Semira Sheikh, personal communication).

A large proportion of the conclusions drawn from the study were based on the use of Tet-on inducible cell lines, where doxycycline addition causes expression of a Flag-tagged protein such as HR23B, HDAC6 or Myd88. Although this is a useful and convenient tool as it allows to observe the effects of increasing a protein of interest, there are drawbacks to this system, such as the possibility of doxycycline addition altering proliferation and metabolism of human cell lines [155], and the possibility that ectopic overexpression of a protein at such high levels may lead to an "unnatural" state whereby cellular functions such as transcription and translation are excessively occupied with production of a single protein, thereby leading to spurious effects of such overexpression. In addition, high levels of a protein may cause it to participate in functions which the endogenous protein would not perform, such as aggregate formation.

It is important to note that the use of any cell line as a model for a tumour has limitations, as there are genomic differences between cancer cell lines and tumour samples [222], as well as the lack of complexity and heterogeneity in a cell line, as opposed to a tumour, and a lack of tumour evolution and development in a cell model [223].

7.7. Compound specificity and potential

A number of small molecule compounds were used during the investigation, including inhibitors of enzymes (SAHA, tubastatin, JMJD3 inhibitors), autophagy inhibitors (3-MA, bafilomycin A), proteasome inhibitors (velcade, Mg-132) and inhibitors of recognition of acetylated lysines (bromosporine). Although these are useful tools in the elucidation of various biological pathways, especially importance of the catalytic activity of enzymes in such pathways, there are concerns associated with their use, particularly regarding specificity and off-target effects.

For example, although tubastatin A is more selective for HDAC6 compared to general HDIs such as SAHA, it is not completely HDAC6 specific, as demonstrated by very low, but detectable levels of acetylated Histone H3 on tubastatin treatment, which means that it inhibits nuclear HDACs as well as HDAC6. This means that care must be taken with interpretation of experiments where tubastatin A is used, as the effects may not be singly due to HDAC6 inhibition but also from effects on other HDACs which cause a variety of effects including changes in gene transcription (as described in introduction section 1.5). However, comparisons between the general HDI SAHA and tubastatin are still of significance as SAHA is highly broad-spectrum HDI compared to tubastatin which is largely HDAC6 specific. HDAC6 siRNA has advantages in experiments designed to establish the role of HDAC6 in certain processes, although it does not allow investigation of the effect of simply inhibiting the catalytic activity of HDAC6 whilst allowing domains such as the BUZ domain to function.

Another potential problem with the use of small-molecules in the investigation of biological pathways is the possibility of off-target effects. For example, bromosporine is a broad-spectrum bromodomain inhibitor, so cellular effects seen when this compound is used may not only be due to Myd88 acetylation no longer being recognised by a bromodomain reader, but due to other signalling pathways involving bromodomain proteins in the cell being disrupted. This is why creation of a mutant of Myd88 which cannot be acetylated was a useful additional tool to investigate the importance of Myd88 acetylation, in addition to bromosporine treatment.

In order to help eliminate conclusions being made based on off-target effects of small molecule inhibitors, more than one compound in order to inhibit the same pathway, for example 3-MA and bafilomycin, which are both autophagy inhibitors, but function in different ways (Introduction section 1.6) were used in combination with Flag-HDAC6 induction, and a reduction in HR23B levels was seen in both cases (section 4.5), increasing the likelihood that the effects seen were due to autophagy inhibition, rather than a non-specific effect of the compound used.

7. 8. HR23B downregulation on SAHA treatment

An interesting observation which was made during the study was the consistent dose-dependent decrease in HR23B treatment on SAHA treatment, which correlates with an increase in autophagy and led to investigation of the role of HDAC6 in the HDI response. However, there may be other explanations for the decrease in HR23B than the autophagosome degradation route. For example, HR23B levels may decrease on SAHA treatment because the proportion of SAHA-resistant cells increases during treatment, and these resistant cells have very low HR23B levels – perhaps this is why they are not sensitive to HDI treatment. This could be investigated further by selection of resistant cells and measurement of HR23B levels in these, which would require lower SAHA concentrations and longer treatments than used during this project, or simply comparisons between different cell lines some of which are HDI treatment resistant. Alternatively, at the high HDI concentration used, a large proportion of the cells may be in the sub-G1 cells in the cell cycle, which could lead to a reduction in HR23B levels due to caspase activation. In order to test this hypothesis, apoptosis could be blocked, for example with caspase inhibitors, and the levels of HR23B monitored.

It would also be a clinically promising future direction to compare levels expression of these proteins of interest in normal and malignant tissue, and to look at HDAC6 expression to see whether the down-regulation of HR23B by HDAC6 seen in cell line experiments can also be observed as a correlation between high HDAC6 and low HR23B levels in human tumours. More extensive

analysis from a larger number of patients is therefore required to make definitive conclusions. Based on the results of this study, it can be expected that tumours with low levels of HR23B and high HDAC6 will be less likely to be responsive to HDI treatment as cells are more likely to undergo autophagy rather than apoptosis (Figure 7.1). However, as discussed above, caution should be exercised when extrapolating conclusions made from cell line based experiments into the clinic.

7.9. HDAC6 and HSP90

HSP90 is a chaperone protein which is necessary for structural maturation and assembly of client proteins, many of which play a key role in cell signalling, such as kinases [224]. It has been shown that HSP90 is a substrate for HDAC6, and when HSP90 is deacetylated it loses chaperone activity as it stops interacting with the cochaperone p23 [30]. It was further identified during the course of this project that HSP90 activity is required for the down-regulation of HR23B by HDAC6, which suggests that there may be regulation of HDAC6 by HSP90, although the catalytic activity of HDAC6 does not appear to be required [168]. In order to investigate this phenomenon further, other experiments are required to establish the mechanism by which HSP90 catalytic activity impacts on HDAC6. One possibility is that HDAC6 is a client protein for HSP90, which could be required for HDAC6 maturation and function. To test this hypothesis, HDAC6-dependent cellular functions such as tubulin acetylation and autophagy would need to be monitored under conditions of HSP90 inhibition and absence. In addition, in vitro folding experiments where HDAC6 folding is monitored in the presence and absence of HSP90 could be performed.

Alternatively, HSP90 may affect HDAC6 indirectly through a different client protein which in turn modulates HDAC6, or, it could be that HDAC6 down-regulates HR23B through HSP90 which may be important for HR23B degradation. This is a particularly likely possibility, as HSP90 has been implicated to have a role in protein degradation through interaction with the E3 ubiquitin ligase CHIP (carboxy terminus of Hsc70 interacting protein), which leads to client protein ubiquitylation and proteasomal degradation [225]

7.10. Which histone acetyl transferase acetylates Myd88?

One of the key novel findings of the above investigation has been the identification of a novel Myd88 lysine acetylation site, at lysine 119. There has also been evidence of which histone deacetylase is responsible for removing this post-translational modification, as an interaction has been seen between wild-type Myd88 and HDAC6, but the K119R-MYD88 mutant which cannot be acetylated does not appear to interact with HDAC6. However, due to time constraints, there has been no investigation into which histone acetyl transferase (HAT) is responsible for acetylation of Myd88. This is an important potential future direction for the investigation, as Myd88 acetylation affects its stability, which may also affect the cellular level of activation TLR signaling. In order to determine which HAT or HATs acetylate Myd88, a screen could be performed where small-molecule inhibitors are used to reduce HAT activity, and Myd88 acetylation level is measured. Although only one Myd88 acetylation site has been identified in this study (Chapter 6), it is also possible that other lysines in Myd88 are acetylation, or that there are other functionally relevant post-translational modifications present, which is of interest for future investigation.

7.11. Investigation of how Myd88 acetylation affects stability

Lysine acetylation affects protein stability in a number of diverse mechanisms. Acetylation may prevent proteasomal degradation by the proteasome by blocking the lysine which is acetylated from being ubiquitinated [213]. This is unlikely to be the case for Myd88, however, as this study has shown that Myd88 acetylation reduces its stability. It is more likely in this case that acetylation facilitates proteasomal degradation, perhaps by a similar mechanism to HIF1α (Hypoxia inducible factor), which, when acetylated, interacts with the E3 ligase pVHL, which ubiquitinates it causing proteasomal degradation [213].

In order to investigate this possibility, Myd88 ubiquitination could be measured by mass spectrometry or immunoblotting, and the levels of this compared under conditions when Myd88 is acetylated (e.g. During HDI treatment), and when it is not acetylated (in the absence of HDI treatment or in the case of the K119R mutant). The involvement of the proteasome in Myd88 degradation under various conditions could be elucidated using proteasome inhibitors such as velcade or Mg-132. It is also possible that the low half-life of acetylated Myd88 is not due to proteasomal degradation, but rather due to other forms of protein degradation such as endoplasmic reticulum associated degradation (ERAD) [226](although this is less likely than proteasomal degradation as Myd88 is a cytoplasmic protein), so these possibilities would need to be addressed.

7.12. Role of bromodomain recognition of Myd88 acetylation

Established functions of bromodomain-containing proteins are primarily concerned with regulation of gene expression, such as chromatin remodeling [227]. However, there also 11 cytoplasmic bromodomain containing proteins, not all of which have clearly identified functions [93]. Myd88 is a cytoplasmic protein which is acetylated and there has been evidence of the recognition of this acetylated site by the BRWD3 bromodomain-containing protein (chapter 7). However, no further investigation of the functional significance of this recognition has been performed, which is an interesting future direction for the project. A simple function of BRWD3 recognition of Myd88 acetylation may be that such recognition leads to Myd88 degradation, which thus explains the lower half-life of acetylated Myd88 (see section 7.13). However, there has been no reports in the literature of BRWD3 playing a role in protein degradation. The established role of BRWD3 in JAK/STAT signaling [206], makes it of interest to determine whether this is connected to the recognition of Myd88 acetylation by BRWD3. As initial future experiments, the levels of BRWD3 could be altered through siRNA depletion or inducible cell line creation, and the impact of this on Myd88 degradation and TLR signaling could be observed. Additionally, a small molecule inhibitor of the bromodomain in BRWD3 or a mutant where the bromodomain is not functional could be used to determine the importance of bromodomain recognition of Myd88. The draw-back of this approach is that BRWD3 may have a number of cellular substrates other than Myd88 therefore effects of modulating BRWD3 bromodomain activity may not be specific to Myd88.

As discussed in section 6.6, there are 11 cytoplasmic bromodomain-containing proteins, and it may be that BRWD3 is not the only one to recognize Myd88. In order to investigate this, a peptide screen could be performed with all the cytoplasmic bromodomain-containing proteins and Myd88, the results of which could be verified by immunoprecipitation.

7.13. Project summary

During the course of this project, the proteins HR23B and Myd88 have been verified as sensitivity determinants to histone deacetylase inhibitor treatment. HR23B has been shown to be regulated by HDAC6, through HSP90, which determines whether HDI treated cells undergo apoptosis or survive through autophagy [228]. Interesting insights into the role of Myd88 during the response to HDI treatment have been obtained, including a novel post-translational modification site and a role for IL-6 release in cell cycle progression and HDI sensitivity.

Initially, the only link between Myd88 and HR23B appears to be that they have been identified during the same shRNA screen for sensitivity determinants to SAHA treatment [15]. As the study progressed, however, it became apparent that HDAC6 acts as a connection between these two proteins, as both HR23B and Myd88 interact with HDAC6. The way in which HDAC6 is important in the function of these two proteins, is different, however: in the case of HR23B, HDAC6 down-regulates levels of this protein, whereas in the case of Myd88, HDAC6 is likely to stabilise Myd88 through removal of the acetylation at lysine K119.

In conclusion, the current study has provided interesting and translationally revelant insights into the functions of HR23B, Myd88 and HDAC6 during the response to histone deacetylase inhibitior treatment.

The findings made during this project can be summarised in the following series of points:

a) General HDI treatment causes a number of cellular outcomes, including apoptosis and autophagy

b) In cell culture, pretreatment HR23B and Myd88 levels affect cell fate on HDI treatment, with higher levels of these proteins leading to greater cell death on HDI treatment

c) The autophagy-promoting enzyme HDAC6 downregulates HR23B, and HSP90 is likely to be required for this down-regulation

d) The cellular outcome on HDI treatment is in part determined by relative levels of HDAC6 and HR23B, with high HDAC6 and low HR23B leading to autophagy rather than apoptosis

e) Myd88-mediated cell death on HDI treatment is dependent on IL-6 release, which affects cell cycle progression, under the conditions used in this study.

f) Myd88 is acetylated on lysine K119, and the acetylated form of Myd88 is less stable

g) HR23B, HDAC6 and Myd88 have important functions in governing response to HDI treatment in cell culture, which may prove translationally relevant as there is potential for these proteins to be used as biomarkers to HDI treatment in the clinic.

References

1. Uchida, A., et al., *The carboxy-terminal domain of the XPC protein plays a crucial role in nucleotide excision repair through interactions with transcription factor IIH.* DNA Repair (Amst), 2002. **1**(6): p. 449-61.
2. Han, J., *MyD88 beyond Toll.* Nat Immunol, 2006. **7**(4): p. 370-1.
3. Fleming, A., et al., *Chemical modulators of autophagy as biological probes and potential therapeutics.* Nat Chem Biol, 2011. **7**(1): p. 9-17.
4. Ohnishi, H., et al., *Structural basis for the multiple interactions of the MyD88 TIR domain in TLR4 signaling.* Proc Natl Acad Sci U S A, 2009. **106**(25): p. 10260-5.
5. Akira, S., S. Uematsu, and O. Takeuchi, *Pathogen recognition and innate immunity.* Cell, 2006. **124**(4): p. 783-801.
6. Mizushima, N., *The pleiotropic role of autophagy: from protein metabolism to bactericide.* Cell Death Differ, 2005. **12 Suppl 2**: p. 1535-41.
7. Arkenau, H.T., R. Kefford, and G.V. Long, *Targeting BRAF for patients with melanoma.* Br J Cancer, 2011. **104**(3): p. 392-8.
8. Mizushima, N., *Autophagy: process and function.* Genes Dev, 2007. **21**(22): p. 2861-73.
9. Jaeger, P.A. and T. Wyss-Coray, *All-you-can-eat: autophagy in neurodegeneration and neuroprotection.* Mol Neurodegener, 2009. **4**: p. 16.
10. Coste, I., et al., *Dual function of MyD88 in RAS signaling and inflammation, leading to mouse and human cell transformation.* J Clin Invest, 2010. **120**(10): p. 3663-7.
11. Bentley, G.A., et al., *The crystal structure of the nucleosome core particle by contrast variation.* Basic Life Sci, 1984. **27**: p. 105-17.
12. Moodley, Y.P., et al., *Inverse effects of interleukin-6 on apoptosis of fibroblasts from pulmonary fibrosis and normal lungs.* Am J Respir Cell Mol Biol, 2003. **29**(4): p. 490-8.
13. Haggarty, S.J., et al., *Domain-selective small-molecule inhibitor of histone deacetylase 6 (HDAC6)-mediated tubulin deacetylation.* Proc Natl Acad Sci U S A, 2003. **100**(8): p. 4389-94.
14. Lee, J.Y., et al., *HDAC6 controls autophagosome maturation essential for ubiquitin-selective quality-control autophagy.* EMBO J, 2010. **29**(5): p. 969-80.
15. Fotheringham, S., et al., *Genome-wide loss-of-function screen reveals an important role for the proteasome in HDAC inhibitor-induced apoptosis.* Cancer Cell, 2009. **15**(1): p. 57-66.
16. Inche, A.G. and N.B. La Thangue, *Chromatin control and cancer-drug discovery: realizing the promise.* Drug Discov Today, 2006. **11**(3-4): p. 97-109.
17. Moniot, S., M. Weyand, and C. Steegborn, *Structures, substrates, and regulators of Mammalian sirtuins - opportunities and challenges for drug development.* Front Pharmacol, 2012. **3**: p. 16.
18. Khan, O. and N.B. La Thangue, *Drug Insight: histone deacetylase inhibitor-based therapies for cutaneous T-cell lymphomas.* Nat Clin Pract Oncol, 2008. **5**(12): p. 714-26.
19. Mistry, A.R., et al., *The molecular pathogenesis of acute promyelocytic leukaemia: implications for the clinical management of the disease.* Blood Rev, 2003. **17**(2): p. 71-97.
20. Witt, O., et al., *HDAC family: What are the cancer relevant targets?* Cancer Lett, 2009. **277**(1): p. 8-21.
21. New, M., H. Olzscha, and N.B. La Thangue, *HDAC inhibitor-based therapies: can we interpret the code?* Mol Oncol, 2012. **6**(6): p. 637-56.

22. Gregoretti, I.V., Y.M. Lee, and H.V. Goodson, *Molecular evolution of the histone deacetylase family: functional implications of phylogenetic analysis.* J Mol Biol, 2004. **338**(1): p. 17-31.
23. Liu, T., P.Y. Liu, and G.M. Marshall, *The critical role of the class III histone deacetylase SIRT1 in cancer.* Cancer Res, 2009. **69**(5): p. 1702-5.
24. Haigis, M.C. and D.A. Sinclair, *Mammalian sirtuins: biological insights and disease relevance.* Annu Rev Pathol, 2010. **5**: p. 253-95.
25. Sjoblom, T., et al., *The consensus coding sequences of human breast and colorectal cancers.* Science, 2006. **314**(5797): p. 268-74.
26. Ropero, S., et al., *A truncating mutation of HDAC2 in human cancers confers resistance to histone deacetylase inhibition.* Nat Genet, 2006. **38**(5): p. 566-9.
27. de Ruijter, A.J., et al., *Histone deacetylases (HDACs): characterization of the classical HDAC family.* Biochem J, 2003. **370**(Pt 3): p. 737-49.
28. Glaser, K.B., et al., *Gene expression profiling of multiple histone deacetylase (HDAC) inhibitors: defining a common gene set produced by HDAC inhibition in T24 and MDA carcinoma cell lines.* Mol Cancer Ther, 2003. **2**(2): p. 151-63.
29. Xu, W.S., R.B. Parmigiani, and P.A. Marks, *Histone deacetylase inhibitors: molecular mechanisms of action.* Oncogene, 2007. **26**(37): p. 5541-52.
30. Kovacs, J.J., et al., *HDAC6 regulates Hsp90 acetylation and chaperone-dependent activation of glucocorticoid receptor.* Mol Cell, 2005. **18**(5): p. 601-7.
31. Li, Y., et al., *HDAC6 is required for epidermal growth factor-induced beta-catenin nuclear localization.* J Biol Chem, 2008. **283**(19): p. 12686-90.
32. Ye, F., et al., *HDAC1 and HDAC2 regulate oligodendrocyte differentiation by disrupting the beta-catenin-TCF interaction.* Nat Neurosci, 2009. **12**(7): p. 829-38.
33. Zhu, P., et al., *Induction of HDAC2 expression upon loss of APC in colorectal tumorigenesis.* Cancer Cell, 2004. **5**(5): p. 455-63.
34. Martinez-Balbas, M.A., et al., *Regulation of E2F1 activity by acetylation.* EMBO J, 2000. **19**(4): p. 662-71.
35. Boyault, C., et al., *HDAC6, at the crossroads between cytoskeleton and cell signaling by acetylation and ubiquitination.* Oncogene, 2007. **26**(37): p. 5468-76.
36. Kwon, S., Y. Zhang, and P. Matthias, *The deacetylase HDAC6 is a novel critical component of stress granules involved in the stress response.* Genes Dev, 2007. **21**(24): p. 3381-94.
37. Kawaguchi, Y., et al., *The deacetylase HDAC6 regulates aggresome formation and cell viability in response to misfolded protein stress.* Cell, 2003. **115**(6): p. 727-38.
38. Zhang, Y., et al., *Mice lacking histone deacetylase 6 have hyperacetylated tubulin but are viable and develop normally.* Mol Cell Biol, 2008. **28**(5): p. 1688-701.
39. Laeng, P., et al., *The mood stabilizer valproic acid stimulates GABA neurogenesis from rat forebrain stem cells.* J Neurochem, 2004. **91**(1): p. 238-51.
40. Dinarello, C.A., G. Fossati, and P. Mascagni, *Histone deacetylase inhibitors for treating a spectrum of diseases not related to cancer.* Mol Med, 2011. **17**(5-6): p. 333-52.
41. Khan, O., et al., *HR23B is a biomarker for tumor sensitivity to HDAC inhibitor-based therapy.* Proc Natl Acad Sci U S A, 2010. **107**(14): p. 6532-7.
42. Stimson, L., et al., *HDAC inhibitor-based therapies and haematological malignancy.* Ann Oncol, 2009. **20**(8): p. 1293-302.
43. Marks, P.A., *The clinical development of histone deacetylase inhibitors as targeted anticancer drugs.* Expert Opin Investig Drugs, 2010. **19**(9): p. 1049-66.
44. Bantscheff, M., et al., *Chemoproteomics profiling of HDAC inhibitors reveals selective targeting of HDAC complexes.* Nat Biotechnol, 2011. **29**(3): p. 255-65.
45. Finnin, M.S., et al., *Structures of a histone deacetylase homologue bound to the TSA and SAHA inhibitors.* Nature, 1999. **401**(6749): p. 188-93.

46. Khan, O. and N.B. La Thangue, *HDAC inhibitors in cancer biology: emerging mechanisms and clinical applications.* Immunol Cell Biol, 2012. **90**(1): p. 85-94.
47. Fischer, A., et al., *Targeting the correct HDAC(s) to treat cognitive disorders.* Trends Pharmacol Sci, 2010. **31**(12): p. 605-17.
48. Butler, K.V., et al., *Rational design and simple chemistry yield a superior, neuroprotective HDAC6 inhibitor, tubastatin A.* J Am Chem Soc, 2010. **132**(31): p. 10842-6.
49. Kaliszczak, M., et al., *A novel small molecule hydroxamate preferentially inhibits HDAC6 activity and tumour growth.* Br J Cancer, 2013. **108**(2): p. 342-50.
50. Rikiishi, H., *Autophagic and apoptotic effects of HDAC inhibitors on cancer cells.* J Biomed Biotechnol, 2011. **2011**: p. 830260.
51. Xu, J., et al., *Sp1-mediated TRAIL induction in chemosensitization.* Cancer Res, 2008. **68**(16): p. 6718-26.
52. Garcia-Morales, P., et al., *Histone deacetylase inhibitors induced caspase-independent apoptosis in human pancreatic adenocarcinoma cell lines.* Mol Cancer Ther, 2005. **4**(8): p. 1222-30.
53. Srivastava, R.K., R. Kurzrock, and S. Shankar, *MS-275 sensitizes TRAIL-resistant breast cancer cells, inhibits angiogenesis and metastasis, and reverses epithelial-mesenchymal transition in vivo.* Mol Cancer Ther, 2010. **9**(12): p. 3254-66.
54. Brochier, C., et al., *Specific Acetylation of p53 by HDAC Inhibition Prevents DNA Damage-Induced Apoptosis in Neurons.* J Neurosci, 2013. **33**(20): p. 8621-32.
55. Ito, A., et al., *MDM2-HDAC1-mediated deacetylation of p53 is required for its degradation.* EMBO J, 2002. **21**(22): p. 6236-45.
56. Kim, M.S., et al., *Histone deacetylases induce angiogenesis by negative regulation of tumor suppressor genes.* Nat Med, 2001. **7**(4): p. 437-43.
57. Kim, S.H., et al., *Regulation of the HIF-1alpha stability by histone deacetylases.* Oncol Rep, 2007. **17**(3): p. 647-51.
58. Qian, D.Z., et al., *Class II histone deacetylases are associated with VHL-independent regulation of hypoxia-inducible factor 1 alpha.* Cancer Res, 2006. **66**(17): p. 8814-21.
59. Liu, L.T., et al., *Histone deacetylase inhibitor up-regulates RECK to inhibit MMP-2 activation and cancer cell invasion.* Cancer Res, 2003. **63**(12): p. 3069-72.
60. Zupkovitz, G., et al., *Negative and positive regulation of gene expression by mouse histone deacetylase 1.* Mol Cell Biol, 2006. **26**(21): p. 7913-28.
61. Yamaguchi, T., et al., *Histone deacetylases 1 and 2 act in concert to promote the G1-to-S progression.* Genes Dev, 2010. **24**(5): p. 455-69.
62. Wilson, A.J., et al., *HDAC4 promotes growth of colon cancer cells via repression of p21.* Mol Biol Cell, 2008. **19**(10): p. 4062-75.
63. Wilson, A.J., et al., *Histone deacetylase 3 (HDAC3) and other class I HDACs regulate colon cell maturation and p21 expression and are deregulated in human colon cancer.* J Biol Chem, 2006. **281**(19): p. 13548-58.
64. Hu, J. and N.H. Colburn, *Histone deacetylase inhibition down-regulates cyclin D1 transcription by inhibiting nuclear factor-kappaB/p65 DNA binding.* Mol Cancer Res, 2005. **3**(2): p. 100-9.
65. Stevens, F.E., et al., *Histone deacetylase inhibitors induce mitotic slippage.* Oncogene, 2008. **27**(10): p. 1345-54.
66. Munshi, A., et al., *Vorinostat, a histone deacetylase inhibitor, enhances the response of human tumor cells to ionizing radiation through prolongation of gamma-H2AX foci.* Mol Cancer Ther, 2006. **5**(8): p. 1967-74.
67. Adimoolam, S., et al., *HDAC inhibitor PCI-24781 decreases RAD51 expression and inhibits homologous recombination.* Proc Natl Acad Sci U S A, 2007. **104**(49): p. 19482-7.

68. Rosato, R.R., et al., *Role of histone deacetylase inhibitor-induced reactive oxygen species and DNA damage in LAQ-824/fludarabine antileukemic interactions.* Mol Cancer Ther, 2008. **7**(10): p. 3285-97.
69. Miller, K.M., et al., *Human HDAC1 and HDAC2 function in the DNA-damage response to promote DNA nonhomologous end-joining.* Nat Struct Mol Biol, 2010. **17**(9): p. 1144-51.
70. Hartl, F.U., A. Bracher, and M. Hayer-Hartl, *Molecular chaperones in protein folding and proteostasis.* Nature, 2011. **475**(7356): p. 324-32.
71. Bali, P., et al., *Inhibition of histone deacetylase 6 acetylates and disrupts the chaperone function of heat shock protein 90: a novel basis for antileukemia activity of histone deacetylase inhibitors.* J Biol Chem, 2005. **280**(29): p. 26729-34.
72. Nimmanapalli, R., et al., *Histone deacetylase inhibitor LAQ824 both lowers expression and promotes proteasomal degradation of Bcr-Abl and induces apoptosis of imatinib mesylate-sensitive or -refractory chronic myelogenous leukemia-blast crisis cells.* Cancer Res, 2003. **63**(16): p. 5126-35.
73. Yu, H., D. Pardoll, and R. Jove, *STATs in cancer inflammation and immunity: a leading role for STAT3.* Nat Rev Cancer, 2009. **9**(11): p. 798-809.
74. Kramer, O.H., et al., *A phosphorylation-acetylation switch regulates STAT1 signaling.* Genes Dev, 2009. **23**(2): p. 223-35.
75. Shakespear, M.R., et al., *Histone deacetylases as regulators of inflammation and immunity.* Trends Immunol, 2011. **32**(7): p. 335-43.
76. Vishwakarma, S., et al., *Tubastatin, a selective histone deacetylase 6 inhibitor shows anti-inflammatory and anti-rheumatic effects.* Int Immunopharmacol, 2013. **16**(1): p. 72-8.
77. Levine, B. and D.J. Klionsky, *Development by self-digestion: molecular mechanisms and biological functions of autophagy.* Dev Cell, 2004. **6**(4): p. 463-77.
78. Sanjuan, M.A., et al., *Toll-like receptor signalling in macrophages links the autophagy pathway to phagocytosis.* Nature, 2007. **450**(7173): p. 1253-7.
79. Yang, Y.P., et al., *Application and interpretation of current autophagy inhibitors and activators.* Acta Pharmacol Sin, 2013. **34**(5): p. 625-35.
80. Kihara, A., et al., *Beclin-phosphatidylinositol 3-kinase complex functions at the trans-Golgi network.* EMBO Rep, 2001. **2**(4): p. 330-5.
81. Liang, X.H., et al., *Induction of autophagy and inhibition of tumorigenesis by beclin 1.* Nature, 1999. **402**(6762): p. 672-6.
82. Sarkar, S., *Regulation of autophagy by mTOR-dependent and mTOR-independent pathways: autophagy dysfunction in neurodegenerative diseases and therapeutic application of autophagy enhancers.* Biochem Soc Trans, 2013. **41**(5): p. 1103-30.
83. Yamamoto, S., et al., *Suberoylanilide hydroxamic acid (SAHA) induces apoptosis or autophagy-associated cell death in chondrosarcoma cell lines.* Anticancer Res, 2008. **28**(3A): p. 1585-91.
84. Carew, J.S., et al., *Autophagy inhibition enhances vorinostat-induced apoptosis via ubiquitinated protein accumulation.* J Cell Mol Med, 2010. **14**(10): p. 2448-59.
85. Mizushima, N., T. Yoshimori, and B. Levine, *Methods in mammalian autophagy research.* Cell, 2010. **140**(3): p. 313-26.
86. Ashford, T.P. and K.R. Porter, *Cytoplasmic components in hepatic cell lysosomes.* J Cell Biol, 1962. **12**: p. 198-202.
87. Kabeya, Y., et al., *LC3, a mammalian homologue of yeast Apg8p, is localized in autophagosome membranes after processing.* EMBO J, 2000. **19**(21): p. 5720-8.
88. Mizushima, N., et al., *In vivo analysis of autophagy in response to nutrient starvation using transgenic mice expressing a fluorescent autophagosome marker.* Mol Biol Cell, 2004. **15**(3): p. 1101-11.

89. Yamamoto, A., et al., *Bafilomycin A1 prevents maturation of autophagic vacuoles by inhibiting fusion between autophagosomes and lysosomes in rat hepatoma cell line, H-4-II-E cells.* Cell Struct Funct, 1998. **23**(1): p. 33-42.
90. Kim, D.H., et al., *mTOR interacts with raptor to form a nutrient-sensitive complex that signals to the cell growth machinery.* Cell, 2002. **110**(2): p. 163-75.
91. Yu, Y., et al., *Targeting microRNA-30a-mediated autophagy enhances imatinib activity against human chronic myeloid leukemia cells.* Leukemia, 2012. **26**(8): p. 1752-60.
92. Zhou, Q., et al., *Screening for therapeutic targets of vorinostat by SILAC-based proteomic analysis in human breast cancer cells.* Proteomics, 2010. **10**(5): p. 1029-39.
93. Filippakopoulos, P., et al., *Histone recognition and large-scale structural analysis of the human bromodomain family.* Cell, 2012. **149**(1): p. 214-31.
94. Mujtaba, S., L. Zeng, and M.M. Zhou, *Structure and acetyl-lysine recognition of the bromodomain.* Oncogene, 2007. **26**(37): p. 5521-7.
95. LeRoy, G., B. Rickards, and S.J. Flint, *The double bromodomain proteins Brd2 and Brd3 couple histone acetylation to transcription.* Mol Cell, 2008. **30**(1): p. 51-60.
96. Reynoird, N., et al., *Oncogenesis by sequestration of CBP/p300 in transcriptionally inactive hyperacetylated chromatin domains.* EMBO J, 2010. **29**(17): p. 2943-52.
97. French, C.A., et al., *BRD4 bromodomain gene rearrangement in aggressive carcinoma with translocation t(15;19).* Am J Pathol, 2001. **159**(6): p. 1987-92.
98. Filippakopoulos, P., et al., *Selective inhibition of BET bromodomains.* Nature, 2010. **468**(7327): p. 1067-73.
99. Muller, S., P. Filippakopoulos, and S. Knapp, *Bromodomains as therapeutic targets.* Expert Rev Mol Med, 2011. **13**: p. e29.
100. Ginsburg, G.S. and H.F. Willard, *Genomic and personalized medicine: foundations and applications.* Transl Res, 2009. **154**(6): p. 277-87.
101. O'Connell, M.J., et al., *Improving adjuvant therapy for rectal cancer by combining protracted-infusion fluorouracil with radiation therapy after curative surgery.* N Engl J Med, 1994. **331**(8): p. 502-7.
102. Duldulao, M.P., et al., *Mutations in Specific Codons of the KRAS Oncogene are Associated with Variable Resistance to Neoadjuvant Chemoradiation Therapy in Patients with Rectal Adenocarcinoma.* Ann Surg Oncol, 2013.
103. van't Veer, L.J. and R. Bernards, *Enabling personalized cancer medicine through analysis of gene-expression patterns.* Nature, 2008. **452**(7187): p. 564-70.
104. Mao, Y., et al., *Stromal cells in tumor microenvironment and breast cancer.* Cancer Metastasis Rev, 2012.
105. Straussman, R., et al., *Tumour micro-environment elicits innate resistance to RAF inhibitors through HGF secretion.* Nature, 2012. **487**(7408): p. 500-4.
106. Tentler, J.J., et al., *Patient-derived tumour xenografts as models for oncology drug development.* Nat Rev Clin Oncol, 2012. **9**(6): p. 338-50.
107. Egeblad, M. and Z. Werb, *New functions for the matrix metalloproteinases in cancer progression.* Nat Rev Cancer, 2002. **2**(3): p. 161-74.
108. Wu, E., et al., *Stromelysin-3 suppresses tumor cell apoptosis in a murine model.* J Cell Biochem, 2001. **82**(4): p. 549-55.
109. Roy, R., J. Yang, and M.A. Moses, *Matrix metalloproteinases as novel biomarkers and potential therapeutic targets in human cancer.* J Clin Oncol, 2009. **27**(31): p. 5287-97.
110. Decock, J., et al., *Matrix metalloproteinases: protective roles in cancer.* J Cell Mol Med, 2011. **15**(6): p. 1254-65.
111. Palavalli, L.H., et al., *Analysis of the matrix metalloproteinase family reveals that MMP8 is often mutated in melanoma.* Nat Genet, 2009. **41**(5): p. 518-20.
112. Korpi, J.T., et al., *Collagenase-2 (matrix metalloproteinase-8) plays a protective role in tongue cancer.* Br J Cancer, 2008. **98**(4): p. 766-75.

113. Ratain, M.J., et al., *Pharmacodynamics in cancer therapy.* J Clin Oncol, 1990. **8**(10): p. 1739-53.
114. van 't Veer, L.J., et al., *Gene expression profiling predicts clinical outcome of breast cancer.* Nature, 2002. **415**(6871): p. 530-6.
115. Wang, Y., et al., *Gene-expression profiles to predict distant metastasis of lymph-node-negative primary breast cancer.* Lancet, 2005. **365**(9460): p. 671-9.
116. Terasawa, T., I. Dahabreh, and T.A. Trikalinos, *BCR-ABL mutation testing to predict response to tyrosine kinase inhibitors in patients with chronic myeloid leukemia.* PLoS Curr, 2010. **2**: p. RRN1204.
117. Slamon, D.J., et al., *Human breast cancer: correlation of relapse and survival with amplification of the HER-2/neu oncogene.* Science, 1987. **235**(4785): p. 177-82.
118. Dawood, S., et al., *Prognosis of women with metastatic breast cancer by HER2 status and trastuzumab treatment: an institutional-based review.* J Clin Oncol, 2010. **28**(1): p. 92-8.
119. La Thangue, N.B. and D.J. Kerr, *Predictive biomarkers: a paradigm shift towards personalized cancer medicine.* Nat Rev Clin Oncol, 2011. **8**(10): p. 587-96.
120. Wooster, R. and B.L. Weber, *Breast and ovarian cancer.* N Engl J Med, 2003. **348**(23): p. 2339-47.
121. Schilsky, R.L., *Personalized medicine in oncology: the future is now.* Nat Rev Drug Discov, 2010. **9**(5): p. 363-6.
122. Yeo, W., et al., *Epigenetic therapy using belinostat for patients with unresectable hepatocellular carcinoma: a multicenter phase I/II study with biomarker and pharmacokinetic analysis of tumors from patients in the Mayo Phase II Consortium and the Cancer Therapeutics Research Group.* J Clin Oncol, 2012. **30**(27): p. 3361-7.
123. Sugasawa, K., et al., *Xeroderma pigmentosum group C protein complex is the initiator of global genome nucleotide excision repair.* Mol Cell, 1998. **2**(2): p. 223-32.
124. Into, T., et al., *Regulation of MyD88 aggregation and the MyD88-dependent signaling pathway by sequestosome 1 and histone deacetylase 6.* J Biol Chem, 2010. **285**(46): p. 35759-69.
125. Su, V. and A.F. Lau, *Ubiquitin-like and ubiquitin-associated domain proteins: significance in proteasomal degradation.* Cell Mol Life Sci, 2009. **66**(17): p. 2819-33.
126. Chen, L. and K. Madura, *Rad23 promotes the targeting of proteolytic substrates to the proteasome.* Mol Cell Biol, 2002. **22**(13): p. 4902-13.
127. Rakoff-Nahoum, S. and R. Medzhitov, *Toll-like receptors and cancer.* Nature Reviews Cancer, 2009. **9**(1): p. 57-63.
128. Takeda, K. and S. Akira, *TLR signaling pathways.* Semin Immunol, 2004. **16**(1): p. 3-9.
129. Kawai, T., et al., *Unresponsiveness of MyD88-deficient mice to endotoxin.* Immunity, 1999. **11**(1): p. 115-22.
130. Hirota, K., et al., *Antitumor effect of inhalatory lipopolysaccharide and synergetic effect in combination with cyclophosphamide.* Anticancer Res, 2010. **30**(8): p. 3129-34.
131. Maslinska, D., M. Laure-Kamionowska, and S. Maslinska, *Toll-like receptors as an innate immunity bridge to neuroinflammation in medulloblastoma.* Folia Neuropathol, 2012. **50**(4): p. 375-81.
132. Dranoff, G., *Cytokines in cancer pathogenesis and cancer therapy.* Nat Rev Cancer, 2004. **4**(1): p. 11-22.
133. Grivennikov, S., et al., *IL-6 and Stat3 are required for survival of intestinal epithelial cells and development of colitis-associated cancer.* Cancer Cell, 2009. **15**(2): p. 103-13.
134. Dhillon, A.S., et al., *MAP kinase signalling pathways in cancer.* Oncogene, 2007. **26**(22): p. 3279-90.
135. Kfoury, A., et al., *MyD88 in DNA Repair and Cancer Cell Resistance to Genotoxic Drugs.* J Natl Cancer Inst, 2013.

136. Ding, W.X. and X.M. Yin, *Sorting, recognition and activation of the misfolded protein degradation pathways through macroautophagy and the proteasome.* Autophagy, 2008. **4**(2): p. 141-150.
137. Ngo, V.N., et al., *Oncogenically active MYD88 mutations in human lymphoma.* Nature, 2011. **470**(7332): p. 115-9.
138. Montesinos-Rongen, M., et al., *Activating L265P mutations of the MYD88 gene are common in primary central nervous system lymphoma.* Acta Neuropathol, 2011. **122**(6): p. 791-2.
139. Egunsola, A.T., et al., *Growth, metastasis, and expression of CCL2 and CCL5 by murine mammary carcinomas are dependent upon Myd88.* Cell Immunol, 2012. **272**(2): p. 220-9.
140. Yue, Z., et al., *Beclin 1, an autophagy gene essential for early embryonic development, is a haploinsufficient tumor suppressor.* Proc Natl Acad Sci U S A, 2003. **100**(25): p. 15077-82.
141. Codogno, P. and A.J. Meijer, *Autophagy and signaling: their role in cell survival and cell death.* Cell Death Differ, 2005. **12 Suppl 2**: p. 1509-18.
142. Fantin, V.R. and V.M. Richon, *Mechanisms of resistance to histone deacetylase inhibitors and their therapeutic implications.* Clin Cancer Res, 2007. **13**(24): p. 7237-42.
143. Janku, F., et al., *Autophagy as a target for anticancer therapy.* Nat Rev Clin Oncol, 2011. **8**(9): p. 528-39.
144. Herceg, Z. and Z.Q. Wang, *Failure of poly(ADP-ribose) polymerase cleavage by caspases leads to induction of necrosis and enhanced apoptosis.* Mol Cell Biol, 1999. **19**(7): p. 5124-33.
145. Soldani, C. and A.I. Scovassi, *Poly(ADP-ribose) polymerase-1 cleavage during apoptosis: an update.* Apoptosis, 2002. **7**(4): p. 321-8.
146. Masutani, C., et al., *Purification and cloning of a nucleotide excision repair complex involving the xeroderma pigmentosum group C protein and a human homologue of yeast RAD23.* EMBO J, 1994. **13**(8): p. 1831-43.
147. Chen, L., et al., *Ubiquitin-associated (UBA) domains in Rad23 bind ubiquitin and promote inhibition of multi-ubiquitin chain assembly.* EMBO Rep, 2001. **2**(10): p. 933-8.
148. Schauber, C., et al., *Rad23 links DNA repair to the ubiquitin/proteasome pathway.* Nature, 1998. **391**(6668): p. 715-8.
149. Mantovani, A., et al., *Cancer-related inflammation.* Nature, 2008. **454**(7203): p. 436-44.
150. Drogaris, P., et al., *Histone deacetylase inhibitors globally enhance h3/h4 tail acetylation without affecting h3 lysine 56 acetylation.* Sci Rep, 2012. **2**: p. 220.
151. Pankiv, S., et al., *p62/SQSTM1 binds directly to Atg8/LC3 to facilitate degradation of ubiquitinated protein aggregates by autophagy.* J Biol Chem, 2007. **282**(33): p. 24131-45.
152. Rao, R., et al., *Combination of pan-histone deacetylase inhibitor and autophagy inhibitor exerts superior efficacy against triple-negative human breast cancer cells.* Mol Cancer Ther, 2012. **11**(4): p. 973-83.
153. Huo, H.Z., et al., *Dramatic suppression of colorectal cancer cell growth by the dual mTORC1 and mTORC2 inhibitor AZD-2014.* Biochem Biophys Res Commun, 2014. **443**(2): p. 406-12.
154. Franken, N.A., et al., *Clonogenic assay of cells in vitro.* Nat Protoc, 2006. **1**(5): p. 2315-9.
155. Ahler, E., et al., *Doxycycline alters metabolism and proliferation of human cell lines.* PLoS One, 2013. **8**(5): p. e64561.
156. Matos, L.L., et al., *Immunohistochemistry as an important tool in biomarkers detection and clinical practice.* Biomark Insights, 2010. **5**: p. 9-20.
157. Reed, N.A., et al., *Microtubule acetylation promotes kinesin-1 binding and transport.* Curr Biol, 2006. **16**(21): p. 2166-72.
158. Fotheringham, *HDAC inhibitor-based therapies and haematological malignancy.* 2009.
159. Hubbert, C., et al., *HDAC6 is a microtubule-associated deacetylase.* Nature, 2002. **417**(6887): p. 455-8.

160. Matthias, P., M. Yoshida, and S. Khochbin, *HDAC6 a new cellular stress surveillance factor.* Cell Cycle, 2008. **7**(1): p. 7-10.
161. Valenzuela-Fernandez, A., et al., *HDAC6: a key regulator of cytoskeleton, cell migration and cell-cell interactions.* Trends Cell Biol, 2008. **18**(6): p. 291-7.
162. Chen, D., et al., *Bortezomib as the first proteasome inhibitor anticancer drug: current status and future perspectives.* Curr Cancer Drug Targets, 2011. **11**(3): p. 239-53.
163. Lu, S. and J. Wang, *The resistance mechanisms of proteasome inhibitor bortezomib.* Biomark Res, 2013. **1**(1): p. 13.
164. Meng, L., et al., *Epoxomicin, a potent and selective proteasome inhibitor, exhibits in vivo antiinflammatory activity.* Proc Natl Acad Sci U S A, 1999. **96**(18): p. 10403-8.
165. Kanematsu, S., et al., *Autophagy inhibition enhances sulforaphane-induced apoptosis in human breast cancer cells.* Anticancer Res, 2010. **30**(9): p. 3381-90.
166. Takatsuka, C., et al., *3-methyladenine inhibits autophagy in tobacco culture cells under sucrose starvation conditions.* Plant Cell Physiol, 2004. **45**(3): p. 265-74.
167. Trepel, J., et al., *Targeting the dynamic HSP90 complex in cancer.* Nat Rev Cancer, 2010. **10**(8): p. 537-49.
168. New, M., et al., *A regulatory circuit that involves HR23B and HDAC6 governs the biological response to HDAC inhibitors.* Cell Death Differ, 2013. **20**(10): p. 1306-16.
169. Yang, Z.J., et al., *The role of autophagy in cancer: therapeutic implications.* Mol Cancer Ther, 2011. **10**(9): p. 1533-41.
170. Pratt, W.B., et al., *Role of hsp90 and the hsp90-binding immunophilins in signalling protein movement.* Cell Signal, 2004. **16**(8): p. 857-72.
171. Schulz, R., et al., *Inhibiting the HSP90 chaperone destabilizes macrophage migration inhibitory factor and thereby inhibits breast tumor progression.* J Exp Med, 2012. **209**(2): p. 275-89.
172. Lord, K.A., B. Hoffman-Liebermann, and D.A. Liebermann, *Nucleotide sequence and expression of a cDNA encoding MyD88, a novel myeloid differentiation primary response gene induced by IL6.* Oncogene, 1990. **5**(7): p. 1095-7.
173. Hultmark, D., *Macrophage differentiation marker MyD88 is a member of the Toll/IL-1 receptor family.* Biochem Biophys Res Commun, 1994. **199**(1): p. 144-6.
174. Takeda, K. and S. Akira, *Toll-like receptors in innate immunity.* Int Immunol, 2005. **17**(1): p. 1-14.
175. Bagchi, A., et al., *MyD88-dependent and MyD88-independent pathways in synergy, priming, and tolerance between TLR agonists.* J Immunol, 2007. **178**(2): p. 1164-71.
176. Blander, J.M. and R. Medzhitov, *Regulation of phagosome maturation by signals from toll-like receptors.* Science, 2004. **304**(5673): p. 1014-8.
177. Picard, C., J.L. Casanova, and A. Puel, *Infectious diseases in patients with IRAK-4, MyD88, NEMO, or IkappaBalpha deficiency.* Clin Microbiol Rev, 2011. **24**(3): p. 490-7.
178. Libermann, T.A. and D. Baltimore, *Activation of interleukin-6 gene expression through the NF-kappa B transcription factor.* Mol Cell Biol, 1990. **10**(5): p. 2327-34.
179. Naugler, W.E., et al., *Gender disparity in liver cancer due to sex differences in MyD88-dependent IL-6 production.* Science, 2007. **317**(5834): p. 121-4.
180. O'Keeffe, M., et al., *Distinct roles for the NF-kappaB1 and c-Rel transcription factors in the differentiation and survival of plasmacytoid and conventional dendritic cells activated by TLR-9 signals.* Blood, 2005. **106**(10): p. 3457-64.
181. Kawai, T. and S. Akira, *Signaling to NF-kappaB by Toll-like receptors.* Trends Mol Med, 2007. **13**(11): p. 460-9.
182. Rocha, S., et al., *Regulation of NF-kappaB and p53 through activation of ATR and Chk1 by the ARF tumour suppressor.* EMBO J, 2005. **24**(6): p. 1157-69.
183. Kruidenier, L., et al., *A selective jumonji H3K27 demethylase inhibitor modulates the proinflammatory macrophage response.* Nature, 2012. **488**(7411): p. 404-8.

184. Alexander, C. and E.T. Rietschel, *Bacterial lipopolysaccharides and innate immunity.* J Endotoxin Res, 2001. **7**(3): p. 167-202.
185. Andreakos, E., et al., *Distinct pathways of LPS-induced NF-kappa B activation and cytokine production in human myeloid and nonmyeloid cells defined by selective utilization of MyD88 and Mal/TIRAP.* Blood, 2004. **103**(6): p. 2229-2237.
186. Dinarello, C.A., *Inhibitors of histone deacetylases as anti-inflammatory drugs.* Ernst Schering Res Found Workshop, 2006(56): p. 45-60.
187. Shankar, S., et al., *Suberoylanilide hydroxamic acid (Zolinza/vorinostat) sensitizes TRAIL-resistant breast cancer cells orthotopically implanted in BALB/c nude mice.* Mol Cancer Ther, 2009. **8**(6): p. 1596-605.
188. Chavey, C., et al., *Interleukin-8 expression is regulated by histone deacetylases through the nuclear factor-kappaB pathway in breast cancer.* Mol Pharmacol, 2008. **74**(5): p. 1359-66.
189. Hubackova, S., et al., *Interleukin 6 signaling regulates promyelocytic leukemia protein gene expression in human normal and cancer cells.* J Biol Chem, 2012. **287**(32): p. 26702-14.
190. Hoshino, Y., et al., *Bevacizumab terminates homeobox B9-induced tumor proliferation by silencing microenvironmental communication.* Mol Cancer, 2014. **13**(1): p. 102.
191. Stoll, S.J., et al., *The transcription factor HOXC9 regulates endothelial cell quiescence and vascular morphogenesis in zebrafish via inhibition of interleukin 8.* Circ Res, 2011. **108**(11): p. 1367-77.
192. Shah, M.A. and G.K. Schwartz, *Cell cycle-mediated drug resistance: an emerging concept in cancer therapy.* Clin Cancer Res, 2001. **7**(8): p. 2168-81.
193. Bhaskara, S., et al., *Histone deacetylases 1 and 2 maintain S-phase chromatin and DNA replication fork progression.* Epigenetics Chromatin, 2013. **6**(1): p. 27.
194. Bhaskara, S., et al., *Deletion of histone deacetylase 3 reveals critical roles in S phase progression and DNA damage control.* Mol Cell, 2008. **30**(1): p. 61-72.
195. Chang, J., et al., *MyD88 is essential to sustain mTOR activation necessary to promote T helper 17 cell proliferation by linking IL-1 and IL-23 signaling.* Proc Natl Acad Sci U S A, 2013. **110**(6): p. 2270-5.
196. Jeffrey, I.W., et al., *Inhibition of protein synthesis in apoptosis: differential requirements by the tumor necrosis factor alpha family and a DNA-damaging agent for caspases and the double-stranded RNA-dependent protein kinase.* Cancer Res, 2002. **62**(8): p. 2272-80.
197. Liu, J., et al., *Imaging protein synthesis in cells and tissues with an alkyne analog of puromycin.* Proc Natl Acad Sci U S A, 2012. **109**(2): p. 413-8.
198. Li, X., et al., *Specific SKN-1/Nrf stress responses to perturbations in translation elongation and proteasome activity.* PLoS Genet, 2011. **7**(6): p. e1002119.
199. Chini, C.C. and J. Chen, *Human claspin is required for replication checkpoint control.* J Biol Chem, 2003. **278**(32): p. 30057-62.
200. Wilsker, D., et al., *Essential function of Chk1 can be uncoupled from DNA damage checkpoint and replication control.* Proc Natl Acad Sci U S A, 2008. **105**(52): p. 20752-7.
201. Lee, J.H., et al., *Histone deacetylase inhibitor induces DNA damage, which normal but not transformed cells can repair.* Proc Natl Acad Sci U S A, 2010. **107**(33): p. 14639-44.
202. Dyson, H.J. and P.E. Wright, *Intrinsically unstructured proteins and their functions.* Nat Rev Mol Cell Biol, 2005. **6**(3): p. 197-208.
203. Oldfield, C.J., et al., *Flexible nets: disorder and induced fit in the associations of p53 and 14-3-3 with their partners.* BMC Genomics, 2008. **9 Suppl 1**: p. S1.
204. Zhou, P., *Determining protein half-lives.* Methods Mol Biol, 2004. **284**: p. 67-77.
205. Zhang, Y., et al., *HDAC-6 interacts with and deacetylates tubulin and microtubules in vivo.* EMBO J, 2003. **22**(5): p. 1168-79.

206. Muller, P., et al., *Identification of JAK/STAT signalling components by genome-wide RNA interference.* Nature, 2005. **436**(7052): p. 871-5.
207. Devasthanam, A.S., *Mechanisms underlying the inhibition of interferon signaling by viruses.* Virulence, 2014. **5**(2): p. 270-7.
208. Choi, J.W., et al., *MYD88 expression and L265P mutation in diffuse large B-cell lymphoma.* Hum Pathol, 2013. **44**(7): p. 1375-81.
209. Wu, X., et al., *Bromodomain and Extraterminal (BET) Protein Inhibition Suppresses Human T Cell Leukemia Virus 1 (HTLV-1) Tax Protein-mediated Tumorigenesis by Inhibiting Nuclear Factor kappaB (NF-kappaB) Signaling.* J Biol Chem, 2013. **288**(50): p. 36094-105.
210. Silasi, D.A., et al., *MyD88 predicts chemoresistance to paclitaxel in epithelial ovarian cancer.* Yale J Biol Med, 2006. **79**(3-4): p. 153-63.
211. Takeda, K. and S. Akira, *TLR signaling pathways.* Seminars in Immunology, 2004. **16**(1): p. 3-9.
212. Oritani, K., et al., *Both Stat3-activation and Stat3-independent BCL2 downregulation are important for interleukin-6-induced apoptosis of 1A9-M cells.* Blood, 1999. **93**(4): p. 1346-54.
213. Singh, B.N., et al., *Nonhistone protein acetylation as cancer therapy targets.* Expert Review of Anticancer Therapy, 2010. **10**(6): p. 935-954.
214. Leoni, F., et al., *The histone deacetylase inhibitor ITF2357 reduces production of pro-inflammatory cytokines in vitro and systemic inflammation in vivo.* Mol Med, 2005. **11**(1-12): p. 1-15.
215. Roger, T., et al., *Histone deacetylase inhibitors impair innate immune responses to Toll-like receptor agonists and to infection.* Blood, 2011. **117**(4): p. 1205-17.
216. Sawai, H. and N. Domae, *Discrimination between primary necrosis and apoptosis by necrostatin-1 in Annexin V-positive/propidium iodide-negative cells.* Biochem Biophys Res Commun, 2011. **411**(3): p. 569-73.
217. Riss, T.L., et al., *Cell Viability Assays.* 2004.
218. Ververis, K., et al., *Histone deacetylase inhibitors (HDACIs): multitargeted anticancer agents.* Biologics, 2013. **7**: p. 47-60.
219. Bonito, N.A., et al., *Control of gp130 expression by the mitogen-activated protein kinase ERK2.* Oncogene, 2014. **33**(17): p. 2255-63.
220. Waldner, M.J., S. Foersch, and M.F. Neurath, *Interleukin-6--a key regulator of colorectal cancer development.* Int J Biol Sci, 2012. **8**(9): p. 1248-53.
221. Huang, R.L., et al., *LPS-stimulated inflammatory environment inhibits BMP-2-induced osteoblastic differentiation through crosstalk between TLR4/MyD88/NF-kappaB and BMP/Smad signaling.* Stem Cells Dev, 2014. **23**(3): p. 277-89.
222. Domcke, S., et al., *Evaluating cell lines as tumour models by comparison of genomic profiles.* Nature Communications, 2013. **4**.
223. van Staveren, W.C., et al., *Human cancer cell lines: Experimental models for cancer cells in situ? For cancer stem cells?* Biochim Biophys Acta, 2009. **1795**(2): p. 92-103.
224. Haupt, A., et al., *Hsp90 inhibition differentially destabilises MAP kinase and TGF-beta signalling components in cancer cells revealed by kinase-targeted chemoproteomics.* BMC Cancer, 2012. **12**: p. 38.
225. McDonough, H. and C. Patterson, *CHIP: a link between the chaperone and proteasome systems.* Cell Stress Chaperones, 2003. **8**(4): p. 303-8.
226. Eisele, F. and D.H. Wolf, *Degradation of misfolded protein in the cytoplasm is mediated by the ubiquitin ligase Ubr1.* FEBS Lett, 2008. **582**(30): p. 4143-6.
227. Sanchez, R. and M.M. Zhou, *The role of human bromodomains in chromatin biology and gene transcription.* Curr Opin Drug Discov Devel, 2009. **12**(5): p. 659-65.
228. New, M., et al., *A regulatory circuit that involves HR23B and HDAC6 governs the biological response to HDAC inhibitors.* Cell Death Differ, 2013.